CSQCD 2026 School

18th May 2026

Cooling and Magnetic fields evolution of isolated neutron stars

Daniele Viganò

vigano@ice.csic.es

Institute of Space Sciences

CSIC IEEC

Consejo Superior de Investigaciones Científicas

European Research Council

Established by the European Commission

P-Pdot diagram for isolated neutron stars

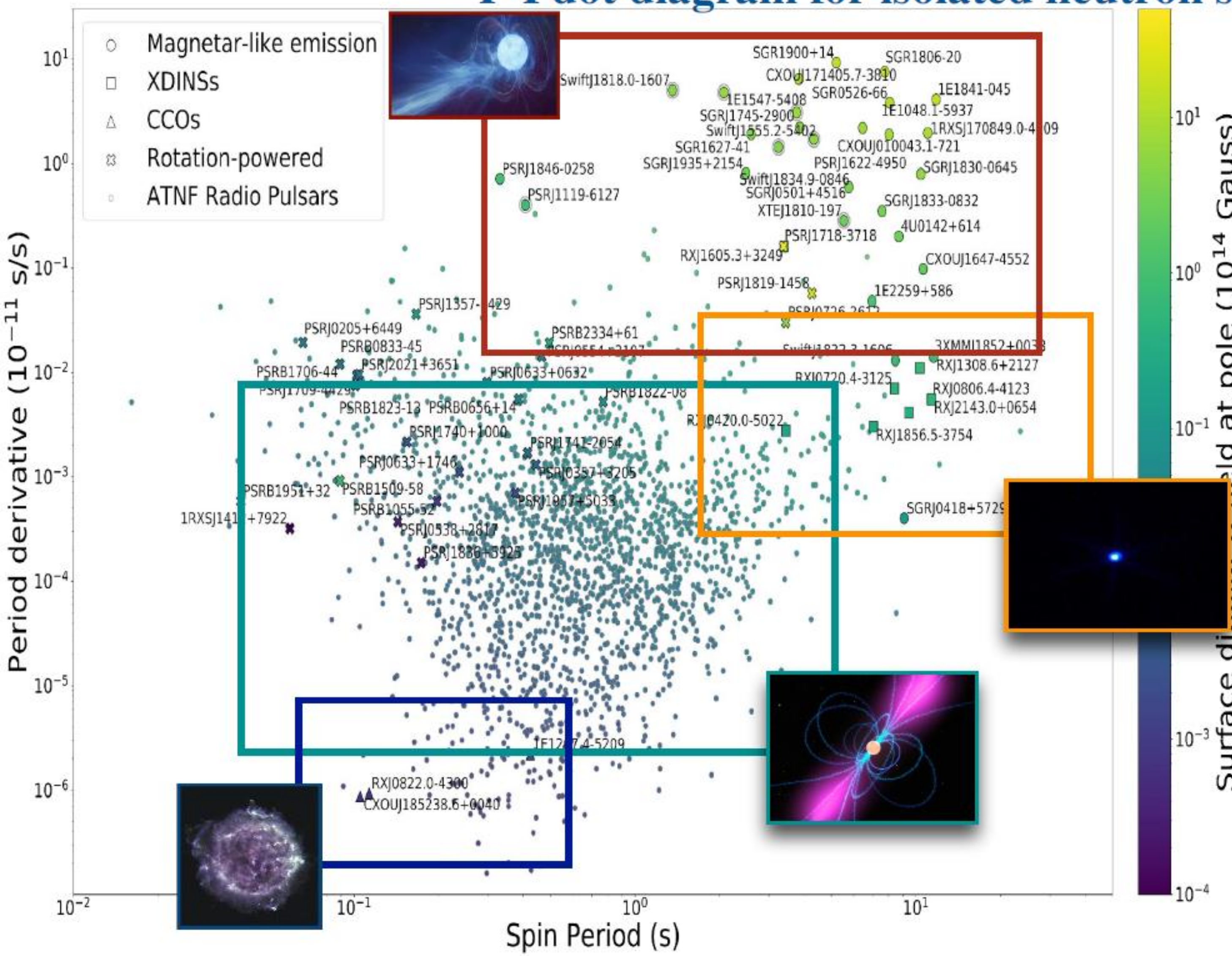

Magnetars

Powered by magnetic energy. Characterised by outbursts and flares. Typically emitting in X-rays

X-ray Dim Isolated Neutron Stars

Powered by magnetic energy. Old, almost pure blackbodies. Typically emitting in X-rays

Central Compact Objects

Powered by magnetic energy. Young with bright SNRs. Typically emitting in X-rays

Rotational-Powered Pulsars

Powered by rotational energy. Typically emitting in radio.

MATINS
MAgneto-Thermal evolution of Isolated Neutron Stars

$$B_p = C_{sd}\sqrt{P[\mathrm{s}]\ \dot{P}}\ ,$$

$$C_{sd} = 6.4 \times 10^{19}\sqrt{\frac{I_{45}}{f_\chi R_6^6}}\ \mathrm{G}$$

[courtesy Clara Dehman]

Observations: thermal X-ray luminosity, real age, P and Pdot

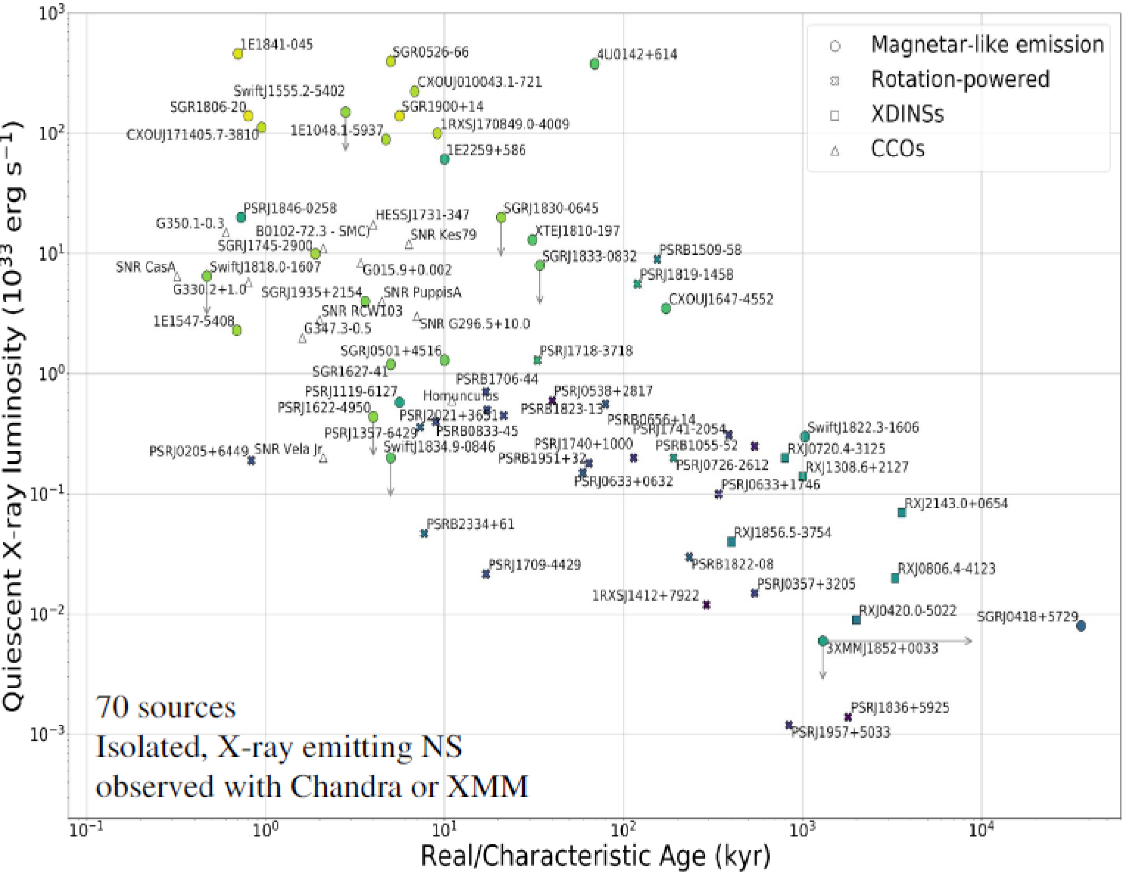

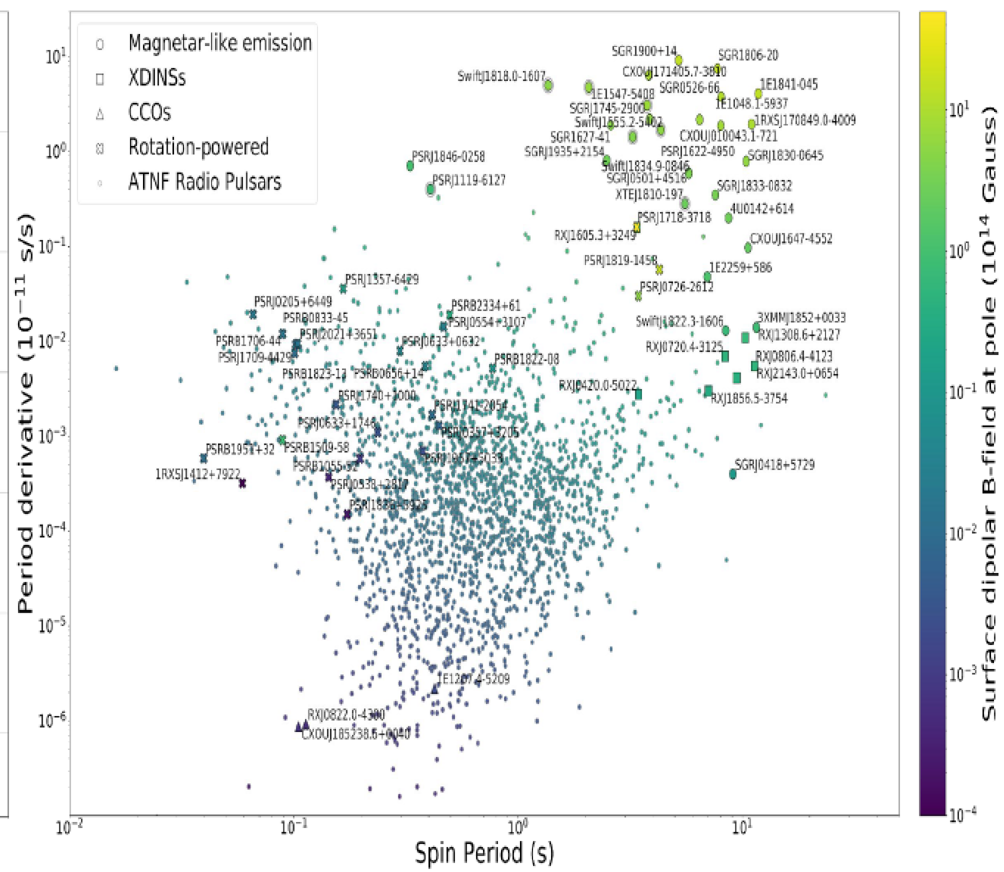

[courtesy Clara Dehman]

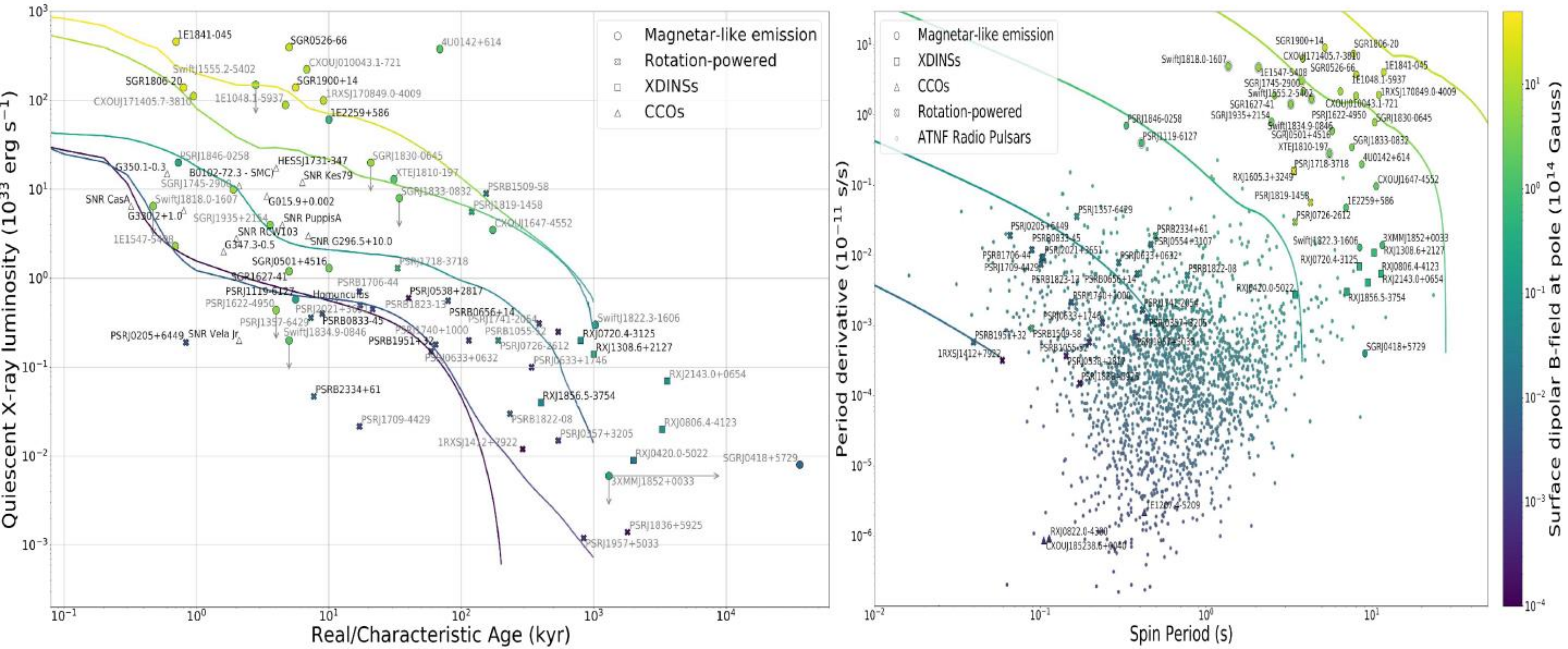

- Realistic magnetic topology: complex and non-axisymmetric
- The need to model cooling curves, that depend on the 3d configuration

"New 3D code MATINS"

MATINS
MAgneto-Thermal evolution of Isolated Neutron Stars

[Dehman, Marino, Kovlakas, Rea et al., in prep.]

[courtesy Clara Dehman]
MATINS: https://ice-csic-astroexotic.github.io/code/matins/

FORMATION OF NEUTRON STARS

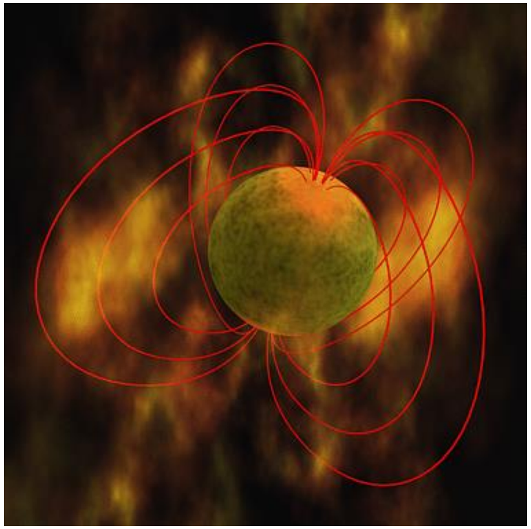

Core collapse of the progenitor

- The warm iron core is supported by radiation pressure.
- The Fe 'ash' cannot fuse: finally gravity wins!
- Rapid contraction with $u \lesssim \frac{1}{2}c$ (in msec!)
- $T_c \gtrsim 3 \times 10^9\,\mathrm{K}$ - the photons cause photo-dissociation:
  $^{56}Ni + \gamma \rightarrow 14\,^4He$
  $^{54}Fe + \gamma \rightarrow 13\,^4He + 2n$
  $^{56}Fe + \gamma \rightarrow 13\,^4He + 4n, \cdots$
- Endothermal reactions, powered by the gravitational energy $\rightarrow$ the core has to contract and heat up. Then: $^4He + \gamma \rightarrow 2\,^1H + 2n$.
- In a second, part of nucleosynthesis products go back to H!
- Secondly, inverse beta decay due to nuclei coming close to each other: $e^- + p \rightarrow n + \overline{\nu}_e$
- **Neutronization** of the core (in 3-10 sec)!

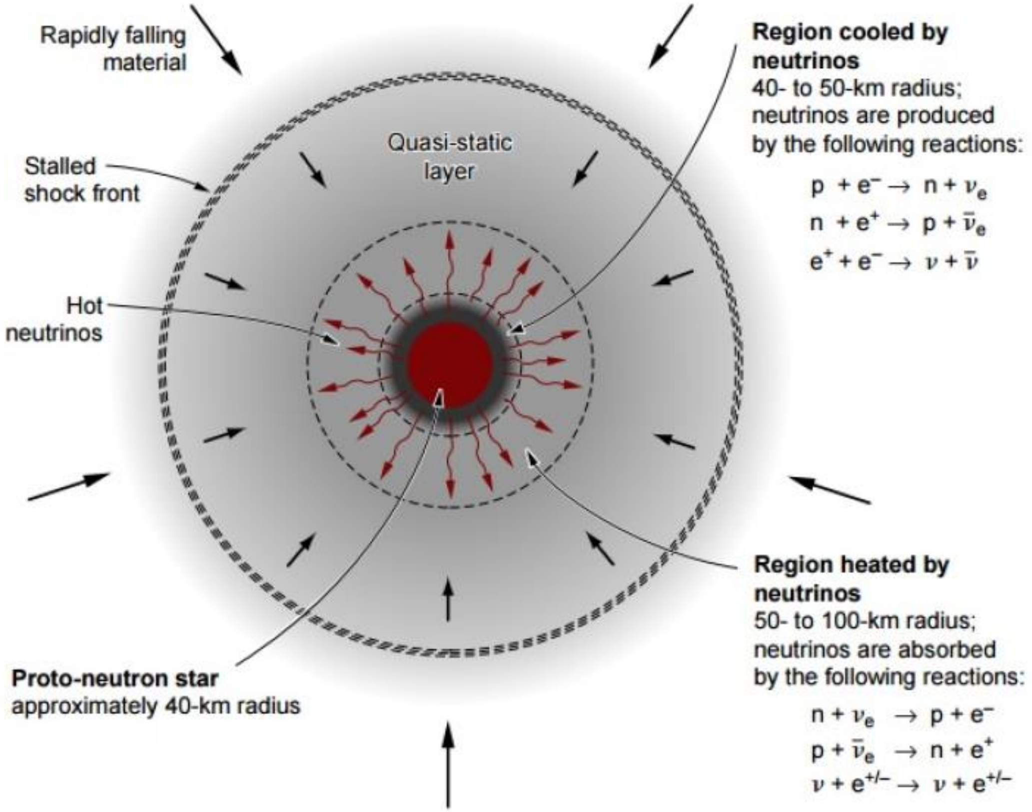

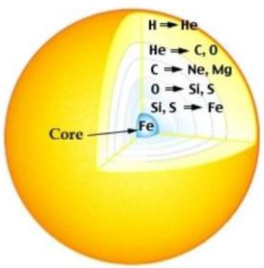

Massive star structure before explosion

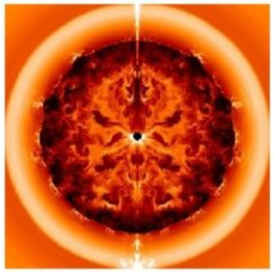

SNII explosion calculations (T. Janka, MPE)

Supernova explosion

Supernova explosion:

- Matter falls onto the neutron-rich core, creating a shock that bounces back ejecting infalling material.
- As matter infalls, high temperatures allowing **photo-neutrino production** ($\gamma + e^- \to e^- + \nu_e + \overline{\nu}_e$) and **pair-annihilation** ($\gamma + \gamma \to \nu_e + \overline{\nu}_e$).
- Many neutrinos, carrying most of the energy $\to$ enough neutrino opacity (despite weak interaction) $\to$ deposition of energy $\to$ envelope explosion!
- Infalling matter fuses in a runaway fashion: more energy ejecting the layers on top!

Supernova outcomes:

- Total energy output: $E_{\mathrm{CC}} \gtrsim 10^{53}\,\mathrm{erg}$ - Milky Way luminosity for one second.
- New elements from capturing neutrons: r-process / s-process.
- The **supernova** forms a neutron star or nothing (?)

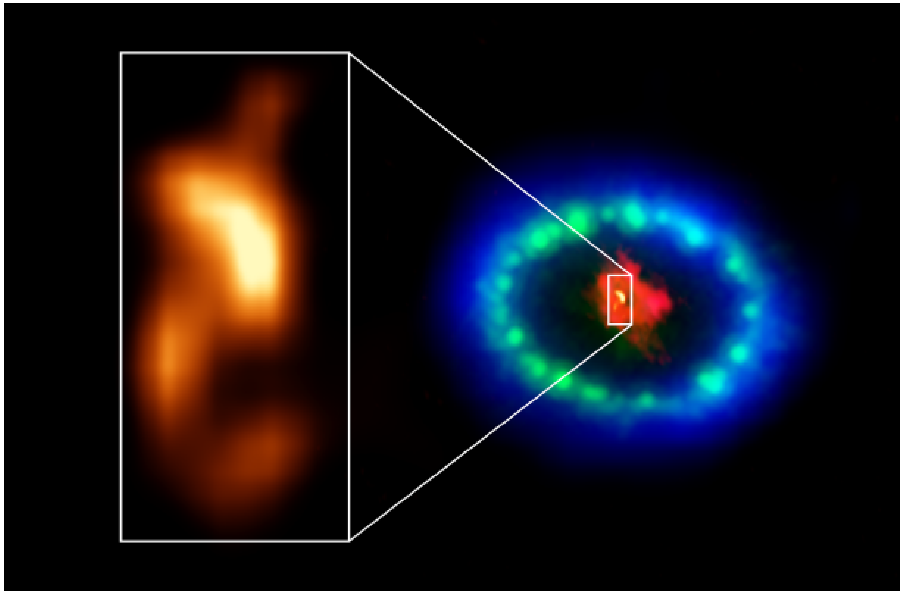

X-ray image of the 39 years old remnant of SN 1987 A. We still don't know if there is a neutron star in the center.

Neutron star formation

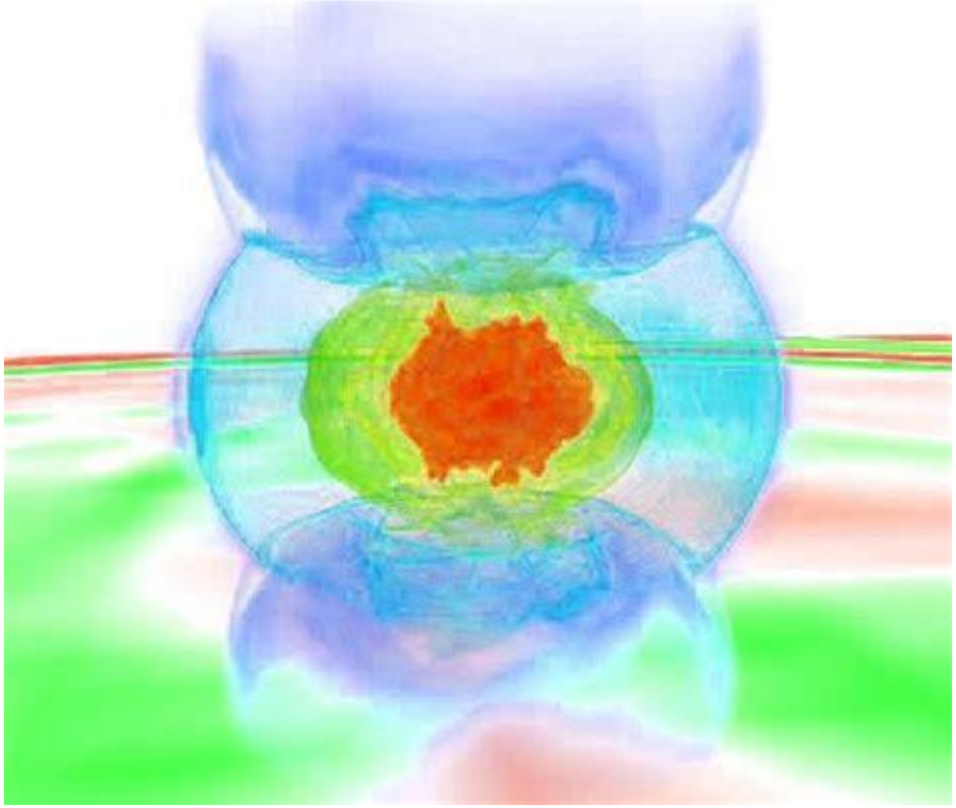

A protoneutron star is the hot remnant of the core collapse, with a radius about 100 km.
The cooling is through electromagnetic radiation.
There is convection with magnetic field amplification.
It's optically thick to neutrino, which interact with matter, for about one minute, after which it becomes optically thin, and neutrinos escape, making the core shrink to the final 10 km size.

MICROPHYSICS OF COOLING

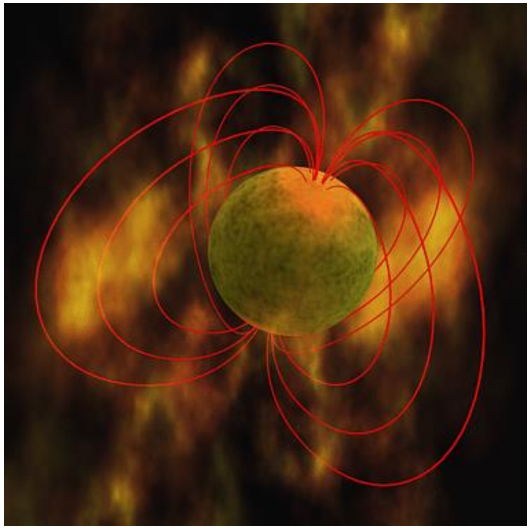

Thermal evolution and persistent properties

Cooling model: diffusion equation

$$c_V \frac{\partial T}{\partial t} + \vec{\nabla} \cdot (-\hat{\kappa} \cdot \vec{\nabla} T) = -Q_\nu + Q_j$$

In case of no extra heating, the only dependence is in the radial direction for spherical symmetry:

$$c_V \frac{\partial T}{\partial t} + \frac{\partial}{\partial r}\left[-\kappa \frac{\partial T}{\partial r}\right] = -Q_\nu$$

Cooling timescale: $\mathbf{c_v T/Q_v}$

Ingredients:

- Neutron star model (structure, EoS)
- Heat capacity c_v (T, density): main contribution by neutrons.
- Thermal conductivity κ, very large in the core (rapidly isothermal). Important timescales given by the electron relaxation time in the crust.
- Neutrino emissivities Q_v: energy lost in production of neutrinos that escape
- Sources of internal heat Q_j: nuclear reactions, **Ohmic dissipation**, accretion
- Superfluid / Superconductivity models
- Boundary condition: model of envelope (i.e., liquid outermost 100 m, with strong gradient of temperature), linking internal T to surface temperature T_s, emission model (atmosphere, blackbody, condensed surface...)

Transport coefficients

(Shear and Bulk) viscosity:
resistance to gradual deformation by shear stress or tensile stress

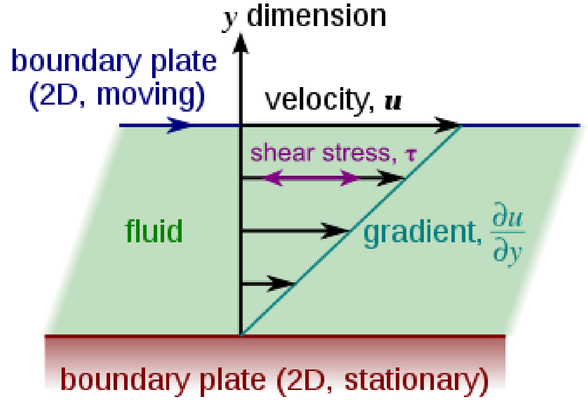

Thermal conductivity:
property of a material to conduct heat

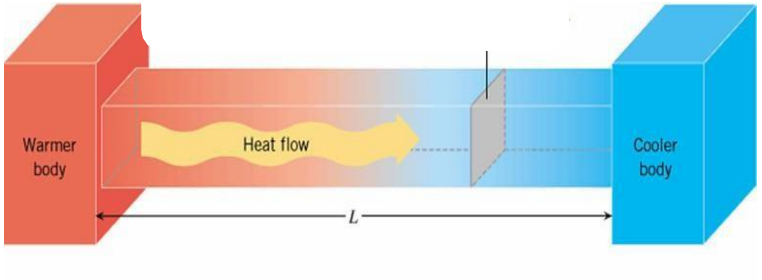

$$P_{cond} = \frac{Q}{t} = kA\frac{T_H - T_C}{L}.$$

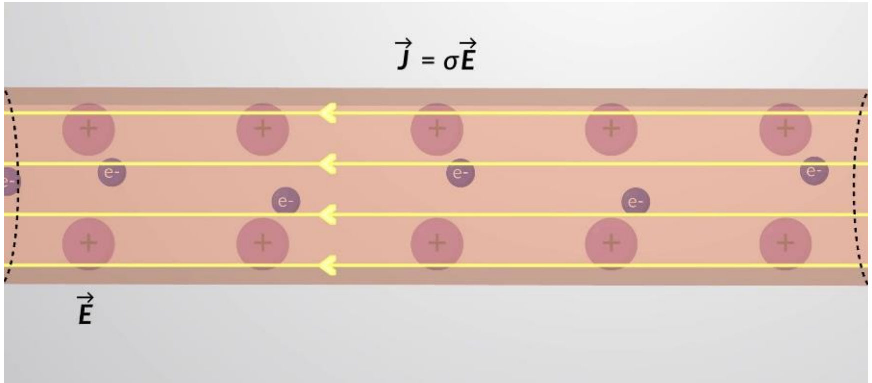

Electrical conductivity: measures a material's ability to conduct an electric current (charge carriers move)

Transport coefficients: viscosity

Analogy:
Shear viscosity = rubbing two decks of cards sideways. They can heat up due to the friction of one card against the other.
Bulk viscosity = repeatedly squeezing a foam ball. The foam heats up slightly when you repeatedly compress it. That heating is bulk viscous dissipation.

Example of viscosity in liquids:
drop of honey or gasoline
laminar vs turbulent flow (high/low viscosity)

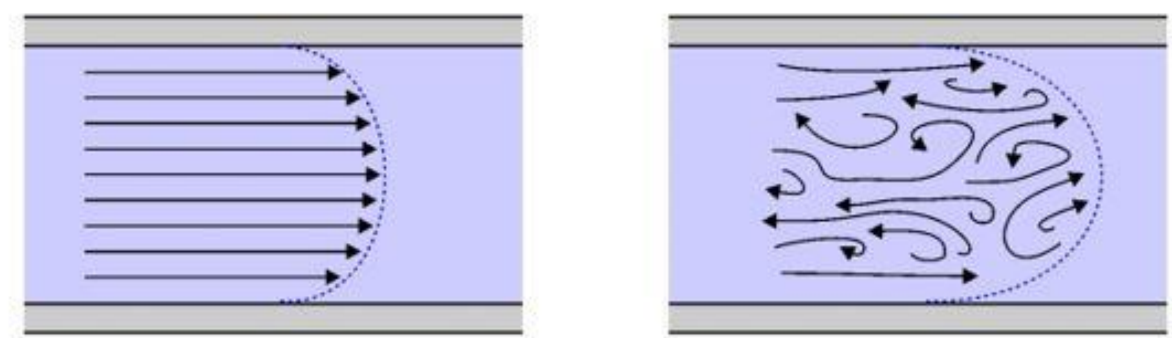

Figure 1 Laminar flow (left) and turbulent flow (right)

Transport coefficients: thermal conductivity

Ways to transfer heat in NSs

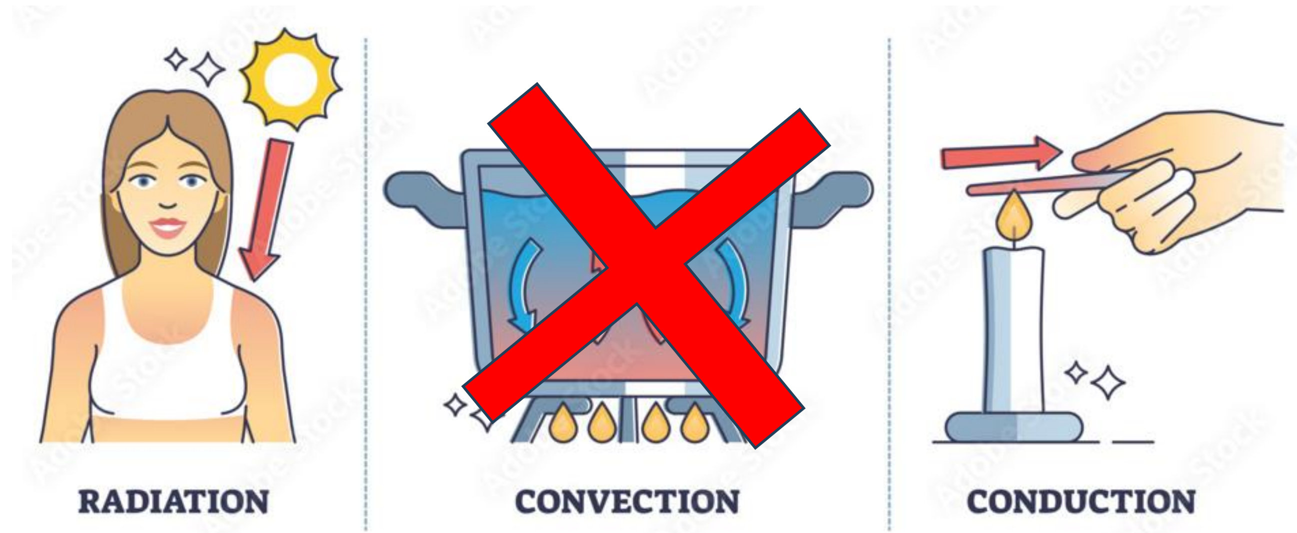

Only in the outermost layers

The matter is strongly stratified: impossible to mix up and down layers (except in the protoNS phase)

The relevant mechanism, effective due to the large density and the large energy (high Fermi momentum)

Transport coefficients: conductivities

Chamel and Haensel '08

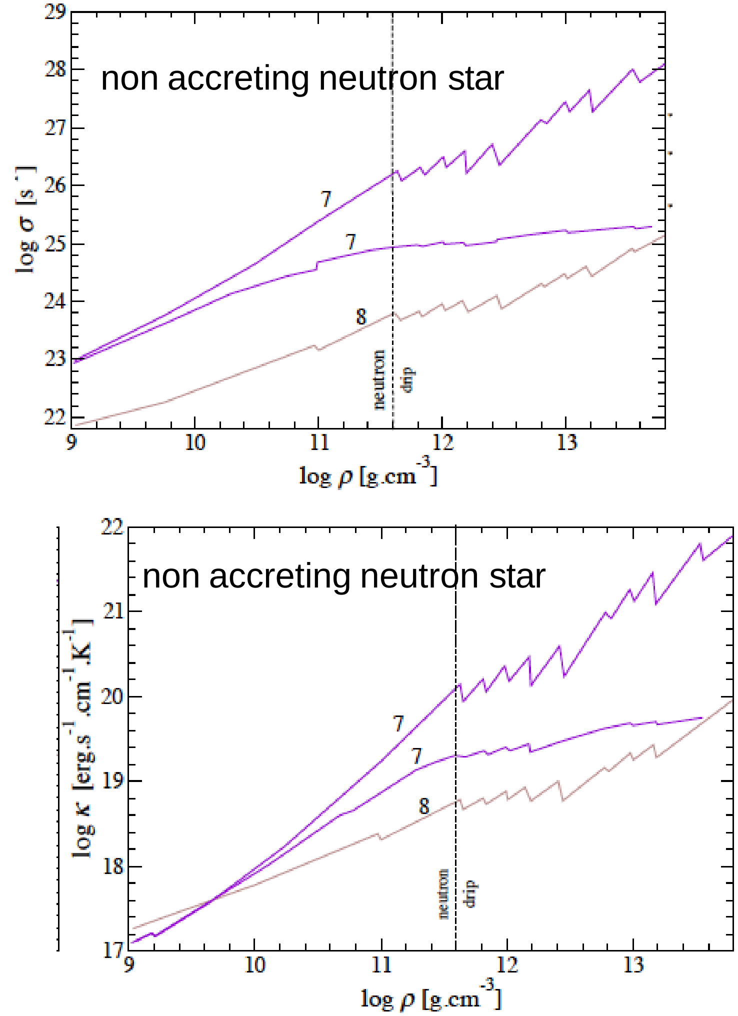

Figure 54: Electrical conductivity σ and thermal conductivity κ of the outer and inner crust, calculate for the ground-state model of Negele & Vautherin [303]. Labels 7 and 8 refer to $\log_{10} T[\mathrm{K}] = 7$ and 8 respectively. The thin line with label 7 corresponds to an impure crust, which contains in the lattice site 5% impurities – nuclei with $|Z_{\rm imp} - Z| = 4$. Based on a figure made by A.Y. Potekhin.

$$\boldsymbol{j}_T = -Q_T T \boldsymbol{j}_e - \kappa \boldsymbol{\nabla} T$$

$$\boldsymbol{j}_e = \sigma \boldsymbol{E}^* + \sigma Q_T \boldsymbol{\nabla} T \,,$$

$$\sigma = \frac{e^2 n_e}{m_e^* \nu_\sigma} \qquad \nu_\sigma = \nu_{e\mathrm{N}}^\sigma + \nu_{\mathrm{imp}}^\sigma$$

$$\kappa = \frac{\pi^2 k_{\mathrm{B}}^2 T n_e}{3 m_e^* \nu_\kappa} \qquad \nu_\kappa = \nu_{e\mathrm{N}}^\kappa + \nu_{ee}^\kappa + \nu_{\mathrm{imp}}^\kappa$$

Outer crust: main carriers of transport are electrons scattering with ions

$$\nu_\kappa = \nu_\sigma \simeq \nu_{e\mathrm{N}}(\mu_e)$$

For low temperatures, impurities dominate

Inner crust: the neutron gas plays a role

$$\kappa = \kappa_e + \kappa_n \qquad \kappa_n^{\mathrm{diff}} = \frac{\pi^2 k_{\mathrm{B}}^2 T n_n}{3 m_n^* \nu_n} \quad \begin{array}{l} \nu_n = \nu_{n\mathrm{N}} + \nu_{nn} \\ \nu_n \approx \nu_{n\mathrm{N}} \end{array}$$

Electron-electron might also be more important than electron-ion interactions (Shternin & Yakovlev '06)

Strong magnetic fields

Transport properties become anisotropic:
magnetic field bends electron trajectories and suppresses the electron transport across B

Along B, electron conduction is bigger than thermal ion conduction
Across B, electron conduction is suppressed

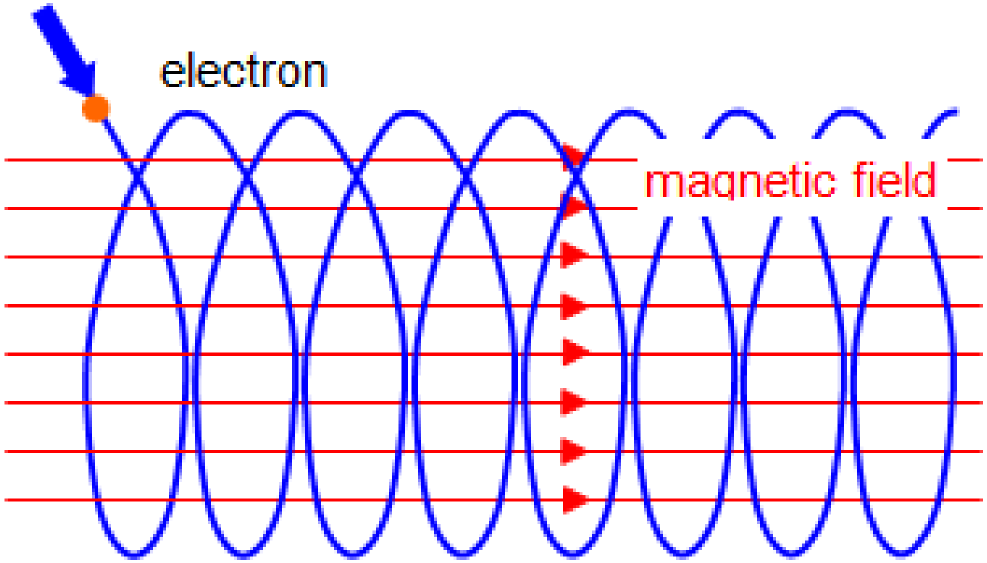

Strong magnetic fields

Nonquantizing magnetic fields: many Landau orbitals are populated and quantum effects smeared by thermal effects

Weakly-quantizing magnetic fields

many Landau orbitals are populated and quantum effects are well pronounced (oscillations due to filling of a new Landau level)

Strongly-quantizing magnetic fields

quantization effects are well pronounced and electrons populate the ground Landau level

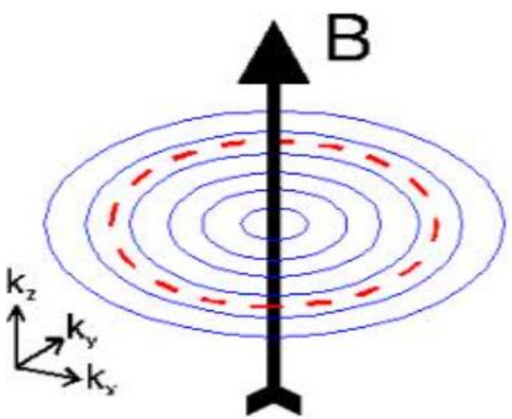

$$E = E_i + \left(N + \frac{1}{2}\right)\hbar\omega_c$$

$$\omega_c = \frac{|q|B}{m}$$

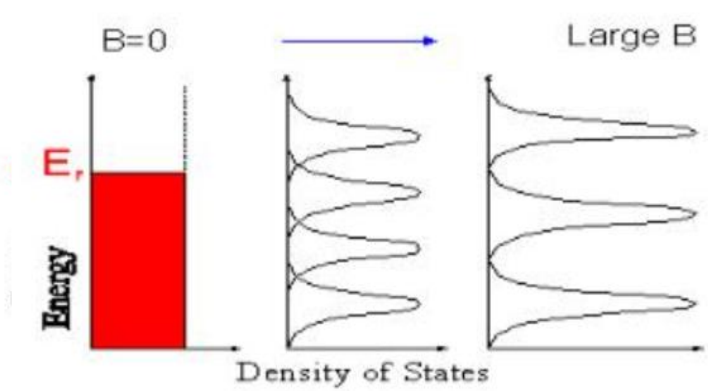

Conductivities

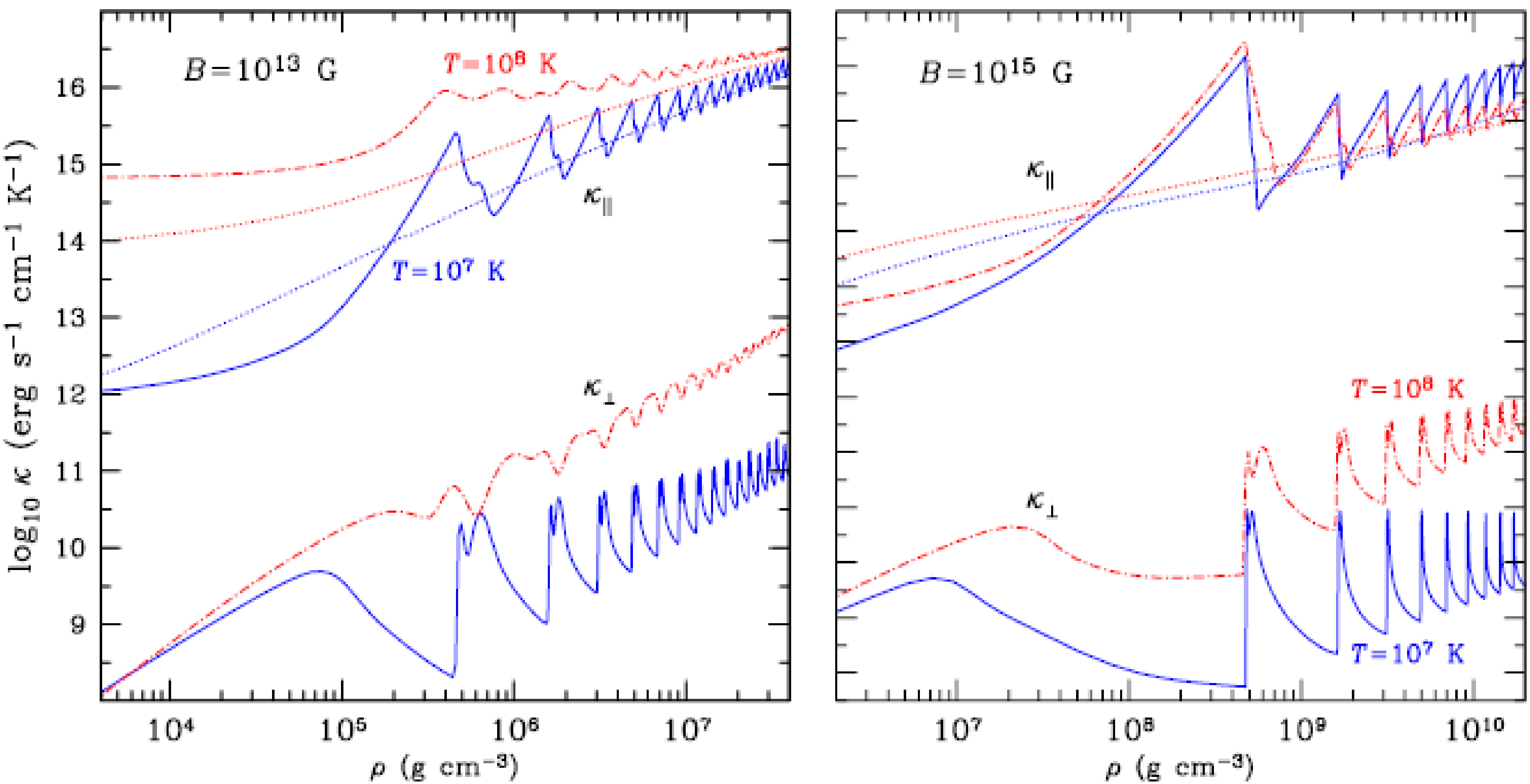

Fig. 9 Electron thermal conductivities along (upper curves) and across (lower curves) magnetic field $B = 10^{13}$ G (left panel) and 10^{15} G (right panel) as functions of mass density at temperatures $T = 10^7$ K (solid lines) and 10^8 K (dot-dashed lines). For comparison, the non-magnetic thermal conductivities are shown by dotted lines.

Conductivities

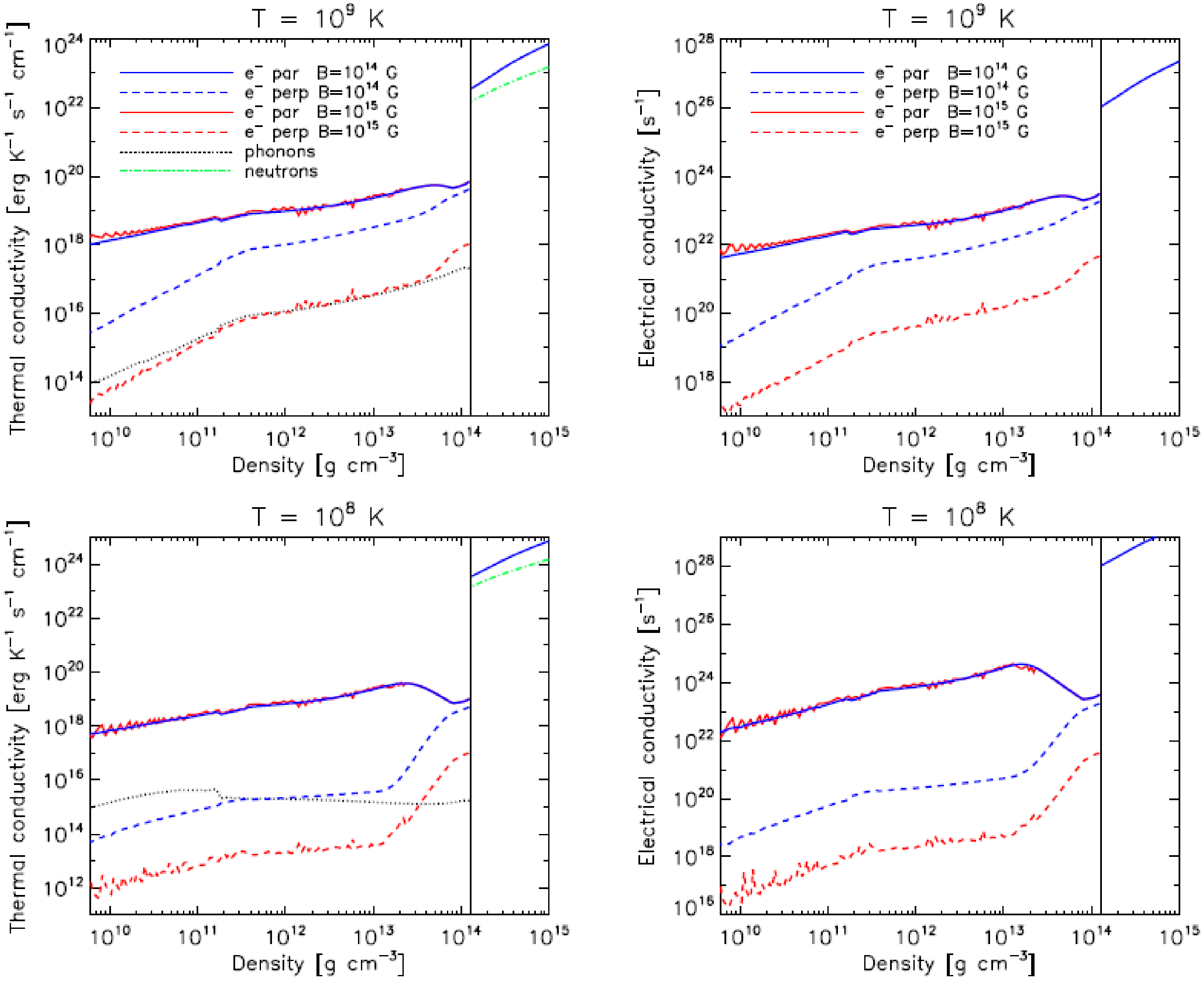

Figure 4.5: Contributions to the thermal (left panels) and electrical (right panels) conductivities, at $T = 10^9$ K (top) and $T = 10^8$ K (bottom), without superfluidity.

Anisotropy in heat conduction

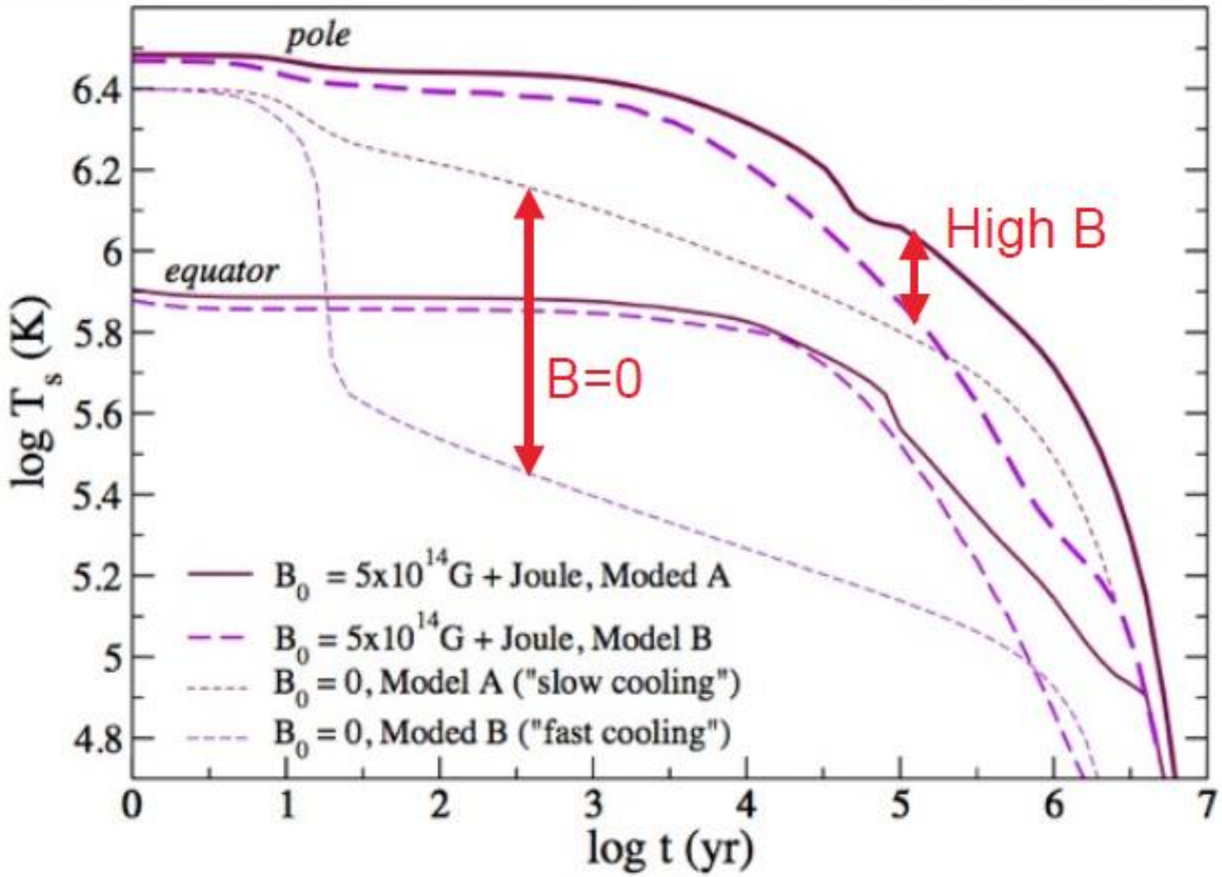

[Pons 2009]

Magnetic field acts as an insulator, so that heat can be conducted easily along the magnetic field lines, and less easily across it, due to the anisotropic conductivity of the electrons.

If you have a dipole, the poles are then thermally connected to the interior, while the equator is partially insulated.

Cooper pairs: an intutitive picture for electron pairing in superconducting metals

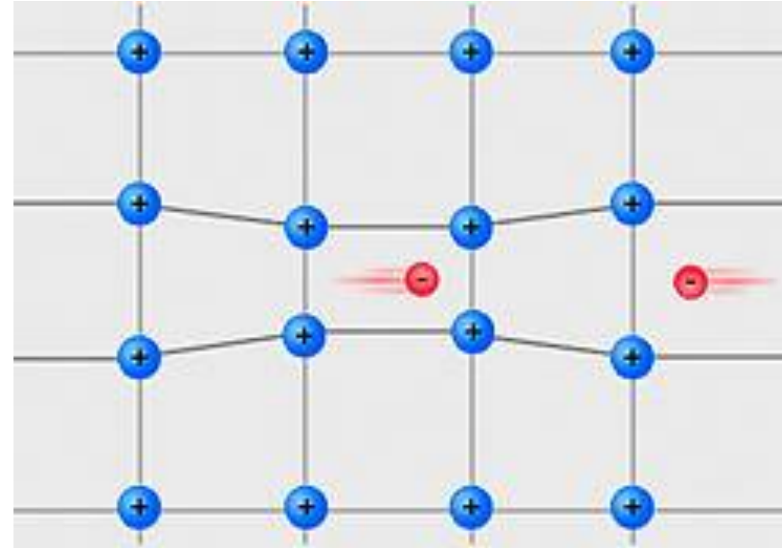

The attractive interactions are due to the presence of phonons (lattice deformation), which induce a small attraction of electrons, which is weak (because there is repulsion between electrons), so thermal energy breaks the pairs easily.

The pairs are not physically close, but they are connected. The composite pair has an integer spin, so it behaves as a boson: they can be in the same ground state and generate condensates (superconductivity).
The pairing creates an energy gap, which basically forbids scattering among electrons, and make the superconductivity/superfluidity appear

In NSs, neutrons and protons become superfluid/superconductive (strong force mediation, which is attractive in the long-range, at contrast with e-e).

Gap models

In 1959 Migdal already proposed that the neutrons in NS would be in a BCS state: n-n and p-p interactions become attractive in some range of densities, and Cooper pairs of n and p are formed

It costs energy to break Cooper pairs: energy gap.

$$E = \sqrt{(\frac{p^2}{2m} - \mu)^2 + \Delta^2} \qquad \Delta \sim (1-3)\mathrm{MeV}$$

It's the binding energy that overcomes the natural repulsion.
This gap correspons to a critical temperature (below which BCS state appears): $T_c \sim 0.57\,\Delta$

Minimal effects on the EoS of the star, but very relevant effects on both the hydrodynamical equations and the transport coefficients (suppression by $\sim e^{-\Delta/T}$): cooling and rotational properties affected

Gap models

Values of the gap as a function of the density.
As the density increases, the attractive n-n interaction becomes repulsive in the s-channel (singlet, isotropic wavefunction, J=0), but there is an attractive interaction in a p-channel (triplet, J=1, e.g. ^{3}He).

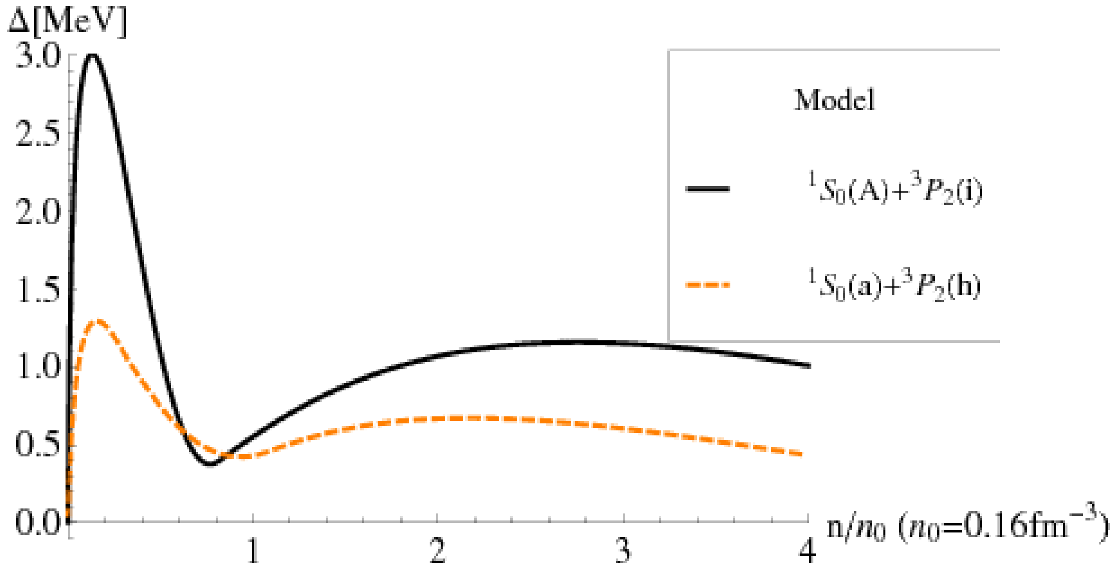

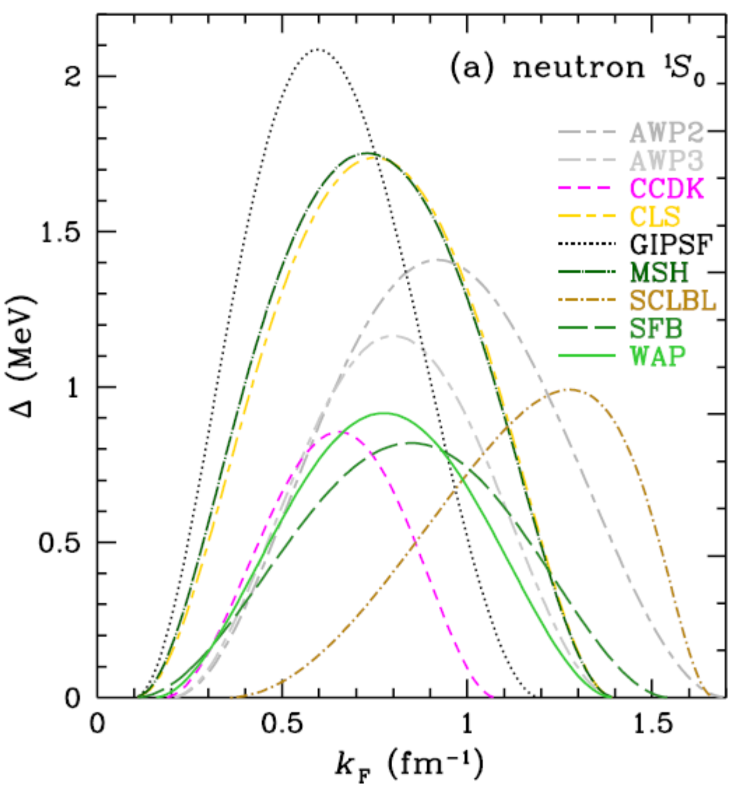

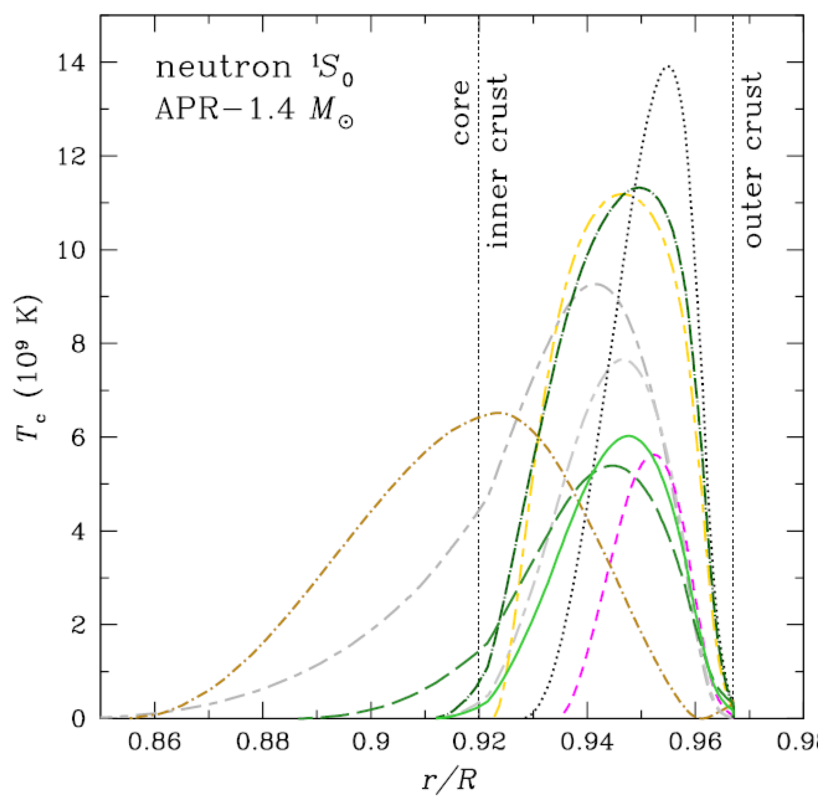

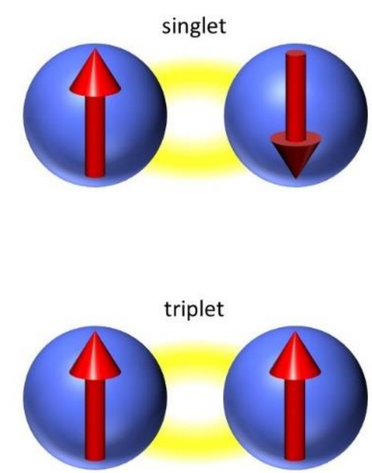

Gap models

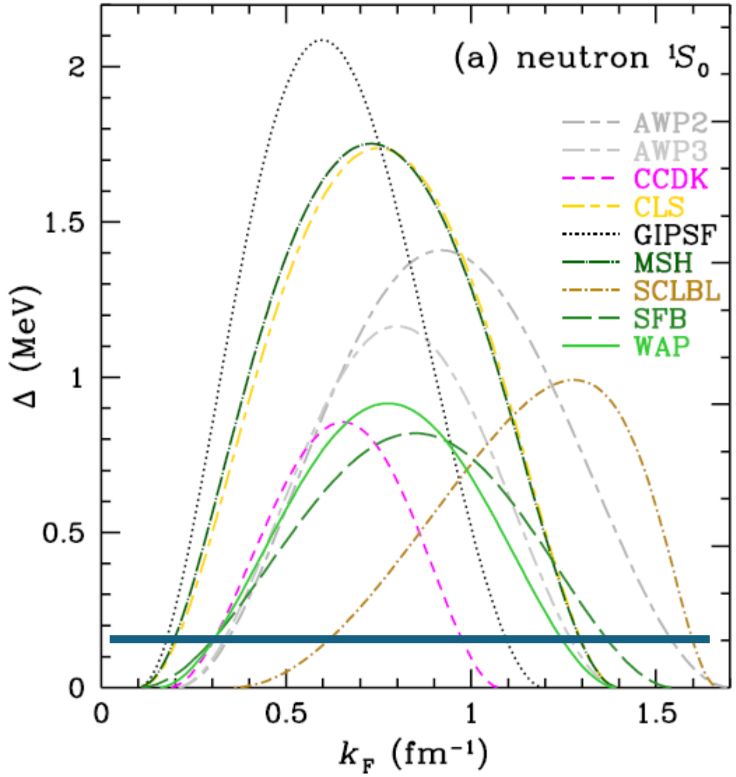

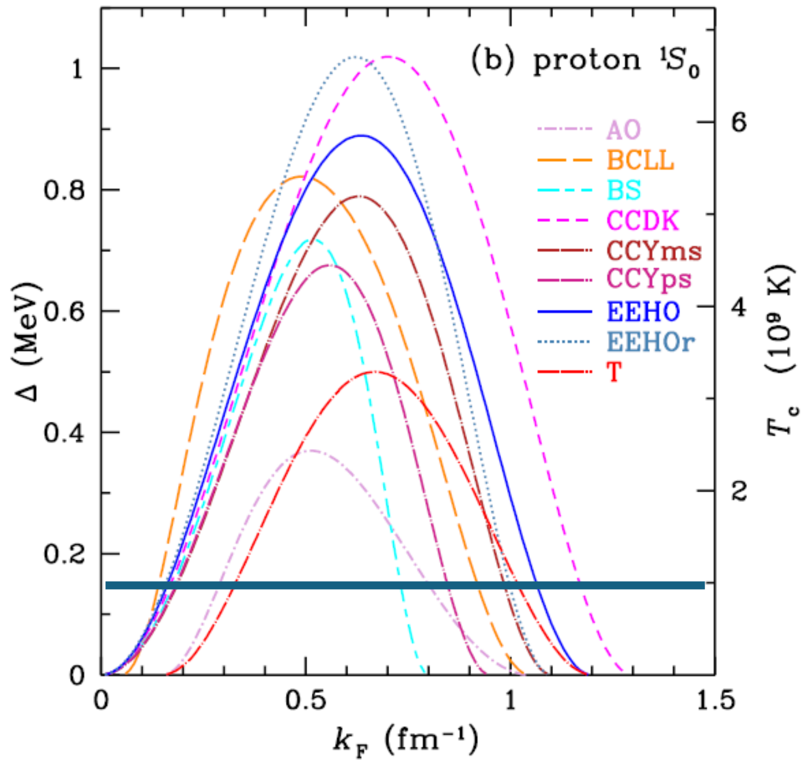

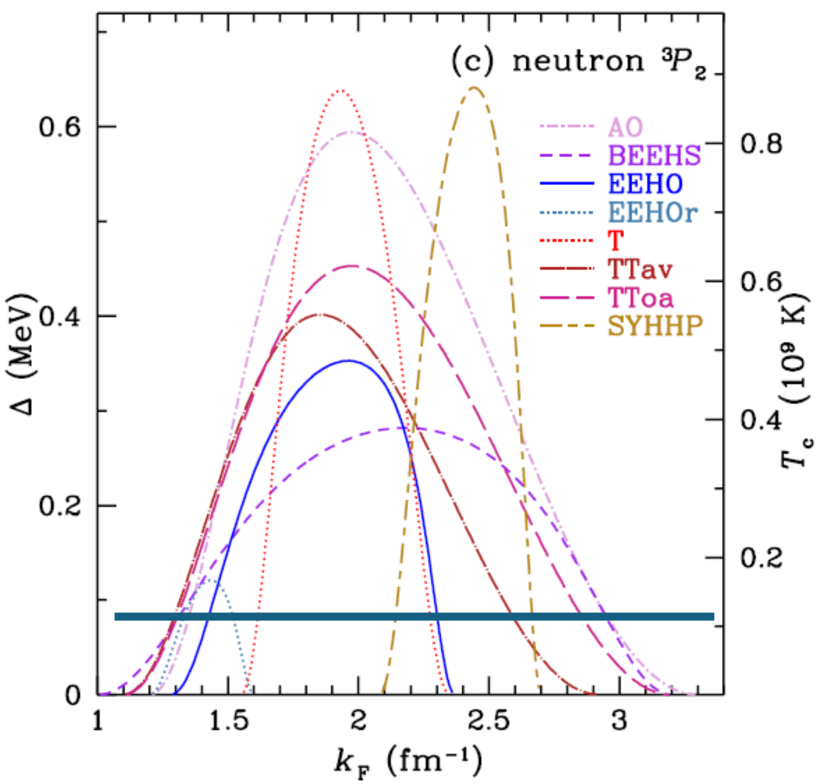

Typical T of a young NS

Convenient purely analytical functional form (neglecting T dependence):

$$\Delta(k_{\rm Fx}) = \Delta_0 \frac{(k_{\rm Fx}-k_0)^2}{(k_{\rm Fx}-k_0)^2+k_1}\frac{(k_{\rm Fx}-k_2)^2}{(k_{\rm Fx}-k_2)^2+k_3}$$

where Δ_0, k_0, k_1, k_2, and k_3 are fit parameters.

$$\hbar k_{\rm Fx} = \hbar(3\pi^2 n_{\rm x})^{1/3}$$

[Wynn Ho et al. 2012]

Gap models

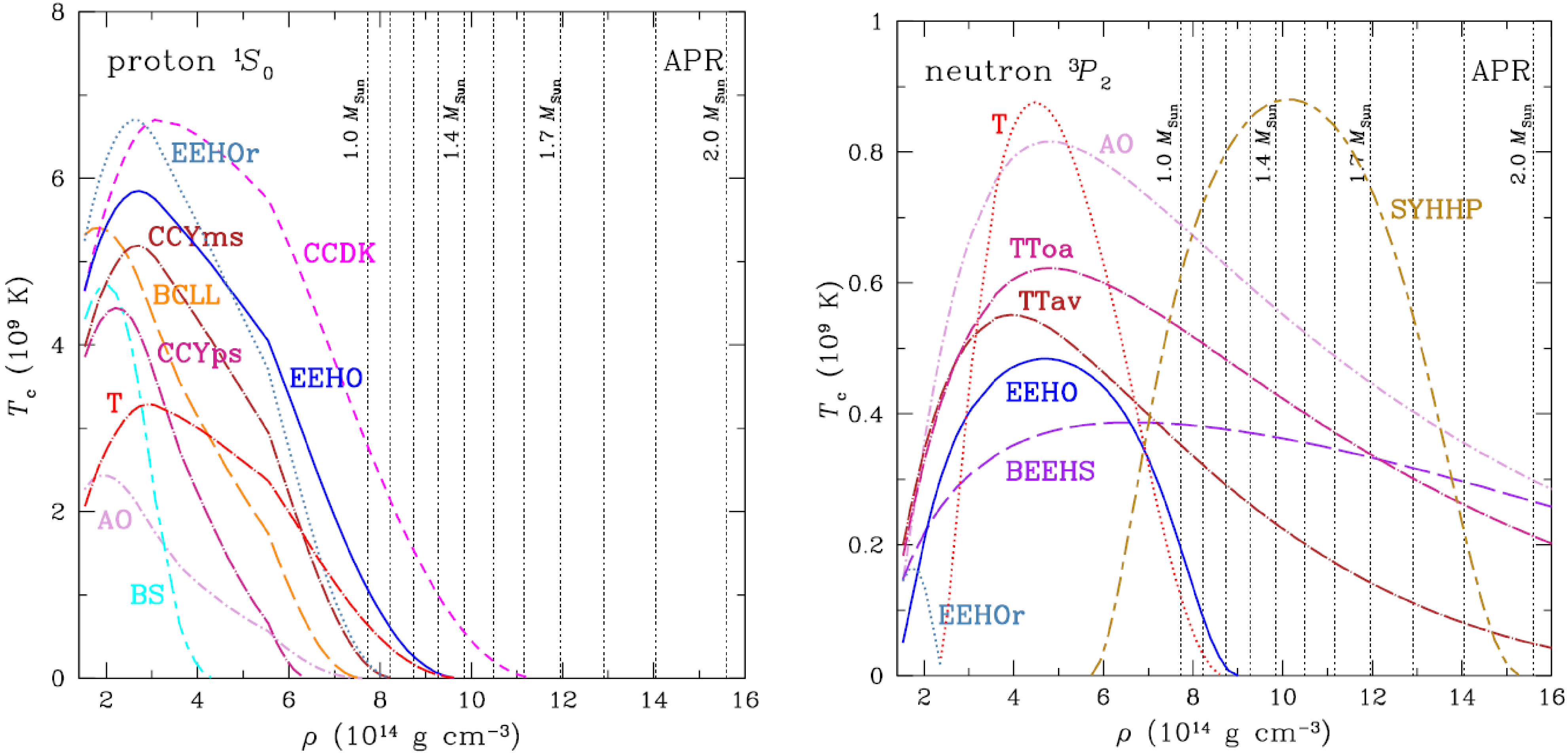

Depending on the EoS and NS mass, and on the gap, we can have more or less SF / SC matter

Superconductivity in quark matter

Quark matter is also in a BCS state at high enough densities

This is due to the fact that quark-quark interactions close to the Fermi interactions are attractive (with gluons mediating the interaction, analogously to phonons with electrons):

COLOR SUPERCONDUCTIVITY

The specific form of the BCS state depends on the different parameters, such as quark masses, quark chemical potentials, etc

If there is democratic pairing between the three light quark flavors, the most preferred phase is COLOR-FLAVOR LOCKED (CFL) phase (one-to-one correspondence between three color pairs, r g b, and three flavor pairs, u d s, with the pairs being color-neutral and favour-neutral).

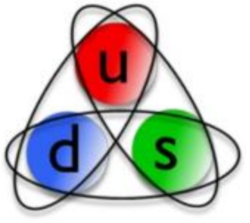

Neutrino emissivity

Momentum conservation implies the fast cooling by DUrca possible only for minimum proton fraction Y_p>1/9 (momentum conservation), which happens only for certain EoS and high enough mass

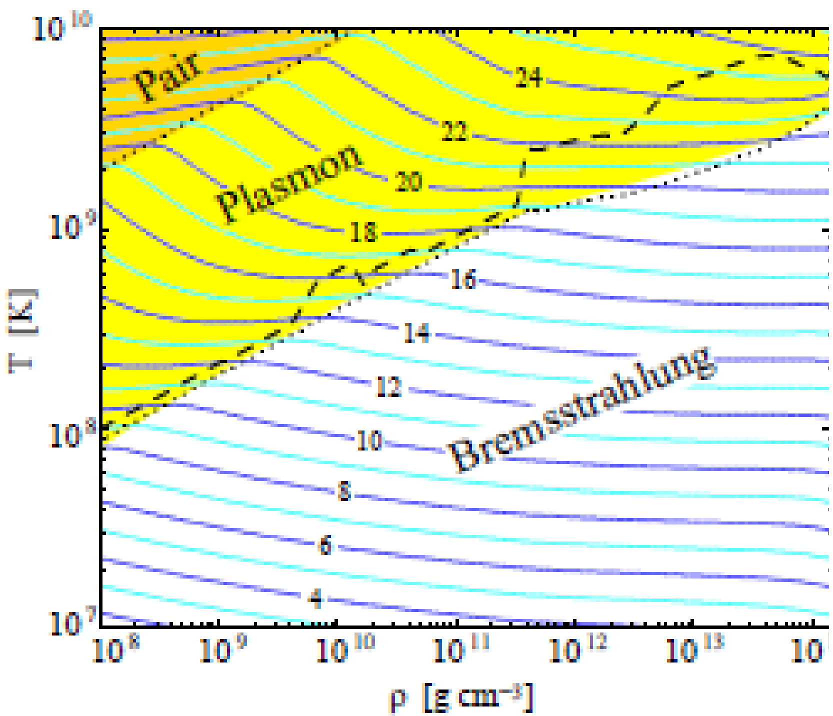

Steep temperature dependence (T^8, T^6, T^5..)!

Process	Q_ν [erg cm^{-3}s^{-1}]	Onset	Ref
Core			
Modified URCA (n-branch)			
$nn \to pne\bar{\nu}_e$, $pne \to nn\nu_e$	$8 \times 10^{21}\,\mathcal{R}_n^{MU}\,n_p^{1/3}\,T_9^8$		1
Modified URCA (p-branch)			
$np \to ppe\bar{\nu}_e$, $ppe \to np\nu_e$	$8 \times 10^{21}\,\mathcal{R}_p^{MU}\,n_p^{1/3}\,T_9^8$	$Y_p^c = 0.01$	1
N-N Bremsstrahlung			
$nn \to nn\nu\bar{\nu}$	$7 \times 10^{19}\,\mathcal{R}^{nn}\,n_n^{1/3}\,T_9^8$		1
$np \to np\nu\bar{\nu}$	$1 \times 10^{20}\,\mathcal{R}^{np}\,n_p^{1/3}\,T_9^8$		1
$pp \to pp\nu\bar{\nu}$	$7 \times 10^{19}\,\mathcal{R}^{pp}\,n_p^{1/3}\,T_9^8$		1
e-p Bremsstrahlung			
$ep \to ep\nu\bar{\nu}$	$2 \times 10^{17}\,n_B^{-2/3}\,T_9^8$		2
Direct URCA			
$n \to pe\bar{\nu}_e, pe \to n\nu_e$	$4 \times 10^{27}\,\mathcal{R}^{DU}\,n_e^{1/3}\,T_9^6$	$Y_p^c = 0.11$	3
$n \to p\mu\bar{\nu}_\mu, p\mu \to n\nu_\mu$	$4 \times 10^{27}\,\mathcal{R}^{DU}\,n_e^{1/3}\,T_9^6$	$Y_p^c = 0.14$	3
Crust			
Pair annihilation			
$ee^+ \to \nu\bar{\nu}$	$9 \times 10^{20}\,F_{\rm pair}(n_e, n_{e^+})$		4
Plasmon decay			
$\tilde{e} \to \tilde{e}\nu\bar{\nu}$	$1 \times 10^{20}\,I_{\rm pl}(T, y_e)$		5
e-A Bremsstrahlung			
$e(A,Z) \to e(A,Z)\nu\bar{\nu}$	$3 \times 10^{12}\,L_{eA}\,Z\,\rho_o\,n_e\,T_9^6$		6
N-N Bremsstrahlung			
$nn \to nn\nu\bar{\nu}$	$7 \times 10^{19}\,\mathcal{R}^{nn}\,f_\nu\,n_n^{1/3}\,T_9^8$		1
Core and crust			
CPBF			
$\tilde{B} + \tilde{B} \to \nu\bar{\nu}$	$1 \times 10^{21}\,n_N^{1/3}\,F_{A,B}\,T_9^7$		7
Neutrino synchrotron			
$e \to (B) \to e\nu\bar{\nu}$	$9 \times 10^{14}\,S_{AB,BC}\,B_{13}^2\,T_9^5$		8

Refs.: (1) Yakovlev & Levenfish (1995); (2) Maxwell (1979); (3) Lattimer et al. (1991); (4) Kaminker & Yakovlev (1994); (5) Yakovlev et al. (2001); (6) Haensel et al. (1996); Kaminker et al. (1999); (7) Yakovlev et al. (1999); (8) Bezchastnov et al. (1997)

Table 4.3: *Neutrino processes and their emissivities Q_ν in the core and in the crust, taken from Aguilera et al. 2008. The third column shows the onset for some processes to operate (critical proton fraction Y_p^c). We indicate the normalized temperature $T_9 = T/10^9$ K; detailed functions and precise factors can be found in the references (last column).*

Neutrino emissivity

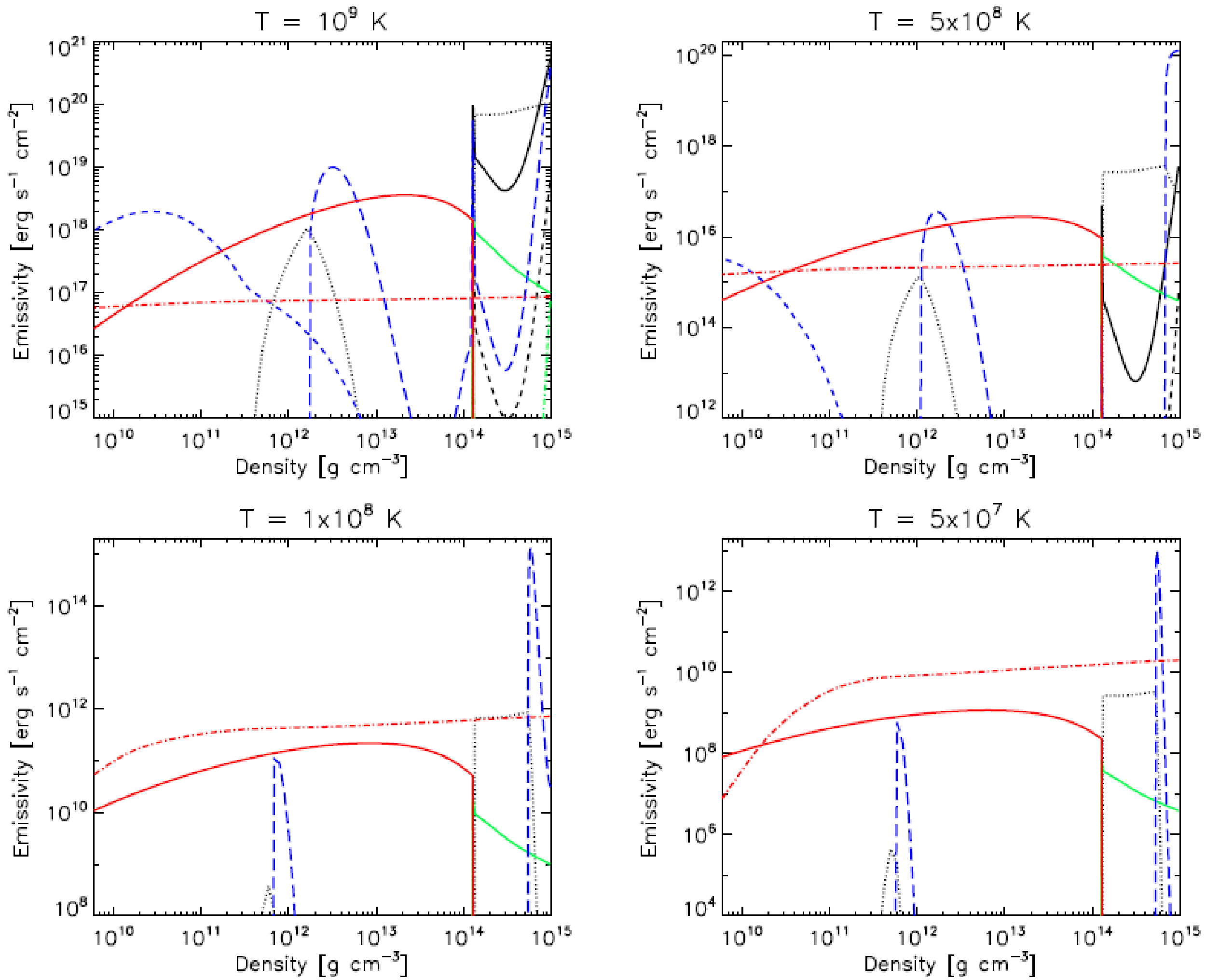

Figure 4.7: Neutrino emissivities in the crust and in the core at the four indicated temperatures, with the chosen equation of state and superfluid gaps (see text), and mass $M = 1.4\ M_\odot$ (no direct URCA). Lines denote: modified URCA (black solid line), n-n Bremsstrahlung (black dots), n-p Bremsstrahlung (black dashes), e-p Bremsstrahlung (green solid), e-A Bremsstrahlung (red solid), plasmon decay (short blue dashes), CPBF (blue long dashes), and ν-synchrotron for $B = 10^{14}$ G (red dot-dashed line).

[Viganò's PhD thesis]

Neutrino processes: magnetic fields opens a new channel

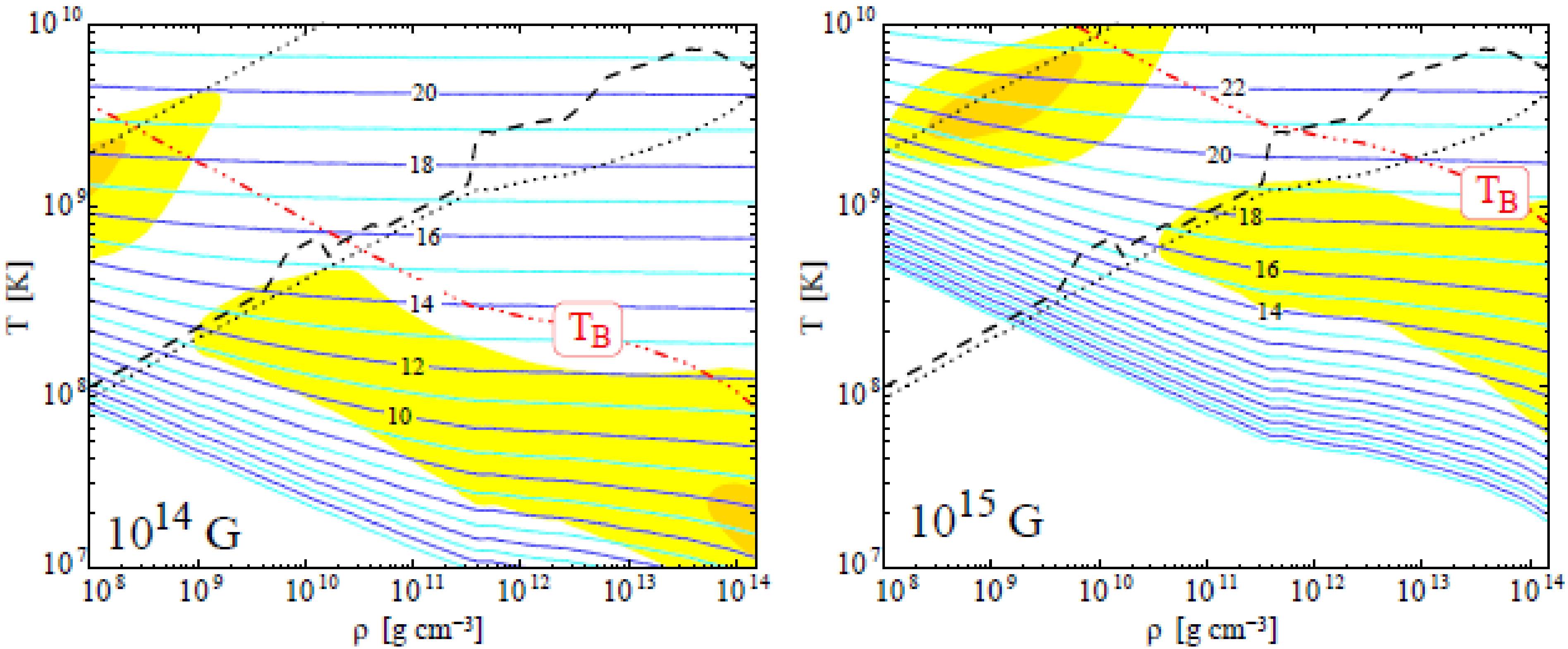

Fig. 8 Neutrino emissivity in a magnetized crust from the synchrotron processes for two, uniform, magnetic field strengths of 10^{14} G (left panel) and 10^{15} G (right panel). The contour lines are labeled by the value of $\log_{10}[Q_\nu/(\mathrm{erg\,cm^{-3}\,s^{-1}})]$. Regions where this process dominates over the ones shown in Fig. 3 are lightly shadowed (in yellow) and regions where it dominates by more than a factor of 10 are darkly shadowed (in orange). The two dotted lines show the dominance transitions between the three processes presented in Fig. 3. (Also indicated is the ion melting curve, dashed line.)

Neutrino emissivity

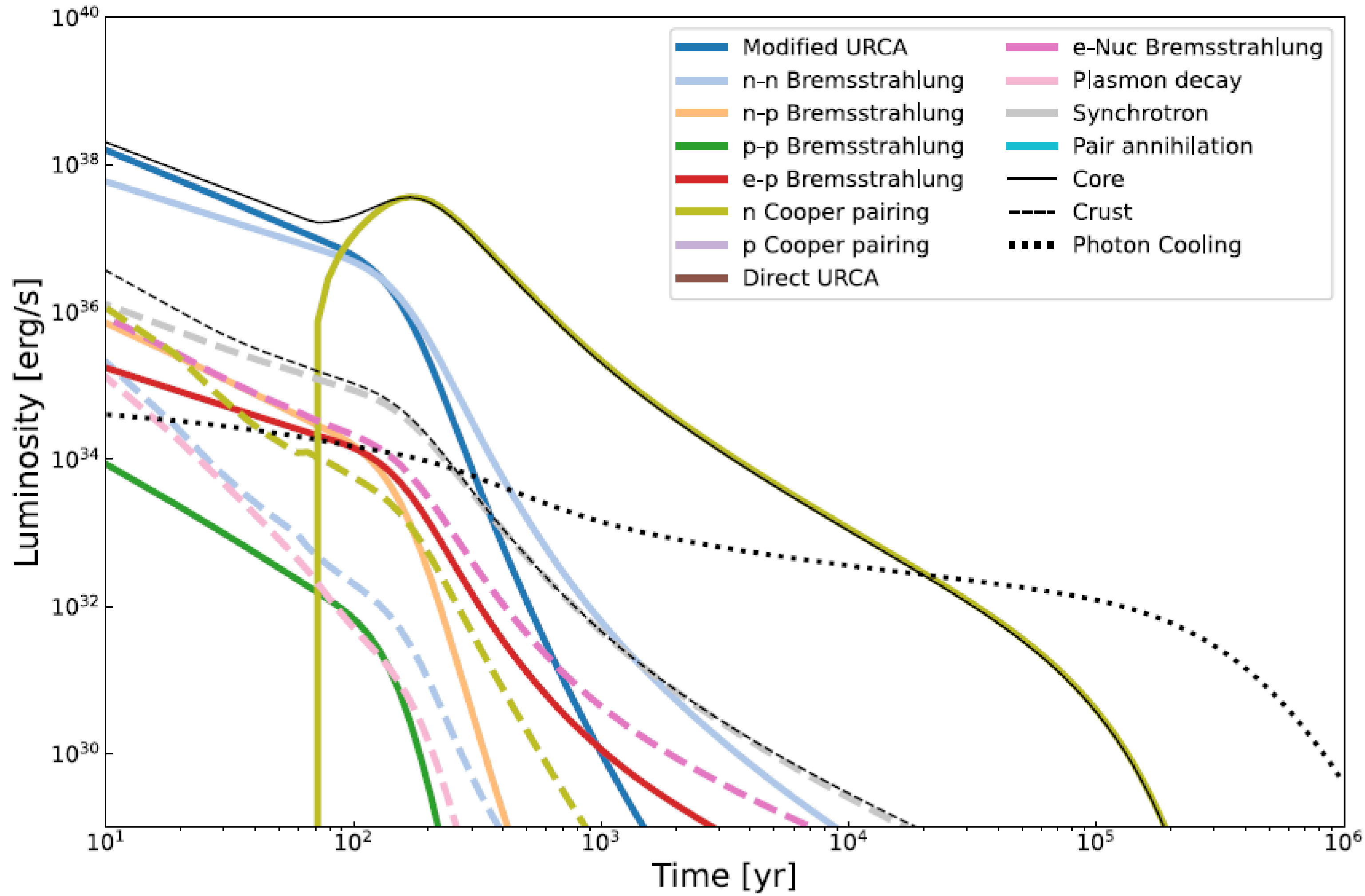

Figure 7. Evolution of neutrino and photon luminosities of all the different emission processes over the NS history for the simulation *Sly4-M1.6-B14-L1*. This run, which uses the SLy4 EOS, is characterized by a mass of $M = 1.6\,\mathrm{M}_\odot$ and a dipolar poloidal magnetic field with a crust-averaged value of $B_{\rm avg} = 6 \times 10^{14}$ G. The chosen resolution is $N_a = 25$, $N_r = 30$. Solid-coloured lines represent different neutrino emission processes occurring in the core. Dashed lines represent different neutrino emission processes occurring in the crust. The same process (marked with a given colour) may involve both the core and the crust. Black lines represent the total neutrino luminosity for processes involving the core (continuous line) and the crust (dashed line), respectively. The black-dots report the surface photon luminosity. It is worth noticing that while the legend includes all the possible neutrino processes included in the simulation, some of them are not effectively active in this particular simulation, as such, they do not appear in the figure. Moreover, in case magnetic fields are present in the core, additional processes can become relevant (Kantor & Gusakov 2021).

[Ascenzi+ 2024]

Specific heat

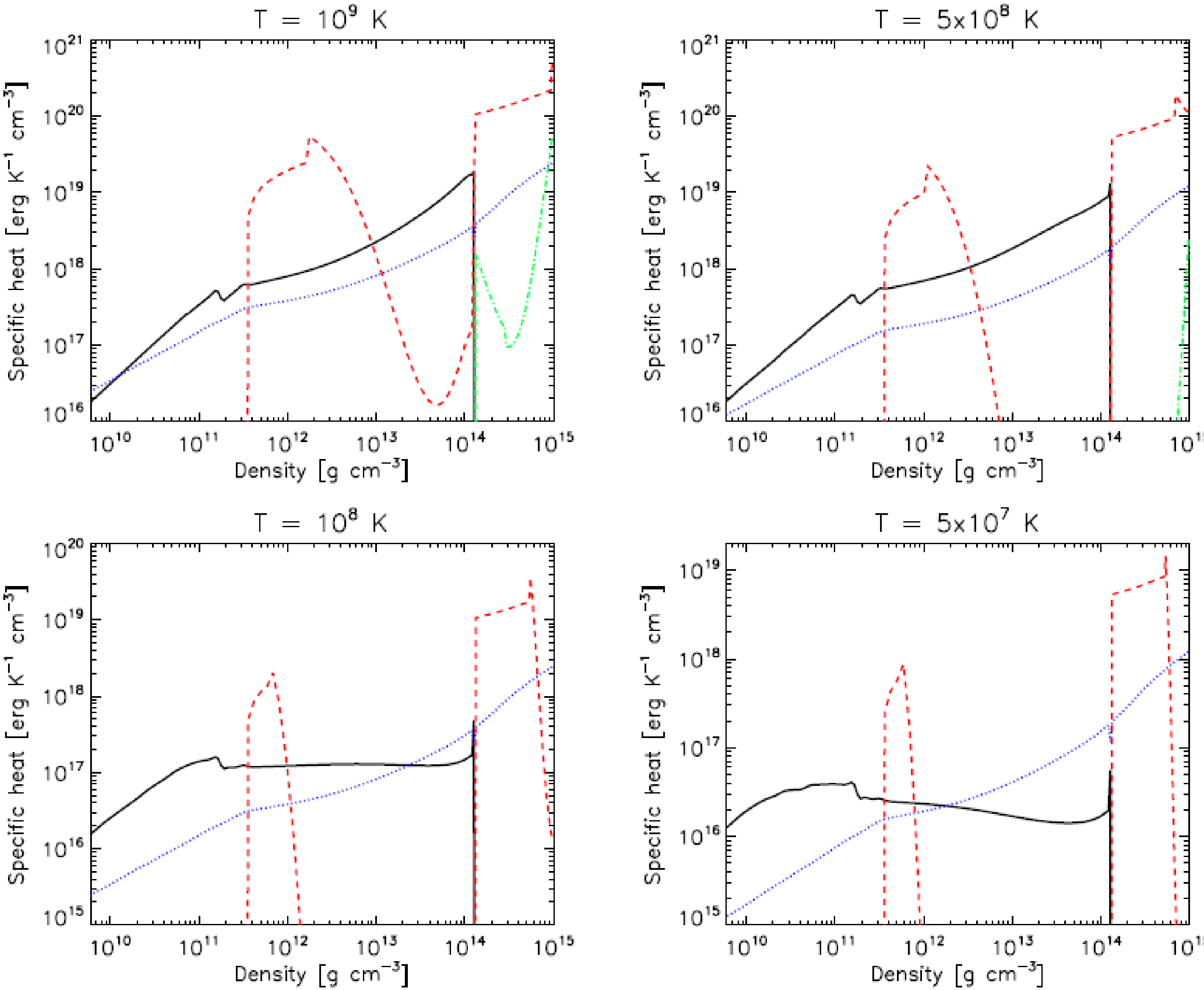

[Viganò's PhD thesis]

Figure 4.4: Contribution to the specific heat as a function of density for different temperatures: neutrons (red dashes), protons (green dot-dashed), electrons (blue dots), and ions (black solid line).

Specific heat

$c_v = \frac{dE}{dT}$

(= how much energy dE is needed to lose to cool the material by a certain dT)

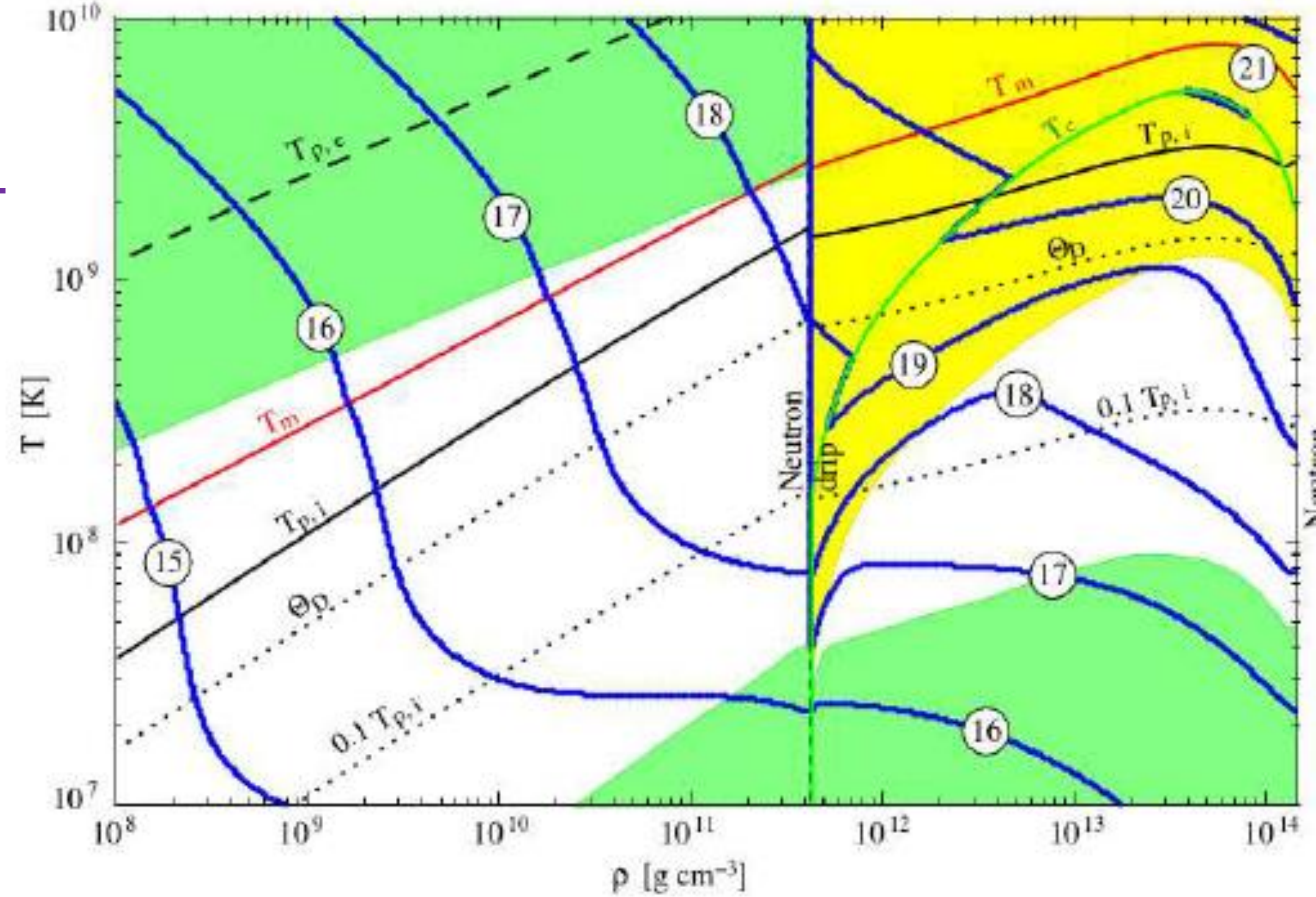

Fig. 2 Iso-contour lines of c_V in the crust, labeled by the value of $\log_{10}(c_V/\mathrm{erg\,cm^{-3}\,K^{-1}})$. Also shown are the melting curve T_m and the critical temperature for neutron $^1S_0$ superfluidity, T_c, the electron and ion plasma temperatures, $T_{p,e}$ and T_p respectively, the Debye temperature, $\Theta_D \simeq 0.45 T_p$, that marks the transition from classical to quantum solid and $0.1 T_p$ below which the wholly quantum crystal regime is realized. The outer crust chemical composition is from Haensel and Pichon (1994) and inner crust from Negele and Vautherin (1973) with the neutron drip point at $\rho_{drip} = 4.3 \times 10^{11}$ g cm $^{-3}$. The electron contribution dominates in the two dark-shadowed (green) regions at high T and ρ below ρ_{drip} and at low T and high ρ, while neutrons dominate in the light-shadowed (yellow) region at high T and ρ above ρ_{drip},

QUESTION

What is the role of heat capacity in cooling?

Using common sense, what has a higher specific heat capacity: the sea or the soil (land)?

1D COOLING (NON-MAGNETIZED) MODELS

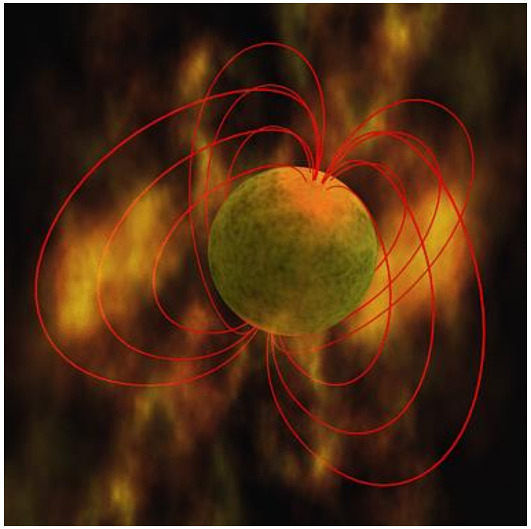

Cooling models

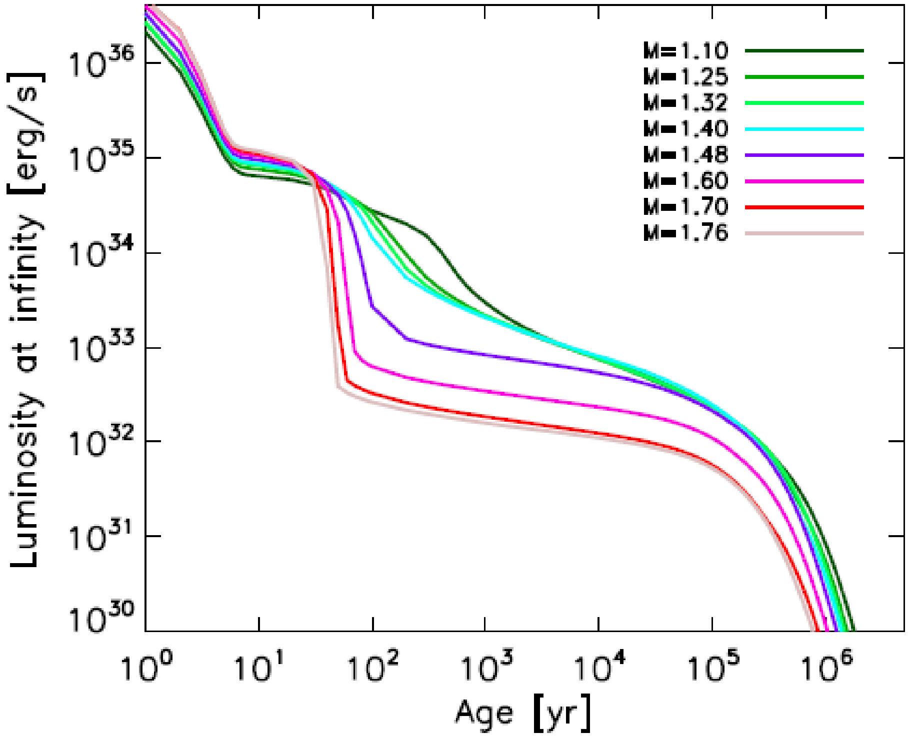

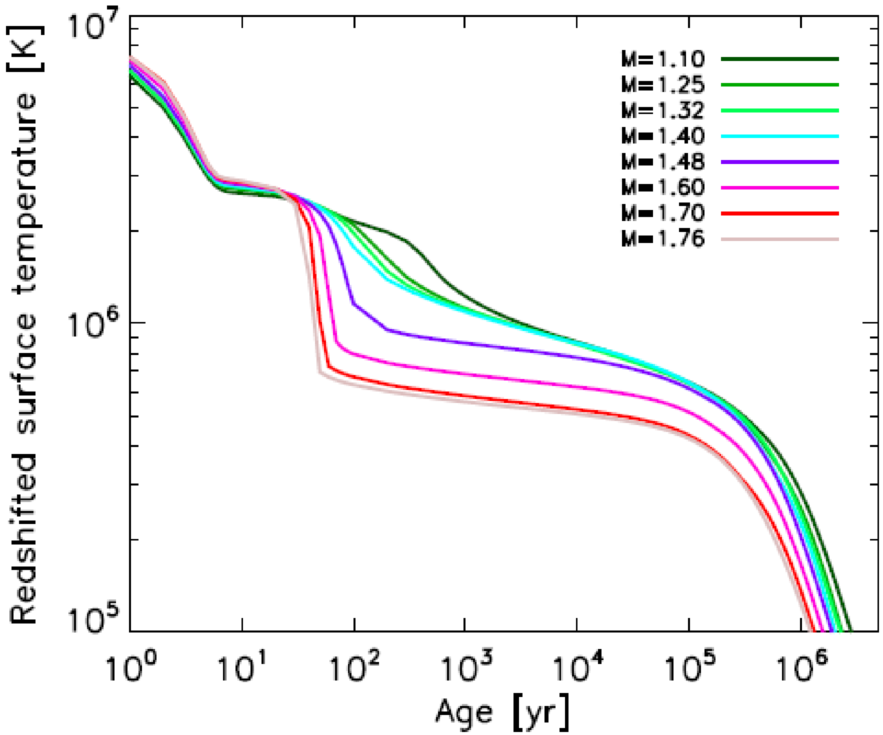

One has two options:

1. look at the theoretical luminosity (more robust) and deal with observational unabsorbed flux and distance

2. look at the effective temperature, by spectral fitting of data assuming an emission mechanism (quite uncertain due to the unknown features of NS surfaces: black body, atmospheric modelling, condensed surfaces…)

In both case, there is an unavoidable systematic uncertainty making hard the comparison between data and models.

Cooling models: infant NS stage

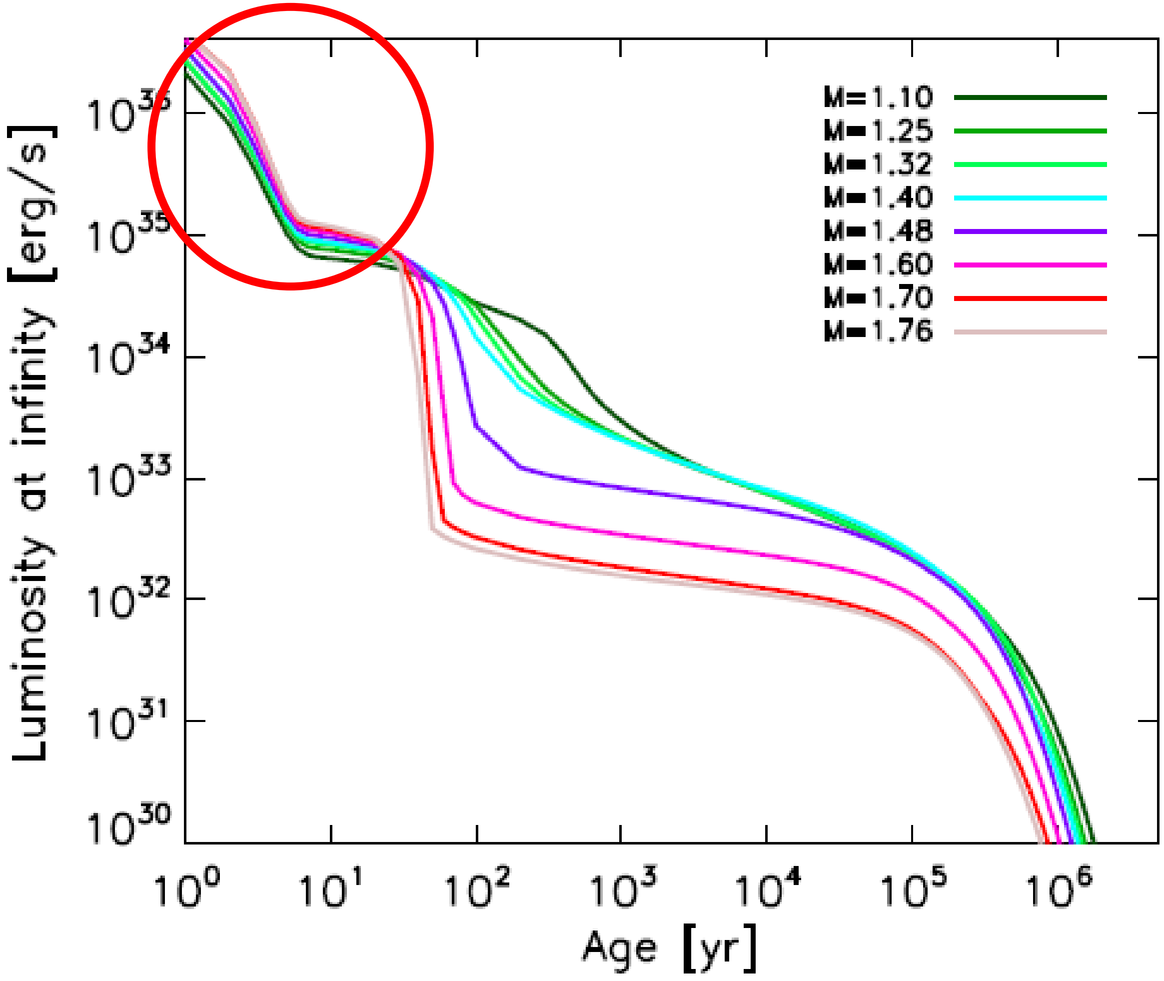

Initial temperature: $10^{10} - 10^{11}$ K
Quickly drops to 10^{35} erg/s
Neutrinos can escape freely and their production is so efficient, that even higher temperature at birth would be forgotten soon after months or years.

Cooling models: fast cooling 1

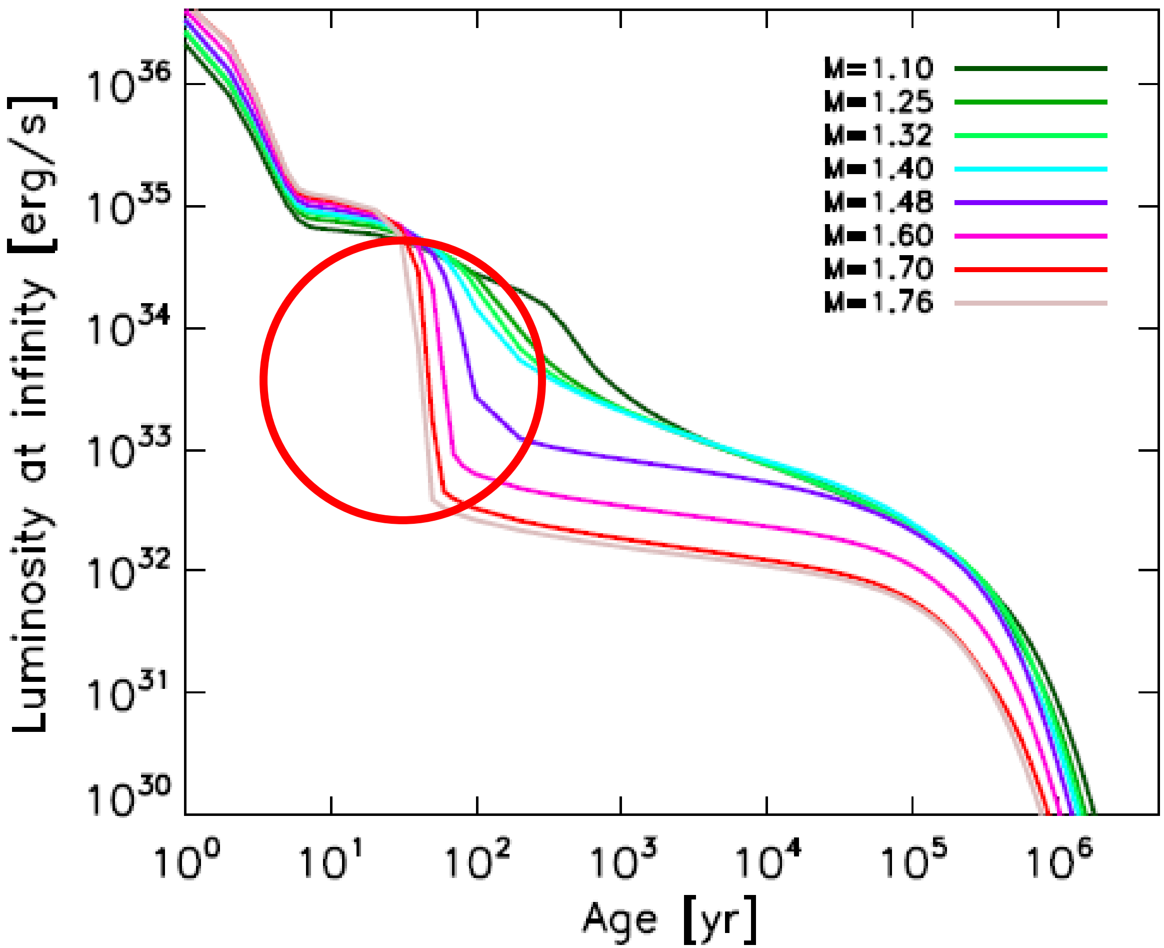

If the star is massive enough, for some equations of state, some additional processes of neutrino production, called Direct URCA, are activated at its centre, leading to an even faster cooling in the first century.

Cooling models: fast cooling 2

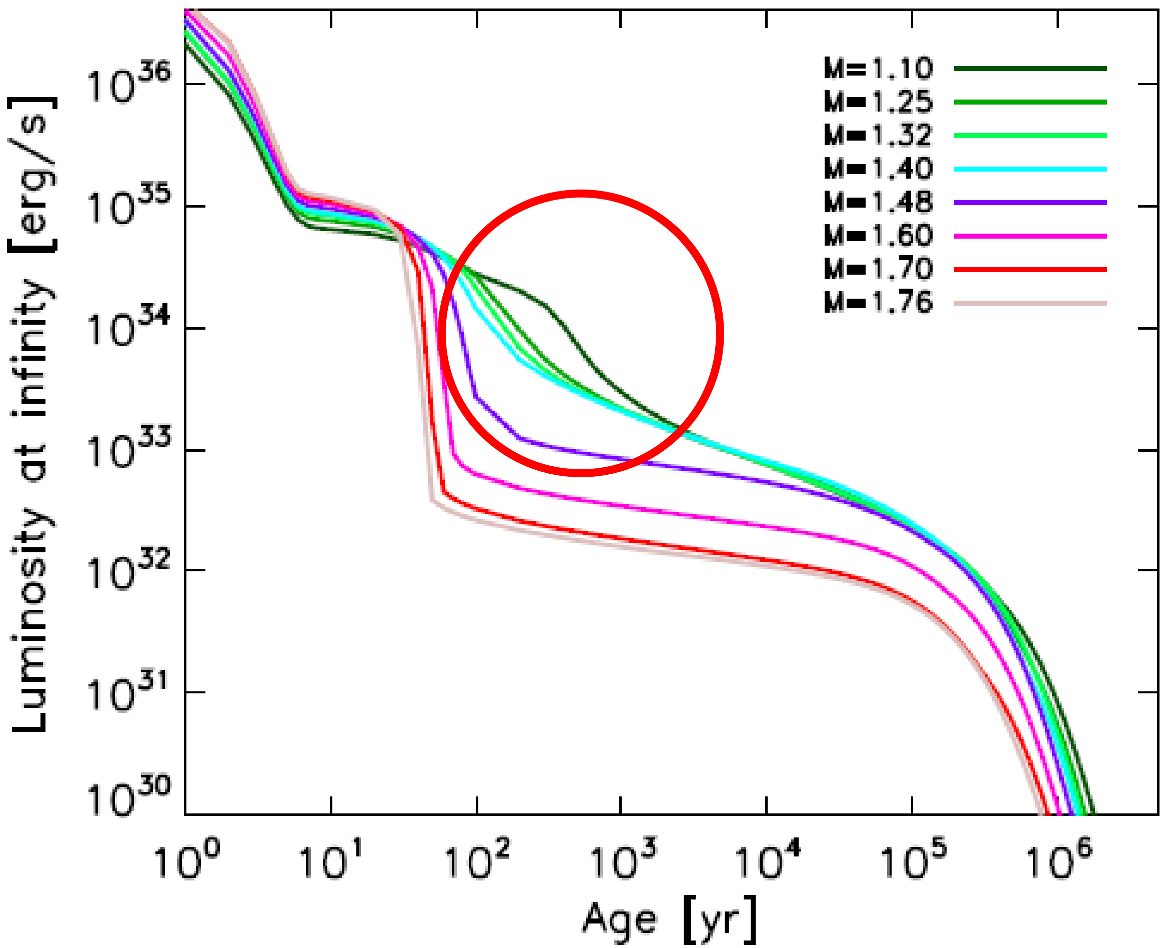

Currently controversial if the fast cooling can be actually measured as significant variation of T inferred from data over a few decades. The case of the NS in Cas A: measured T variation of a few % per decade, disputed due to possible instrumental degradation and calibration uncertainties.

Superfluid transition: it provokes the suppression of the heat capacity, so that for the same extraction of energy by neutrinos, the drop in temperature is larger.

At the same time, neutrino production changes: a new channel is opened, by the formation and breaking of Cooper pair, while other channels are suppressed.

Cooling models: freezing of the crust

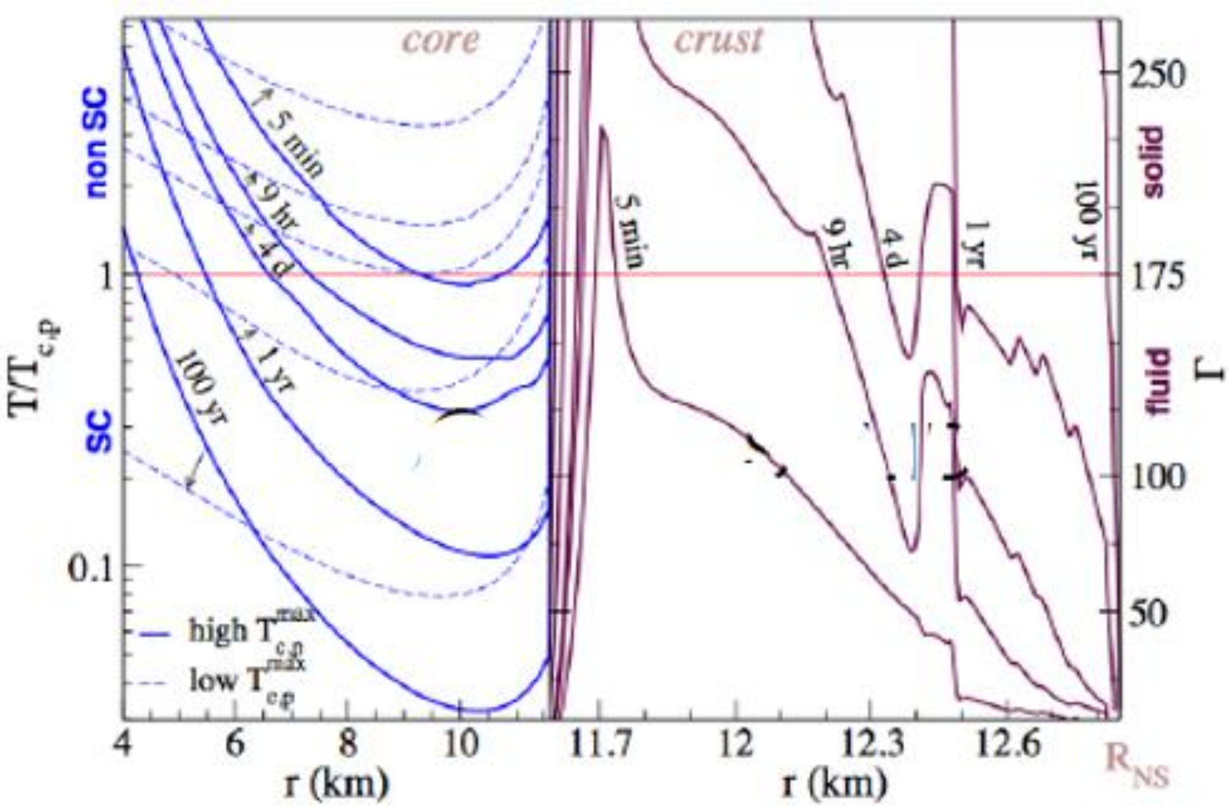

[Aguilera et al. 2008]

Crust freezes, starting from innermost layers after hours/days/weeks

The neutrons in the crust and in the core, and the protons in the core undergo superfluid/superconducting transition.

$$\Gamma_{coul} \equiv \frac{(Ze)^2}{kTa_i} \approx 4.77\,\frac{Z^2}{T_8}\left(\frac{\rho_{10}}{A}\right)^{1/3}\;, \tag{4.10}$$

where T_8 is the temperature in units of 10^8 K, and a_i has been defined in eq. (4.5). When $\Gamma_{coul} < 1$, the ions form a Boltzmann gas, when $1 \leq \Gamma_{coul} < \Gamma_m$ their state is a coupled Coulomb liquid, and when $\Gamma_{coul} > \Gamma_m$ the liquid freezes into a Coulomb lattice. For a

Cooling model: thermal relaxation of the crust

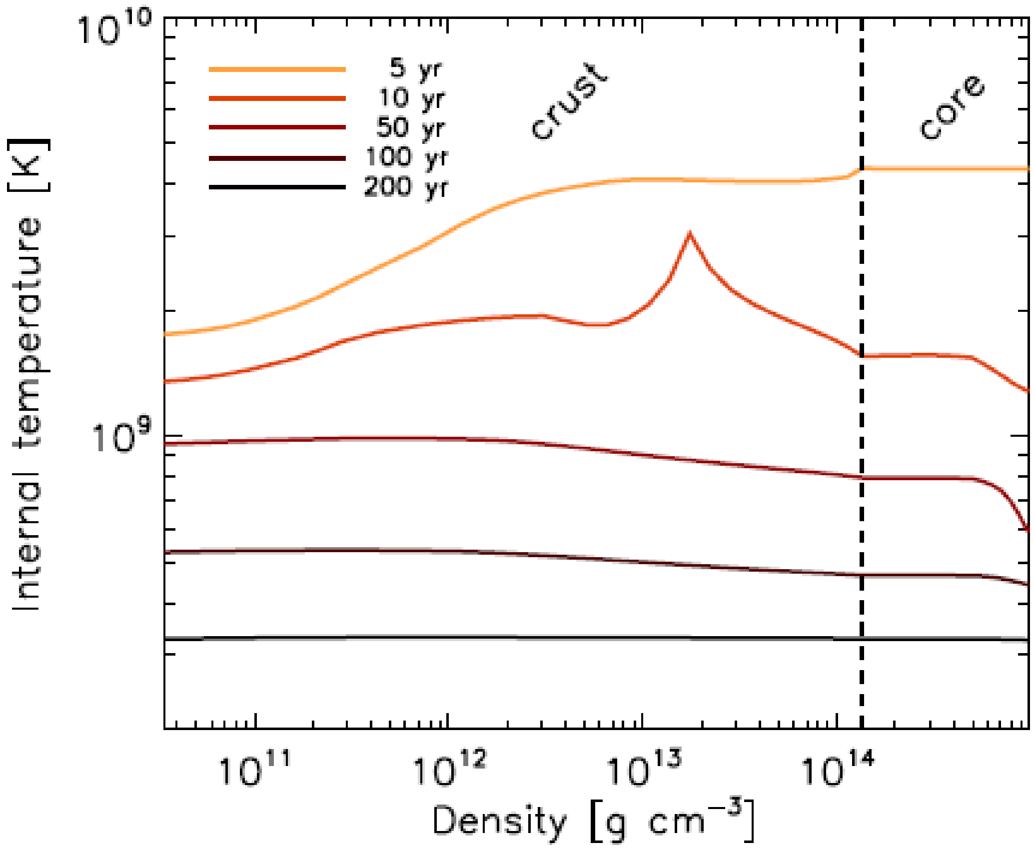

Figure 5.1: Evolution of internal temperature in the early stages ($t = 5, 10, 50, 100$ and 200 yr), starting with $T_{init} = 10^{10}$ K, for a non-magnetized neutron star with $M = 1.4\ M_{\odot}$.

All these early (< 100 years) are hardly comparable with observation, since the Galactic Supernova rate is probably 1-2 per century.

It's more important to look at longer timescales

Cooling models: neutrino vs photon cooling stages

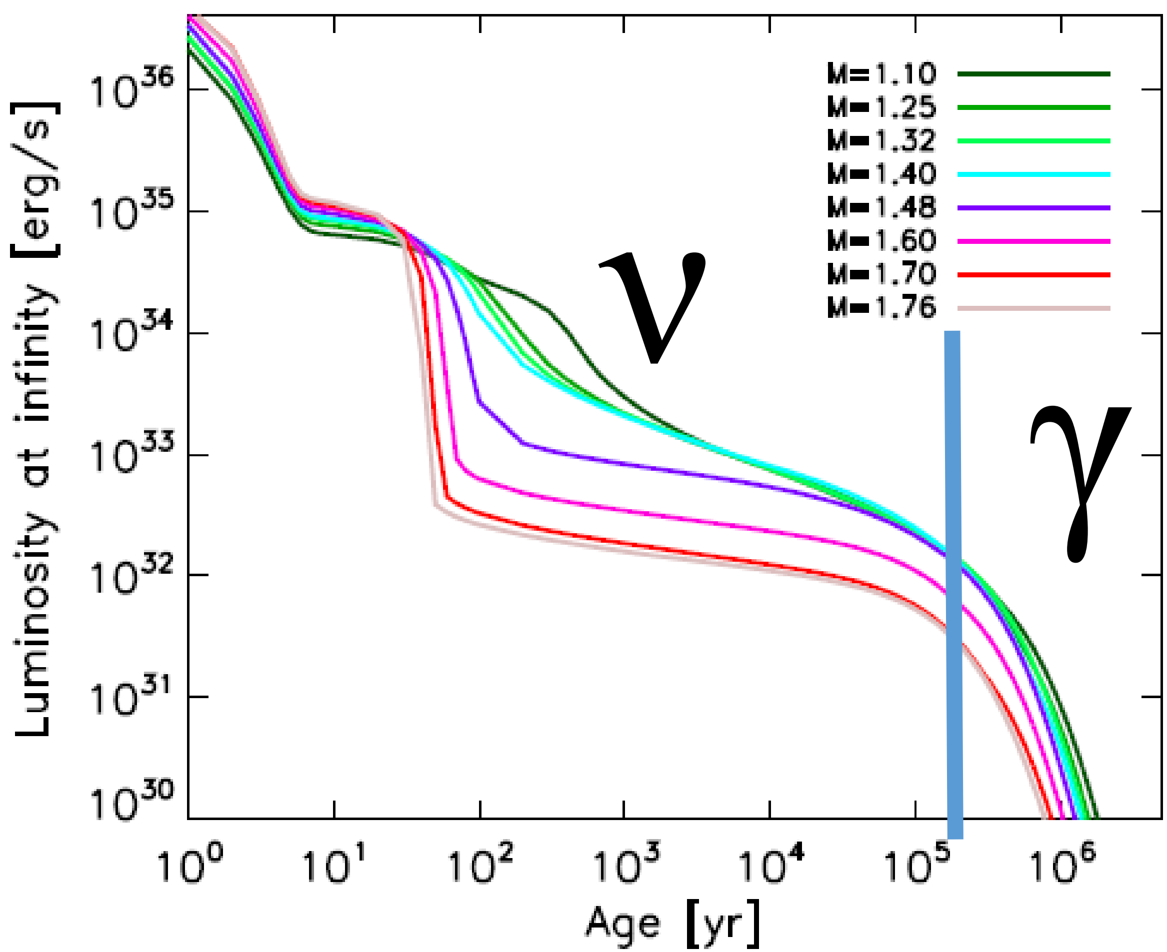

Neutrino cooling dominates during the first 10-100 kyr: the star cools from inside.

Photon cooling dominates when the star is cold enough, so that neutrino production is much less efficient, and heat is mostly transferred to the surface and radiated.

QUESTION

How a hot cup of tea, your body and a young Neutron Star differ in the fundamental cooling mechanism?

X-ray luminosity & Cooling

This marks the first direct measurement of enhanced cooling. Magneto-thermal simulation and machine learning techniques were used to understand this finding.

A suitable EoS should elucidate both exceptionally bright objects like magnetars (Joule heating) and extremely faint objects at young ages.

Taking into account a simplified meta-modeling approach (Margueron et al., 2018), the excluded range is estimated to encompass approximately 75% of the proposed nuclear EoSs.

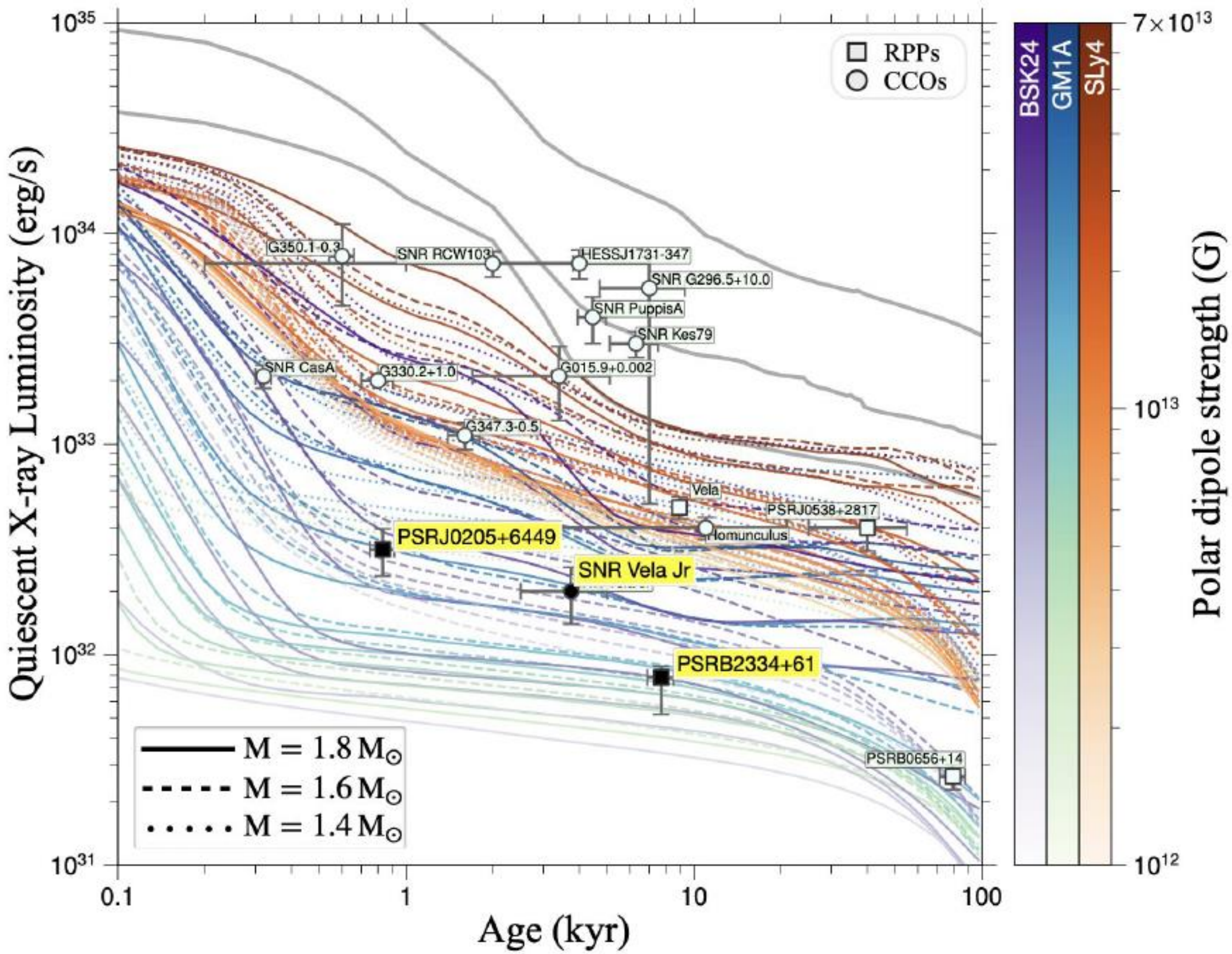

[Anzuini, Melatos, Dehman et al. 2021, MNRAS]
[Anzuini, Melatos, Dehman et al. 2022, MNRAS]

GM1A — with hyperons in the core

[Marino, Dehman, Kovlakas, Rea et al. 2024, Nature Astronomy]

MATINS
MAgneto-Thermal evolution of Isolated Neutron Stars

X-ray luminosity & Cooling

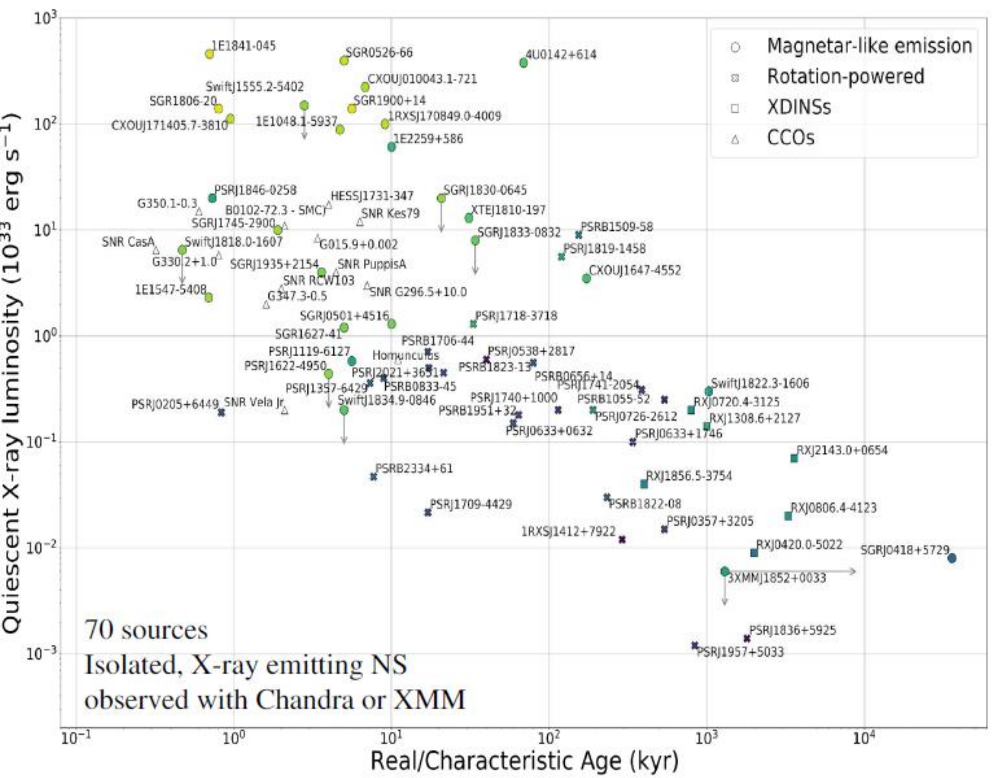

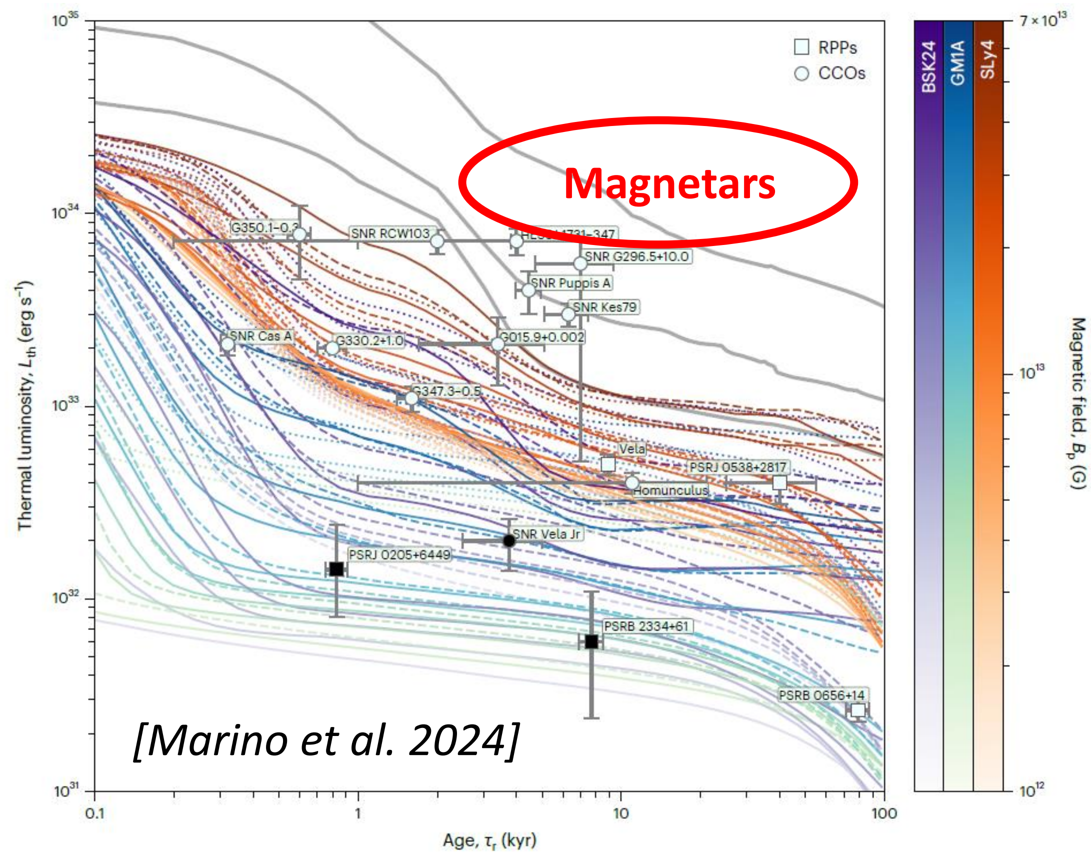

Isolated neutron stars are X-ray bright at the beginning, visible as thermal emitters.

Explore different masses, equations of state, superfluid gap models, without magnetic fields. This can explain only some ordinary pulsars and other young isolated neutron stars (CCO), not magnetars. It can give hints for fast coolers.

MAGNETO-THERMAL MODELS

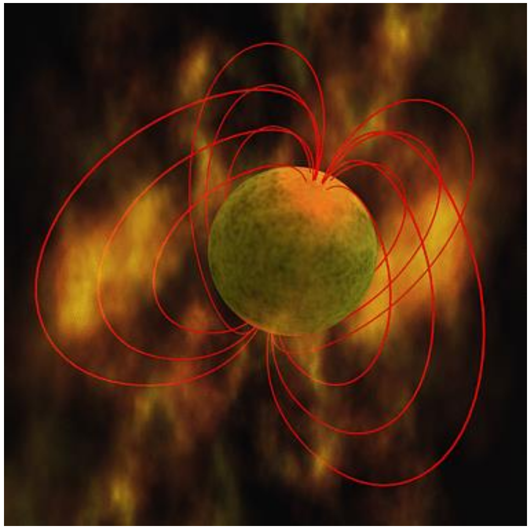

Impact of magnetic fields on cooling

Energy balance equation *[Aguilera+ 2008, Pons+ 2009]*

$$c_v \frac{\partial T}{\partial t} + \vec{\nabla} \cdot (-\hat{\kappa} \cdot \vec{\nabla} T) = -Q_\nu + Q_j$$

Ingredients:

- Neutron star model (structure, EOS)
- Specific heat $c_v(T, \rho)$: main contribution by neutrons
- Thermal and electrical conductivities: $\hat{\kappa}(T, \rho)$. Very large in the core: important timescales given by the electron relaxation time in the crust.
- Neutrino emissivities $Q_\nu(T, \rho)$
- Boundary condition: envelope model (i.e., liquid outermost ~ 100 m, with strong gradient of temperature), linking internal T_b to surface T_s; emission model (atmosphere, BB...)

Temperature-MF interplay:

1. Joule dissipation (source of heat $Q_j = J^2/\sigma$)
2. anisotropic thermal conductivity $\hat{\kappa}$
3. envelope model $T_s(T_b, \vec{B})$ incl. all these effects
4. neutrino synchrotron process
5. quantizing effects (unimportant in the crust)

How to sustain a magnetic field?

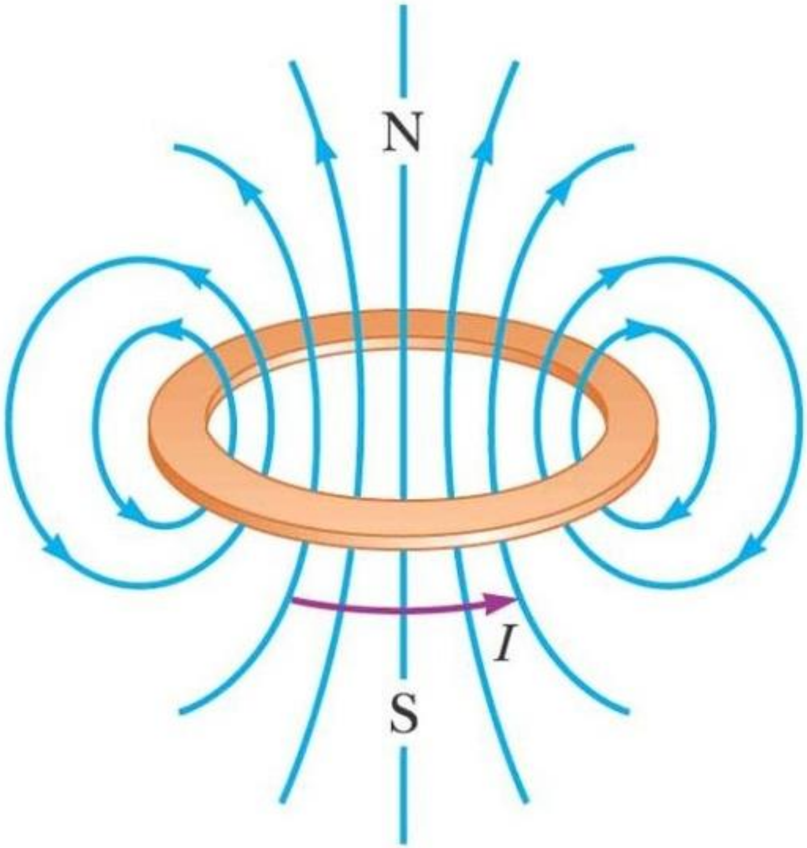

Recipe:

1. An electrically conducting fluid
2. Currents circulating due to the motion of the carriers: differential rotation, convection, MHD velocity…
3. The timescales of survival of the field will depend on how long the motion (energy input) can be sustained and/or on the decay timescale of the magnetic field

Molten iron alloys in the outer core (Earth, Mercury)
Metallic hydrogen in the deep layers of gas giants (Jupiter, Saturn)
Salty oceans (Uranus, Neptune)
Ionized atmosphere/plasma (hot Jupiters, Sun, neutron star’s core)
Free electrons (white dwarfs, neutron stars’ crust)

Magneto-hydro dynamics

Maxwell's Equations of the Electromagnetic Field Theory

$$\nabla \cdot \mathbf{E} = \frac{\rho}{\varepsilon_0}$$

Gauss's Law – ***charge*** makes an ***electric field***

$$\nabla \cdot \mathbf{B} = 0$$

The magnetic field is solenoidal (no monopole sources).

$$\nabla \times \mathbf{E} = -\frac{\partial \mathbf{B}}{\partial t}$$

Faraday's Law of electromagnetic induction -- **E** curls around a changing **B**.

$$\nabla \times \mathbf{B} = \mu_0 \mathbf{J} + \cancel{\mu_0 \varepsilon_0 \frac{\partial \mathbf{E}}{\partial t}}$$

Ampère's Law – ***current*** makes a ***magnetic field***

Maxwell's "Displacement Current"

8/5/08 Lecture 2 Part 2 1

MHD = Hydrodynamic + Maxwell equations for conducting fluids.

The basic MHD approximation is to neglect the displacement current (dE/dt) in the Maxwell equations, because any readjustment of the electric field happens on timescales much shorter than the evolutionary timescales of interest.

Therefore, there is a direct relation between B and J.

Magneto-hydro dynamics: a complex game

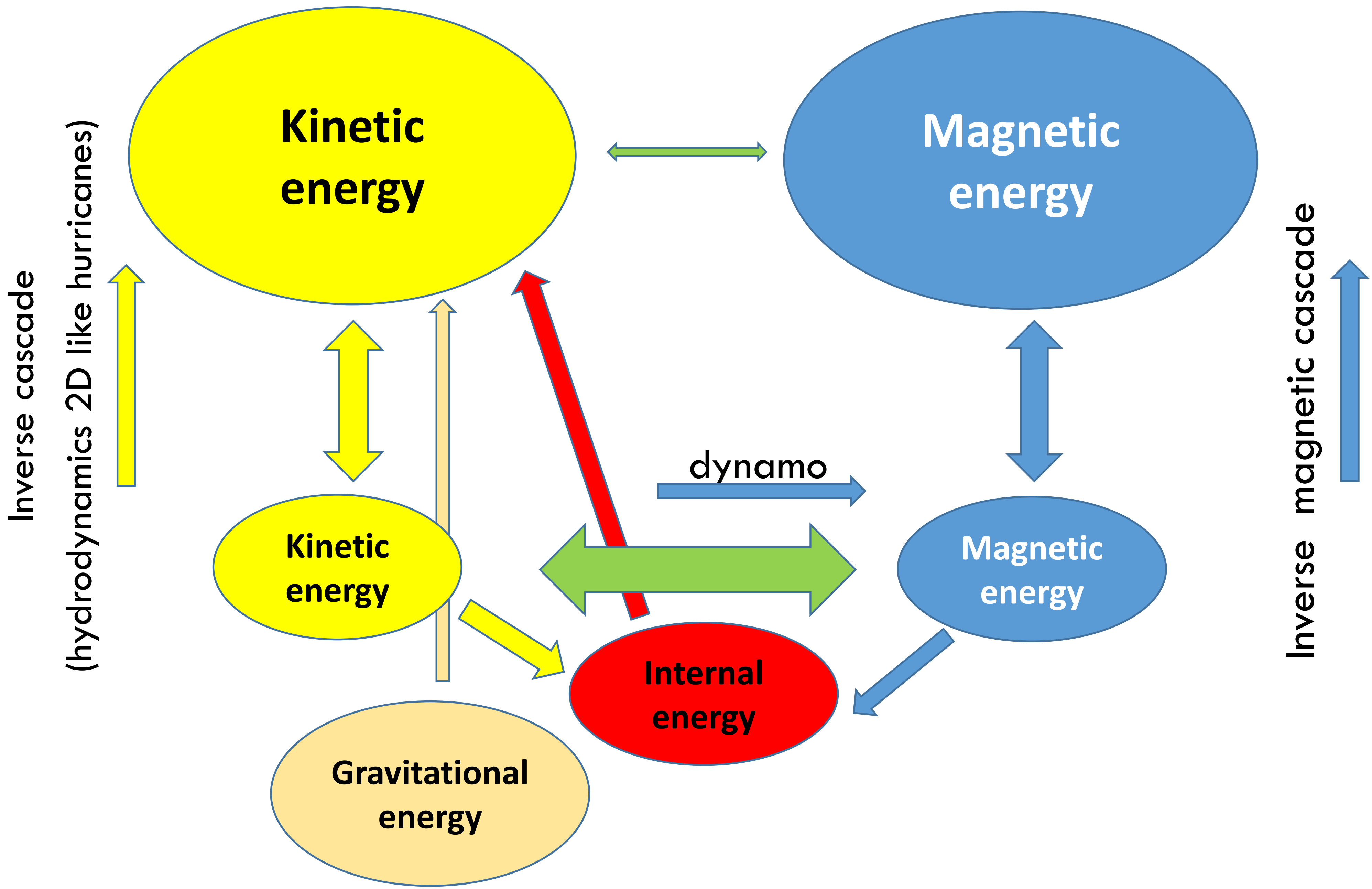

Ideal MHD

You need to assume a Ohm's law to relate electric field and currents.

Ideal MHD: it applies to perfect conductors, within which charges (electrons in metals) are free to move, so they immediately reorganize to produce an electric field and make sure that the total electromagnetic force on them is zero:

$$\nabla \times \vec{B} = \mu_0 \vec{J}$$

$$\mathbf{E} + \mathbf{v} \times \mathbf{B} = 0.$$

$$\partial \vec{B} / \partial t = -\nabla \times \vec{E}$$

Magnetic field lines are advected by the fluid motions. This is responsible for magnetic flux conservation.

See Alfvén's theorem, or the frozen-in flux theorem.

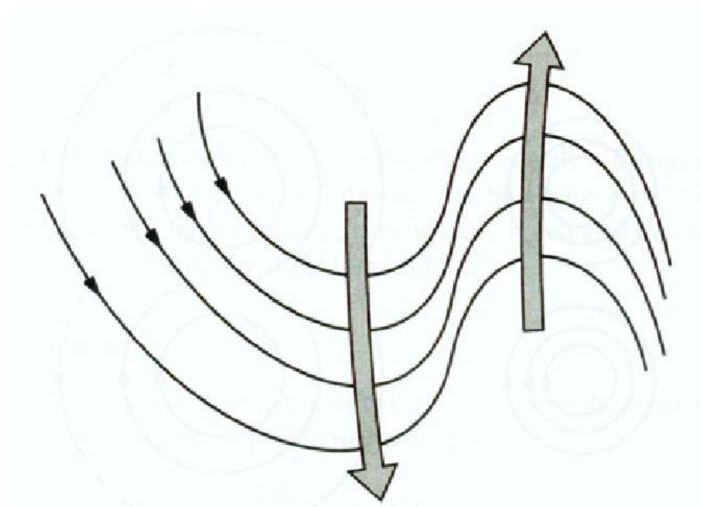

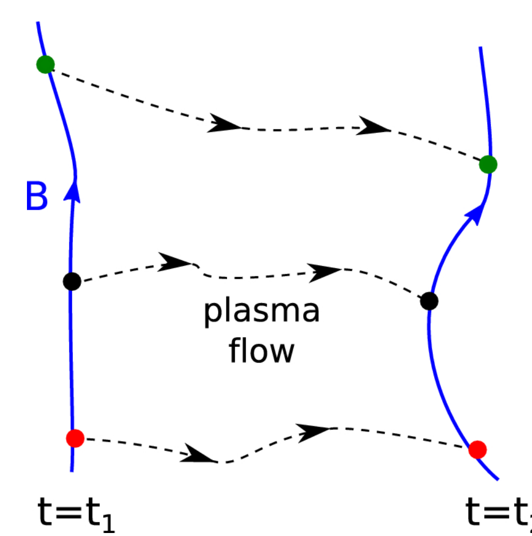

Resistive MHD

$$\partial \vec{B} / \partial t = -\nabla \times \vec{E}$$

$$\vec{E} + \vec{V} \times \vec{B} = \eta \vec{J} \qquad \eta = \frac{1}{\mu_0 \sigma}$$

$$\nabla \times \vec{B} = \mu_0 \vec{J}$$

η is the magnetic diffusivity, inversely proportional to the electrical conductivity, σ, and tries to simplify the field configuration, by dissipating currents Ohmically.

The more tangled the field, the stronger the dissipation

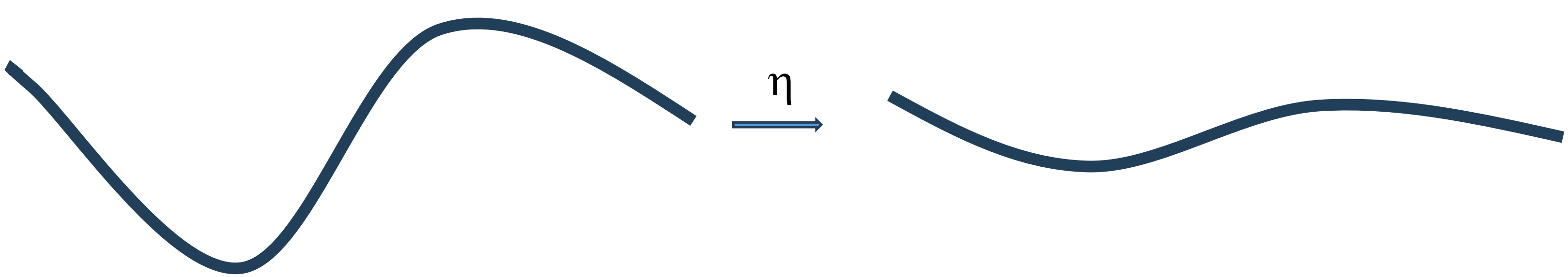

Non-linear MHD: adding Hall drift and ambipolar diffusion

$$\partial \vec{B} / \partial t = -\nabla \times \vec{E}$$

$$\mathbf{E} = -\mathbf{v} \times \mathbf{B} + \frac{\mathbf{J}}{\sigma} + \frac{\mathbf{J} \times \mathbf{B}}{e n_{\mathrm{e}}} - \frac{(\mathbf{J} \times \mathbf{B}) \times \mathbf{B}}{\nu_{\mathrm{in}} \rho_i}$$

e is the elementary charge, n_e the number density of electrons, ρ_i the mass density of ions, ν_{in} the collision rate between ions and neutrals

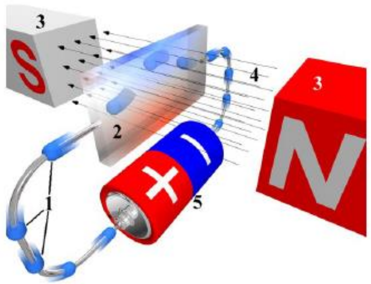

Hall term (Hall drift) arises from the Lorentz force. It distorts the field by diverting the current pattern, usually leading to smaller scale field (field more tangles and twisted).
The process is quadratic with B.

Non-linear MHD: adding Hall drift and ambipolar diffusion

$$\partial\vec{B} / \partial t = -\nabla \times \vec{E}$$

$$\mathbf{E} = -\mathbf{v} \times \mathbf{B} + \frac{\mathbf{J}}{\sigma} + \frac{\mathbf{J} \times \mathbf{B}}{en_e} - \frac{(\mathbf{J} \times \mathbf{B}) \times \mathbf{B}}{\nu_{in}\rho_i}$$

e is the elementary charge, n_e the number density of electrons, ρ_i the mass density of ions, v_{in} the collision rate between ions and neutrals

Ambipolar diffusion arises in partially ionized plasma where neutrals and two different carriers of currents are present (usually electrons and protons/ions, e.g. in the Solar corona or in the interstellar medium). In the absence of neutrals, electrons and ions are perfectly coupled due to the Coulomb interaction: they move together and one can consider a single component. If neutral are present, they collide much more with ions than electrons, and this slows down the charged component.

It's highly non linear with the magnetic field (B^3).

Magnetism in the Universe

Magnetism in the Universe:

- within galaxies or clusters: 0.1-10 μG
- planetary nebulae: 0.1-1 mG
- planets: 0 – 10 G
- brown dwarfs: up to 10^3 G
- main sequence stars: 1 - 10^3 G
- white dwarfs: 10^3 – 10^8 G
- **neutron stars**: 10^8 – 10^{15} G

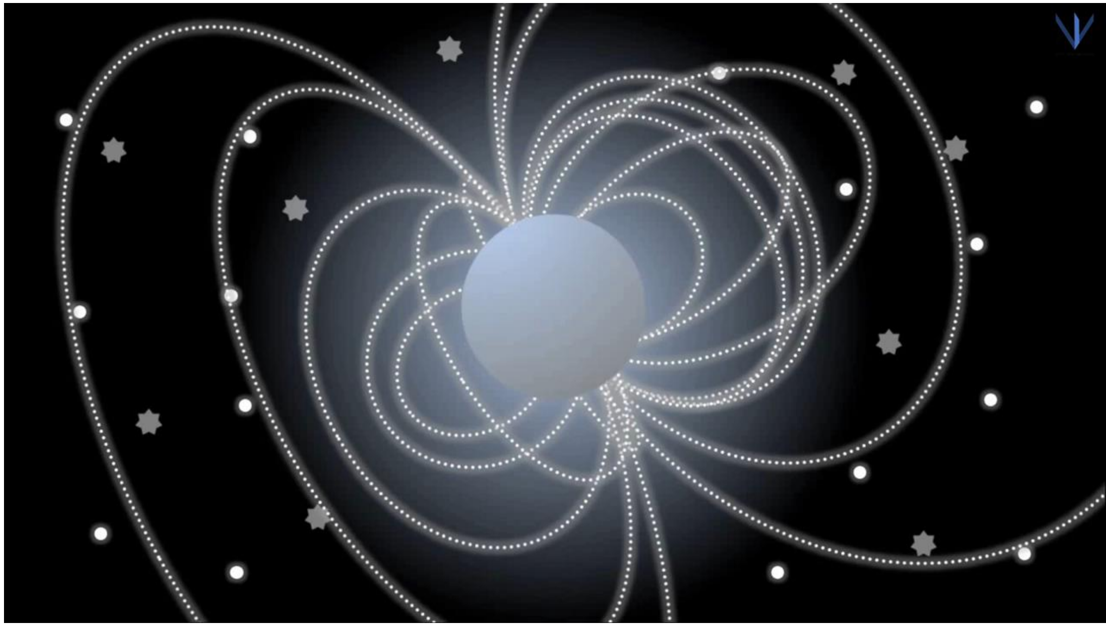

Differences:

- Physical conditions and composition
- Convection in stars, brown dwarfs
- Dynamo not active in WD(?) & NS

Magnetic field estimation

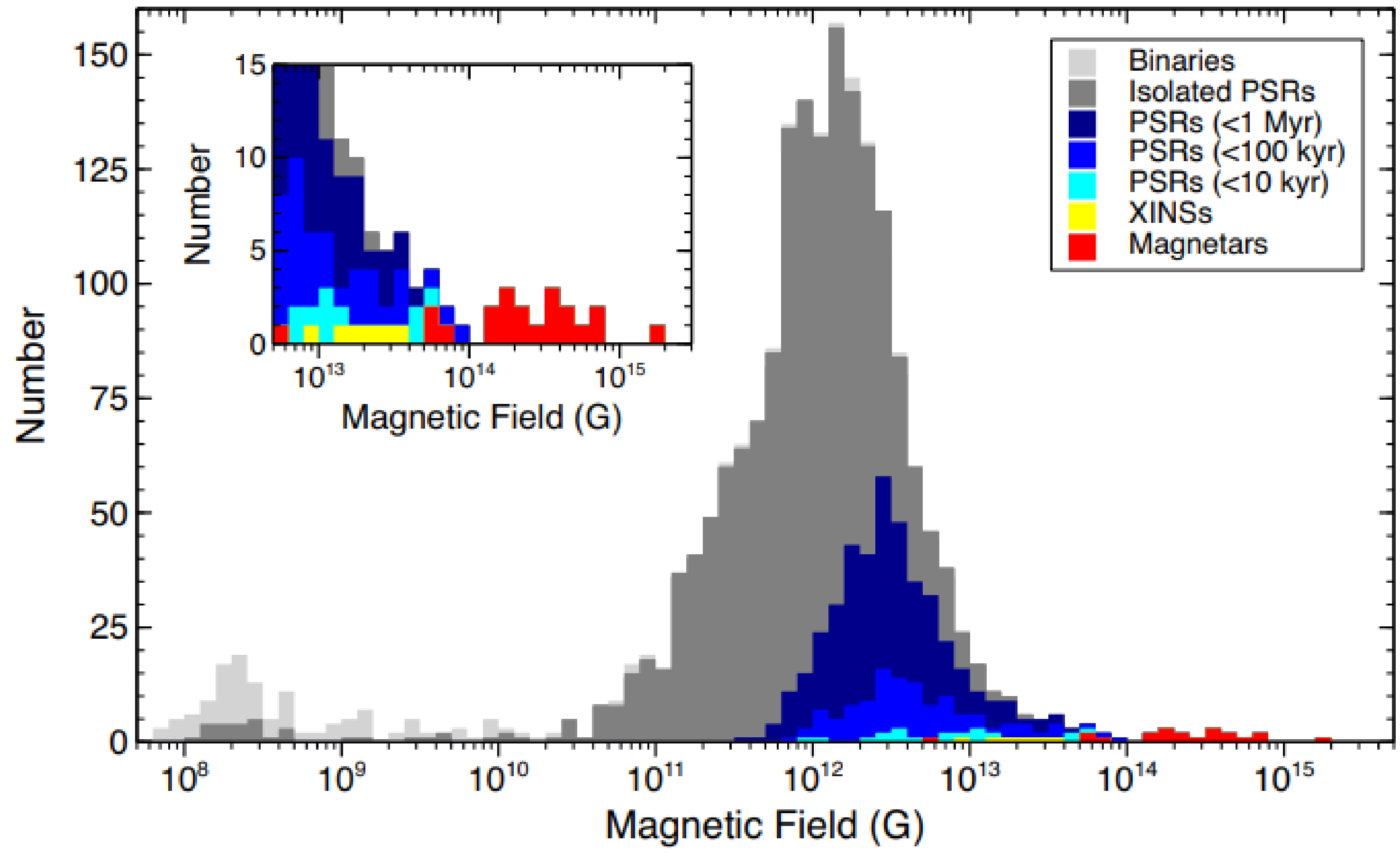

[Olausen & Kaspi 2014]

Magnetic fields mapping in neutron stars

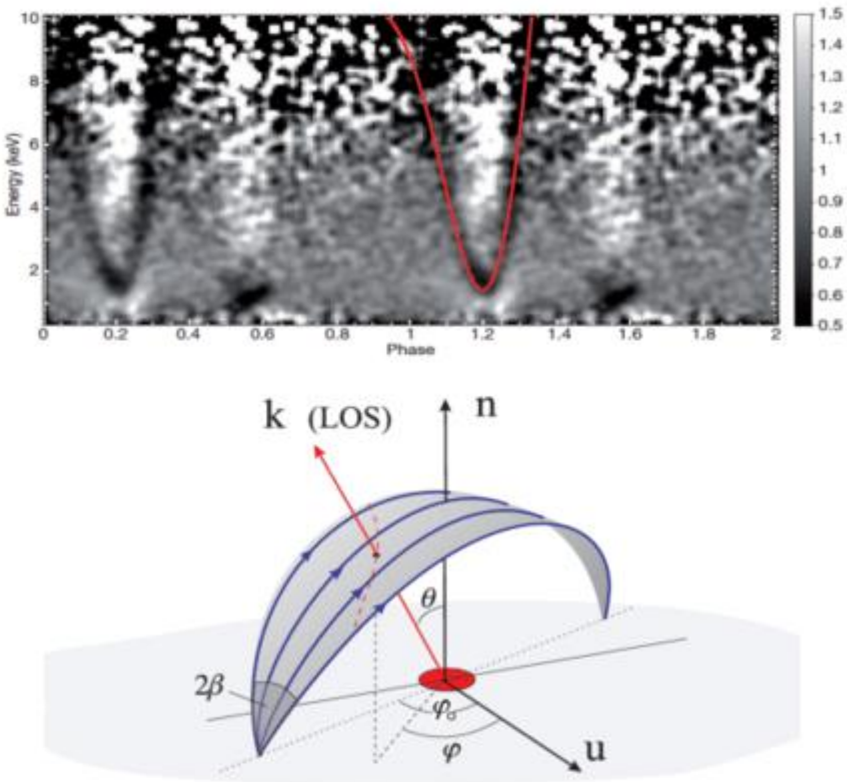

[Tiengo+ 2013]

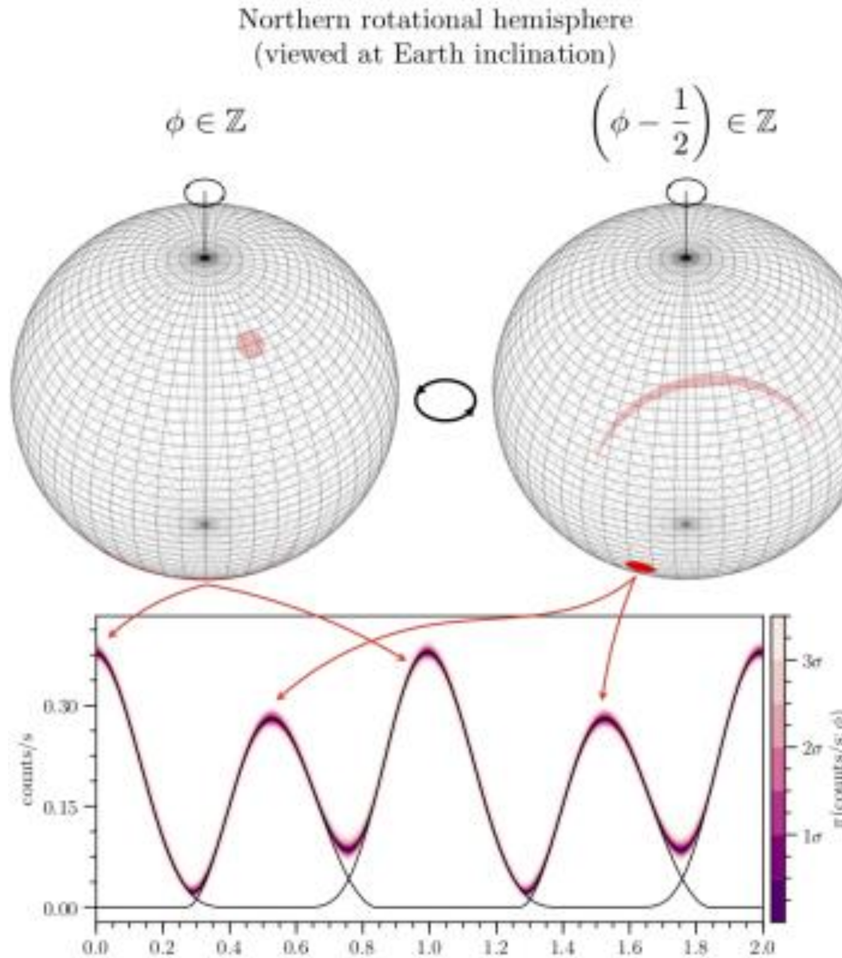

[Riley+ 2019]

Hints for non-dipolarity in several neutron stars inferred from X-rays:
- absorption lines indicating coronal structures
- light curves indicating non-antipodal surface temperature distribution

Energy sources of neutron star radiation

From a macroscopic point of view, the detected radiation from neutron stars can come from the loss/dissipation of:

1. Rotational energy to kinetic energy of magnetospheric plasma, which acquire energy and radiate part of it from radio to gamma rays
2. Residual heat: X-rays from the hot surface (10^5-10^6 K)
3. Magnetic fields
4. Accretion in binary systems
5. Collision (binary neutron star mergers)

Observables:

Timing properties: spin period (very accurately) and its derivative (accurate in many cases), light curve profiles.

Spectral properties: how energy is emitted through different wavelengths, in quiescence and in transient phenomena (bursts, outbursts, flares…).

Magnetic fields at NS birth

Two options to explain the huge magnetic fields

Fossil fields: giant star fields are compressed and amplified by the collapse. Since in ideal MHD the magnetic flux across a moving surface is conserved, shrinking a magnetized conductor leads to amplification: $B_{ns} = B_{gs}*(R_{gs}/R_{ns})^2$, maintaining a similar topology. This cannot however explain very large magnetic fields.

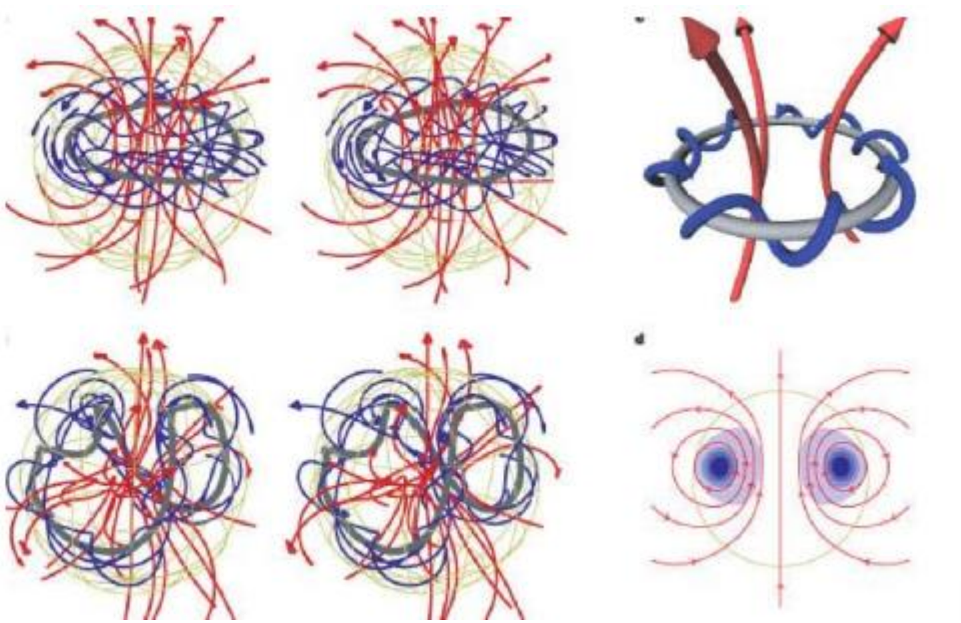

[Braithwaite & Spruit 2005-2006]

Amplification by instabilities and MHD dynamo [Thompson & Duncan works 1992-1996]
Differential rotation and convection in the early stages can twist the field lines, amplifying it. The mechanism is non-linear, non-trivial, and only a few simulations in the last 15 years have provided some quantitative results. Such results show the presence of an organized dipolar poloidal field, and a toroidal torus in the equatorial region.

The second option seems much more likely. Overall, it's still not clear, especially at a quantitative level.

Dipoles (large-scale fields)

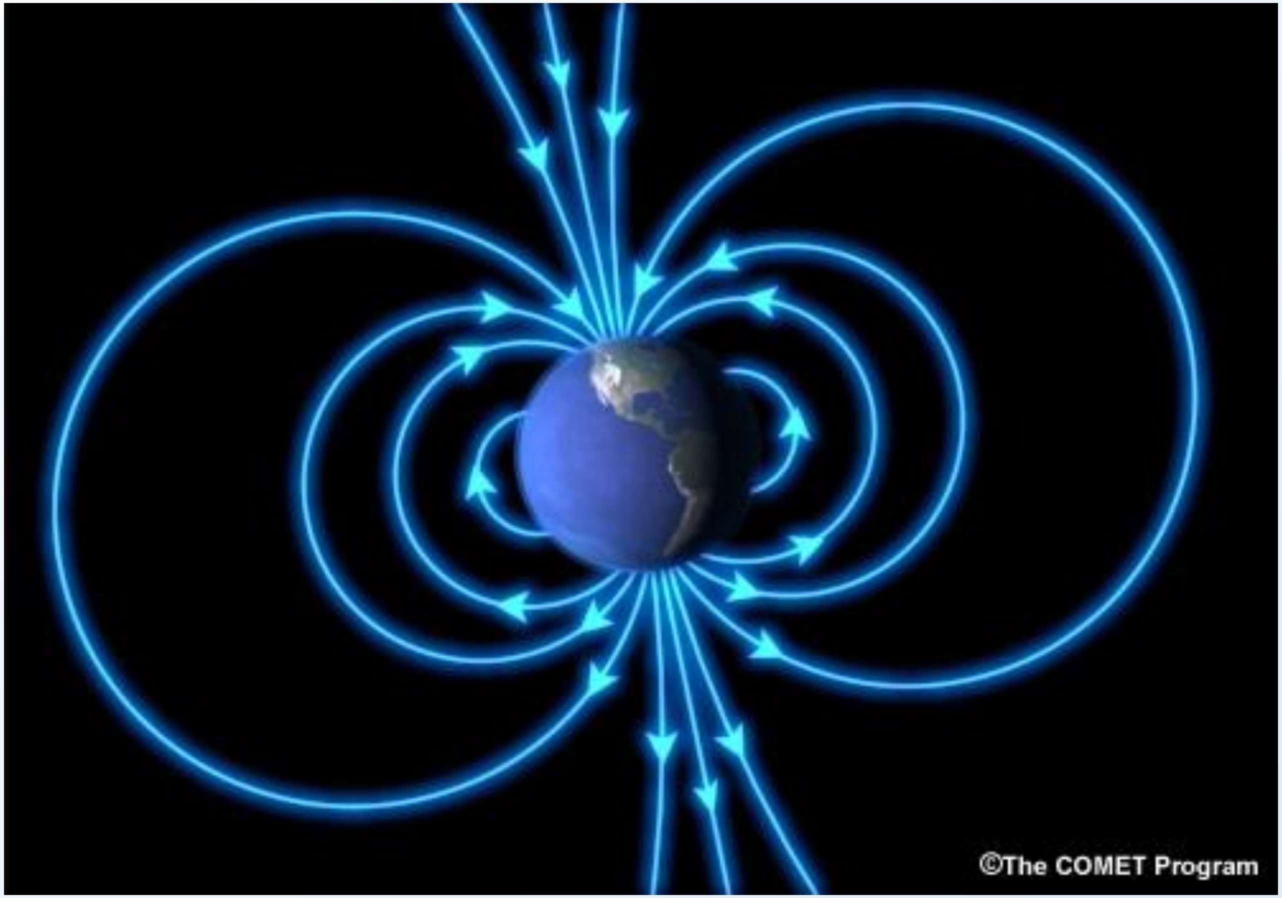

It's the simplest possible configuration, since div(B)=0.
However, such simple, pure "magnets" don't exist in nature

Some magnetic terminology: multipoles

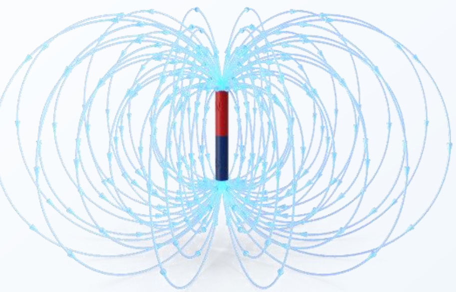

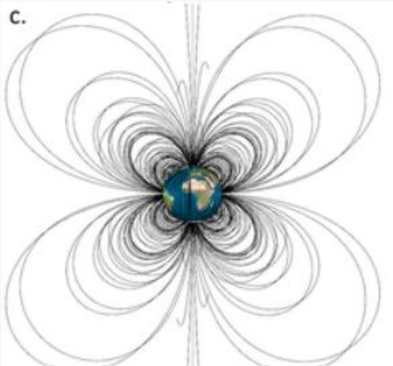

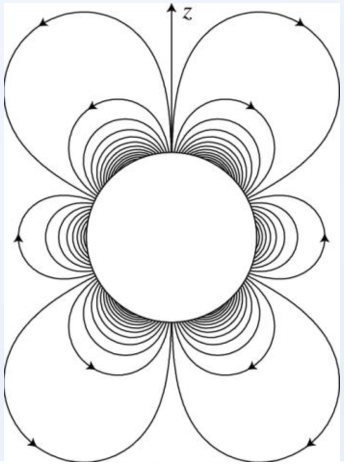

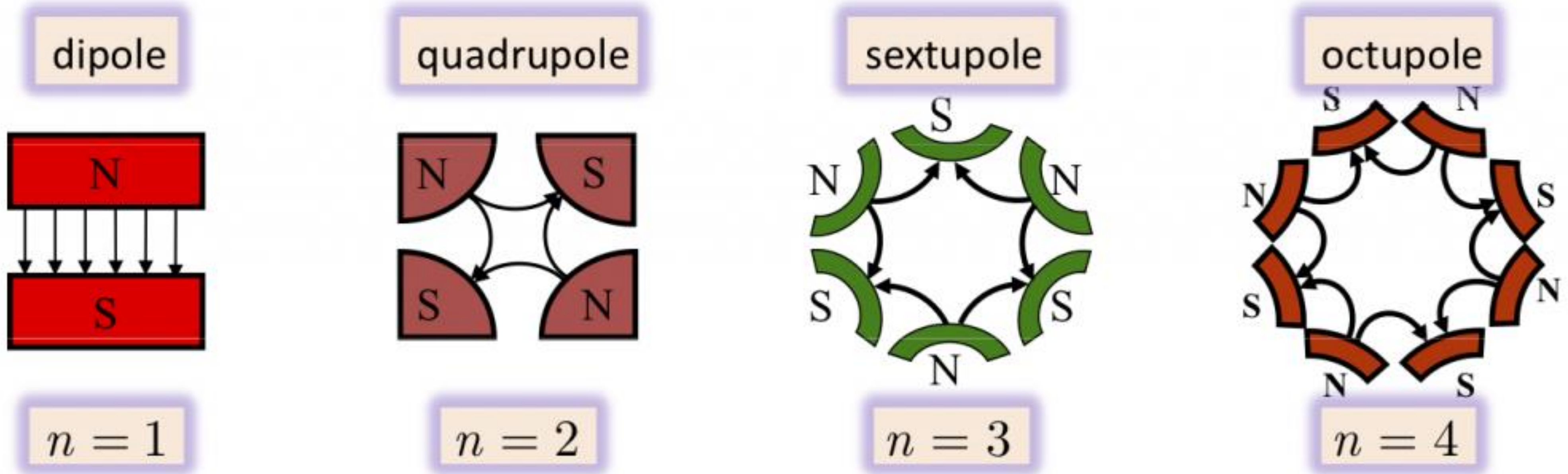

Some magnetic terminology: Poloidal – Toroidal

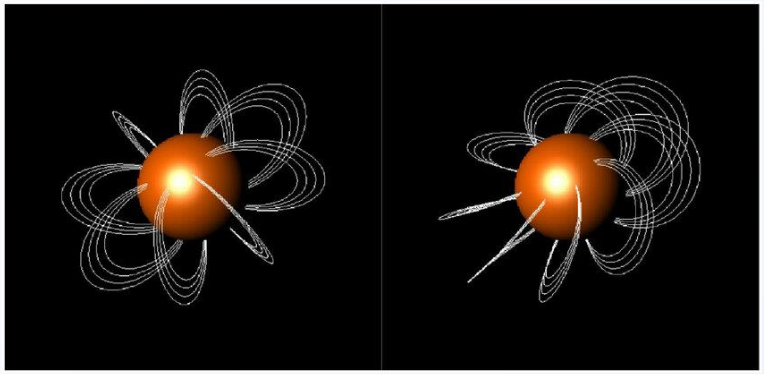

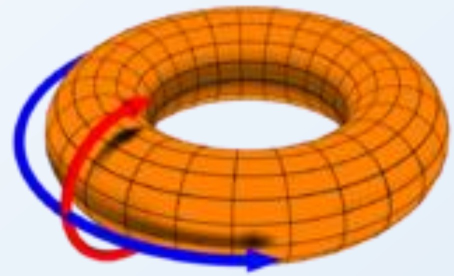

$\vec{B}$ can also be expressed by two scalar functions $\Phi(\vec{x})$, $\Psi(\vec{x})$, that define its *poloidal* and *toroidal* components as follows:

$$\vec{B}_{pol} = \vec{\nabla} \times (\vec{\nabla}\Phi \times \vec{r}) \ ,$$
$$\vec{B}_{tor} = \vec{\nabla}\Psi \times \vec{r} \ .$$

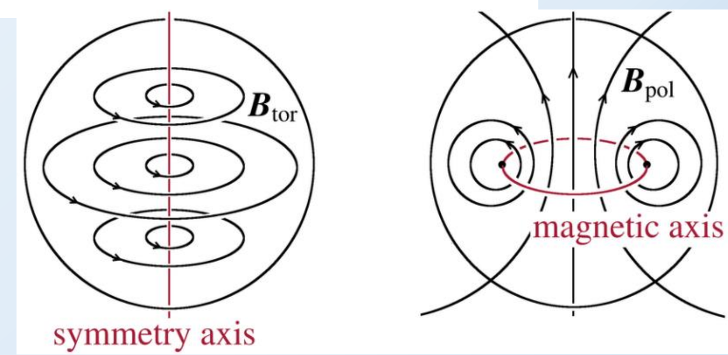

In axial symmetry:
Poloidal = meridional components of the field (r, θ)
Toroidal = azimuthal component (φ)

In 3D poloidal has all (r, θ, φ), toroidal has the tangential ones (θ, φ).

In the absence of currents (curl(B)=0), you can only have a poloidal field.

MAGNETIC FIELDS IN NEUTRON STARS' INTERIOR

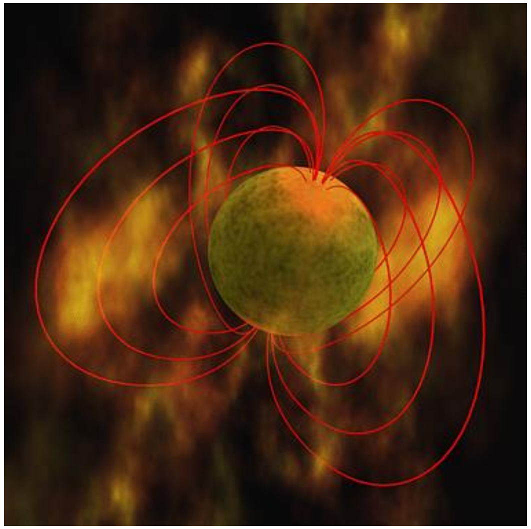

Magnetic field in NSs

The advective term is neglected because:

There is no convection, no differential rotation: the rotation is rigid, so there is no twisting or bending of magnetic field lines, they are simply advected with the rotation.

Therefore, one can recast the magnetic field equation considering only the non-ideal effects.

The MHD equations have to take into account the relativistic effects (10-20% corrections in the derivatives) $\mathrm{d}s^2 = -\mathrm{e}^{2\nu(r)}c^2\mathrm{d}t^2 + \mathrm{e}^{2\lambda(r)}\mathrm{d}r^2 + r^2(\mathrm{d}\theta^2 + \sin^2\theta\,\mathrm{d}\varphi^2)$,

$$\frac{\partial \mathbf{B}}{\partial t} = -c\nabla \times (\mathrm{e}^{\nu}\mathbf{E})$$

$$\mathbf{j} = \mathrm{e}^{-\nu}\frac{c}{4\pi}\nabla \times \left(\mathrm{e}^{\nu}\mathbf{B}\right)$$

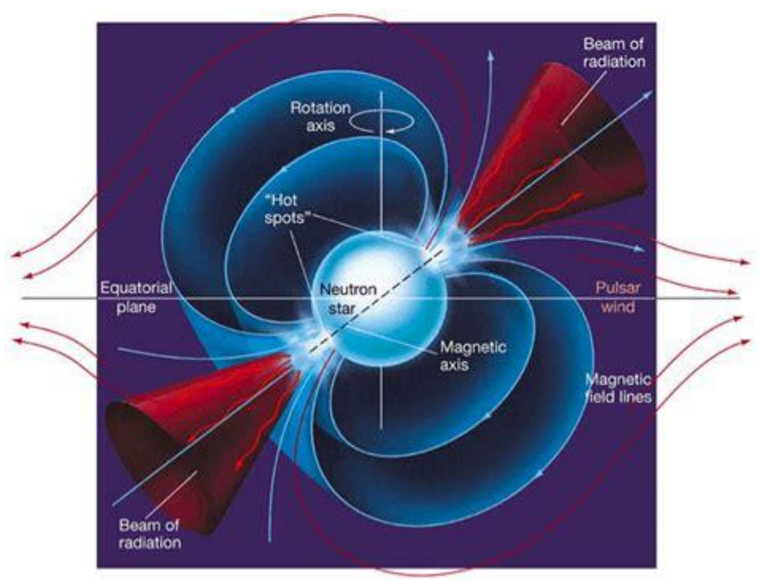

Magnetic field long-term evolution in the crust

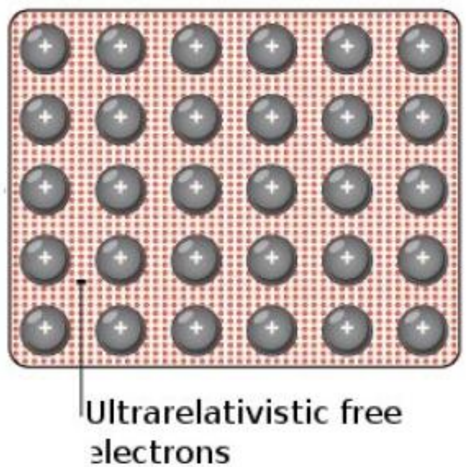

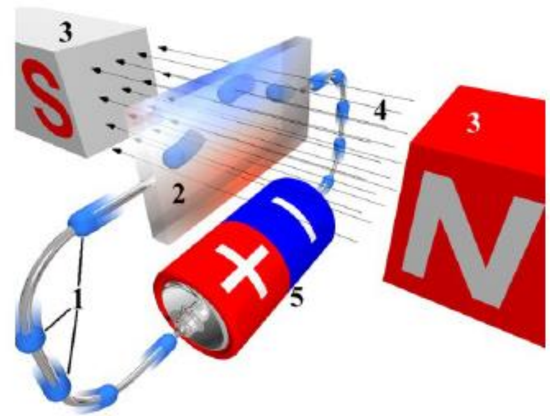

$$\frac{\partial \vec{B}}{\partial t} = -\vec{\nabla} \times \left\{ \eta \vec{\nabla} \times (e^{\nu} \vec{B}) - \left[\frac{c e^{-\nu}}{4\pi e n_e} \vec{\nabla} \times (e^{\nu} \vec{B}) \right] \times (e^{\nu} \vec{B}) \right\}$$

Resistivity Hall term

The solid crust can be considered a simplified version of a Hall plasma: ions have very restricted mobility and only electrons can move freely through the lattice, carrying currents and heat. If ions are strictly fixed in the lattice (ignore plasticity), the limit is known as electron MHD.

η is the magnetic diffusivity, it strongly depends on T, n_e is the electron density

Magnetic field evolution in the core

In the core, physics is very unclear. A mixture of neutrons, protons, electrons, muons (and others?) is expected: multi-fluid MHD, giving rise to the additional effect of **ambipolar diffusion**. Moreover, very soon superfluidity (neutrons) and superconductivity (protons) set in, which complicates the picture. Formalism and simulations exist only for the non superfluid case, simple n-p-e mixture.

In general, we expect the evolution to be slower in the core than in the crust, but there are many open questions.

[Castillo+ 2020]

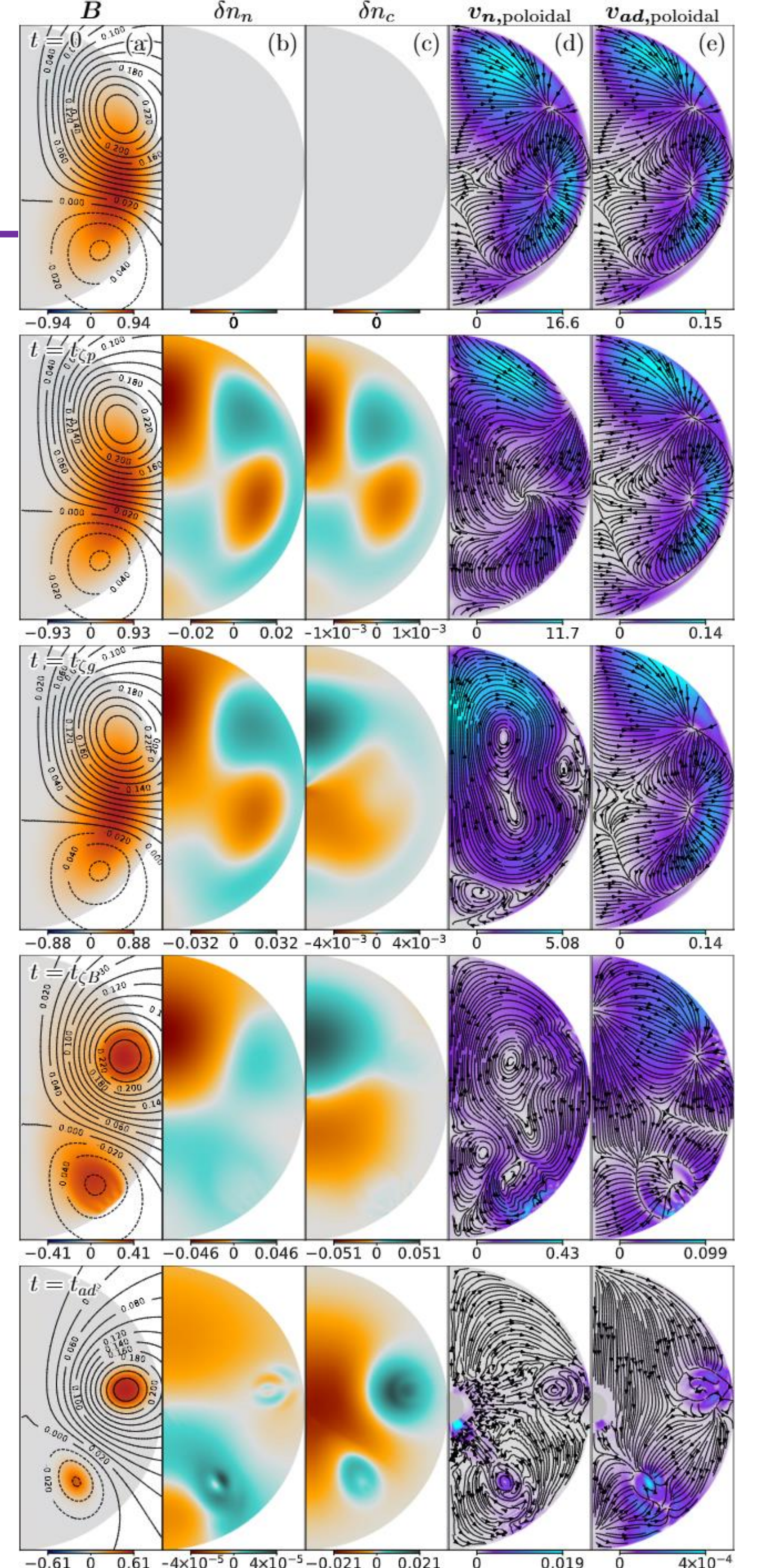

Magnetic field evolution in the core

Below a critical magnetic field and temperature, protons become superconducting, of type II (b), with the magnetic flux contained in tiny vortexes (fluxtubes); for lower B, Meissner effect (type I, (a)).

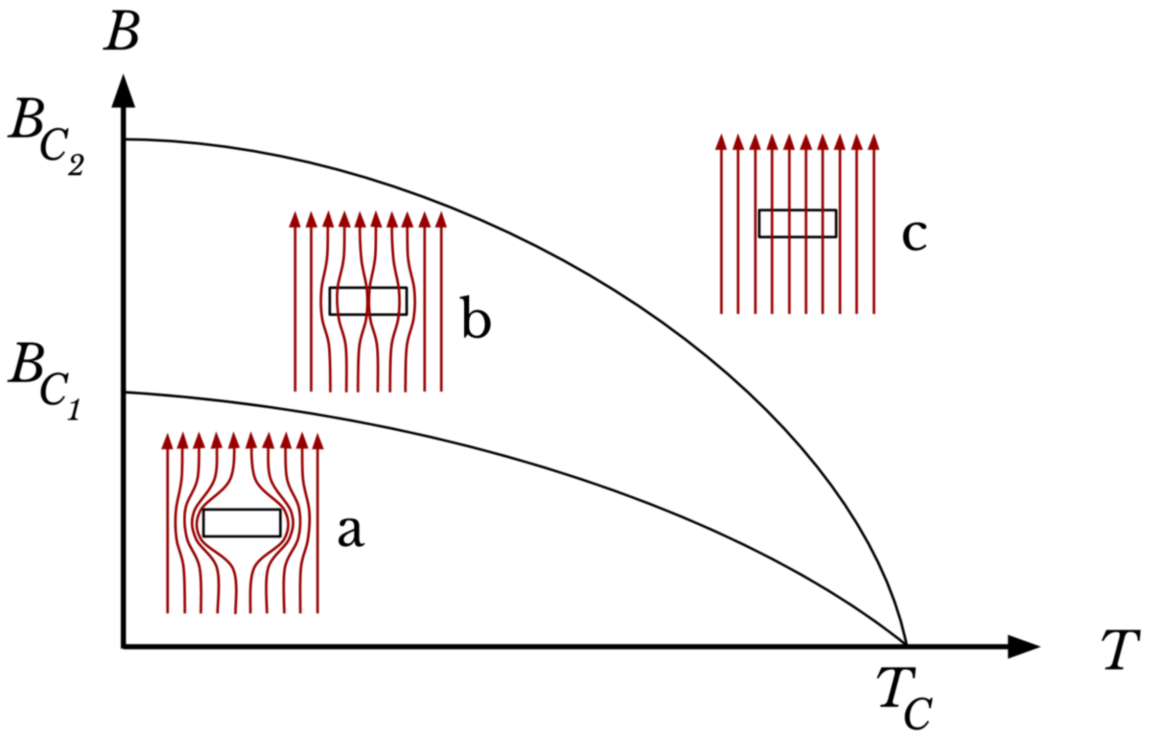

Yttrium barium copper oxide type-II superconductivity

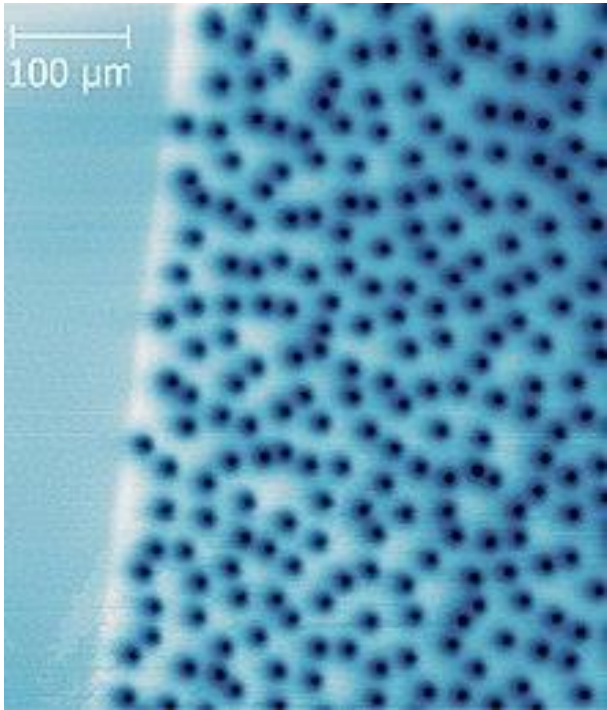

Superconductivity type II

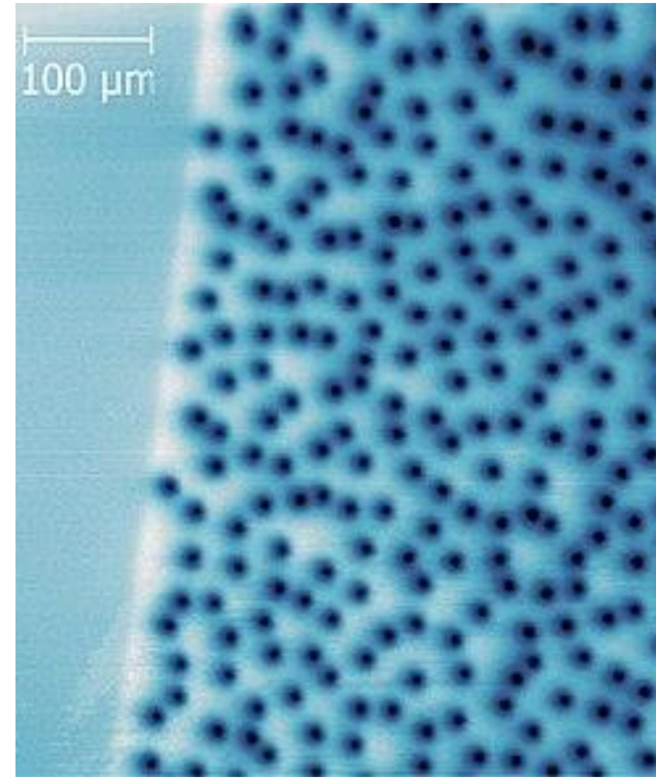

- Type II: magnetic flux is concentrated in tiny fluxtubes
- Not common, but seen in laboratory (e.g. Yttrium barium copper oxide, YBCO)
- Magnetic flux quantized

$$\phi_0 = \pi\hbar c/e \approx 2 \times 10^{-7} \text{ G cm}^2$$

- Exhibits flux pinning: magnetic fluxtubes are pinned to specific places.

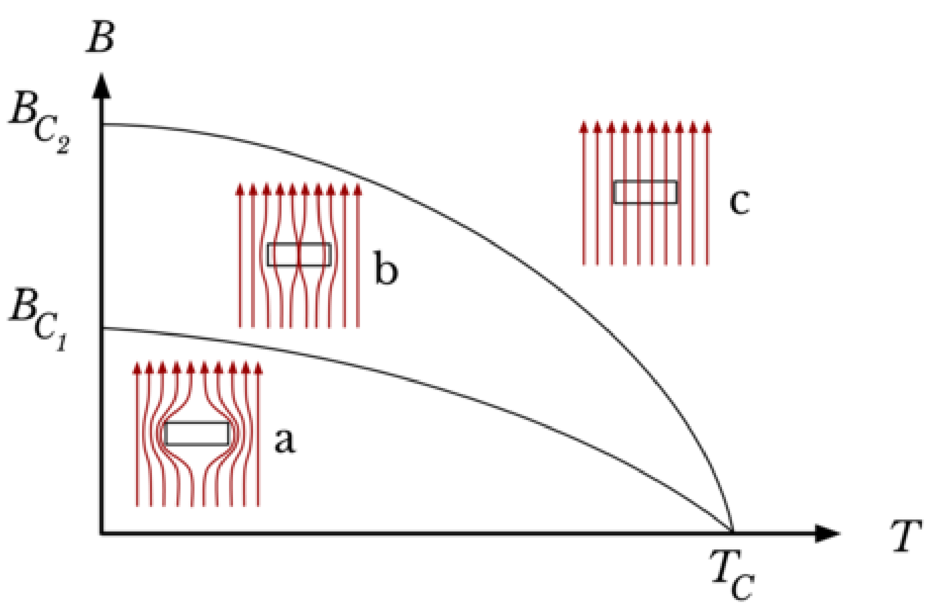

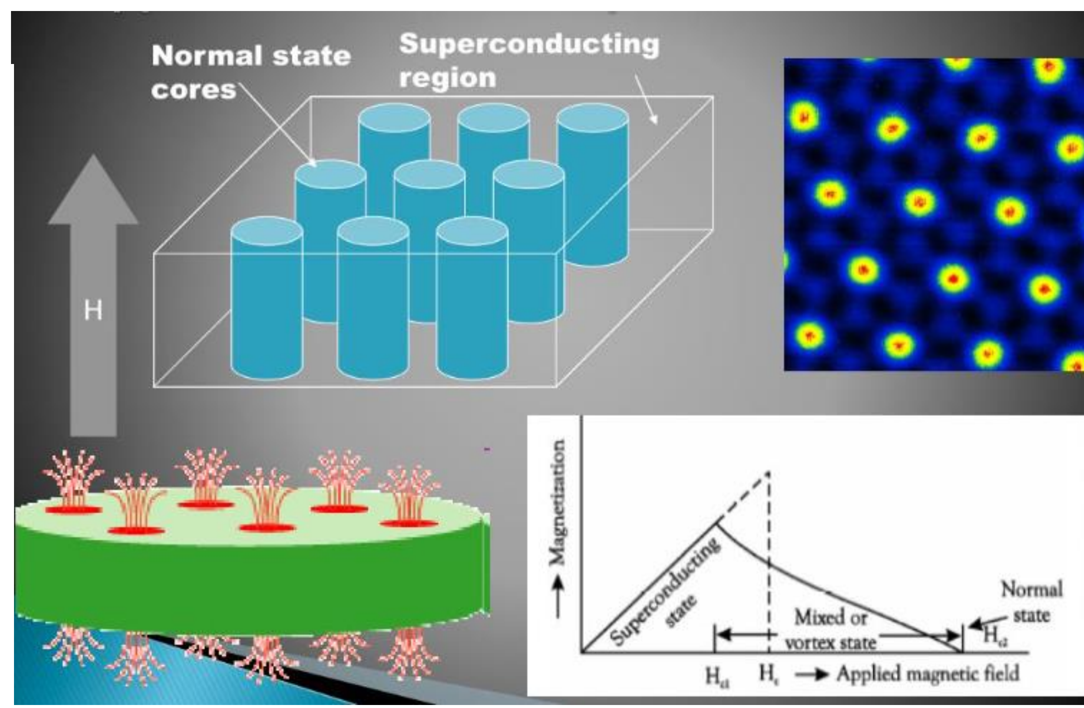

Superconductivity & flux pinning

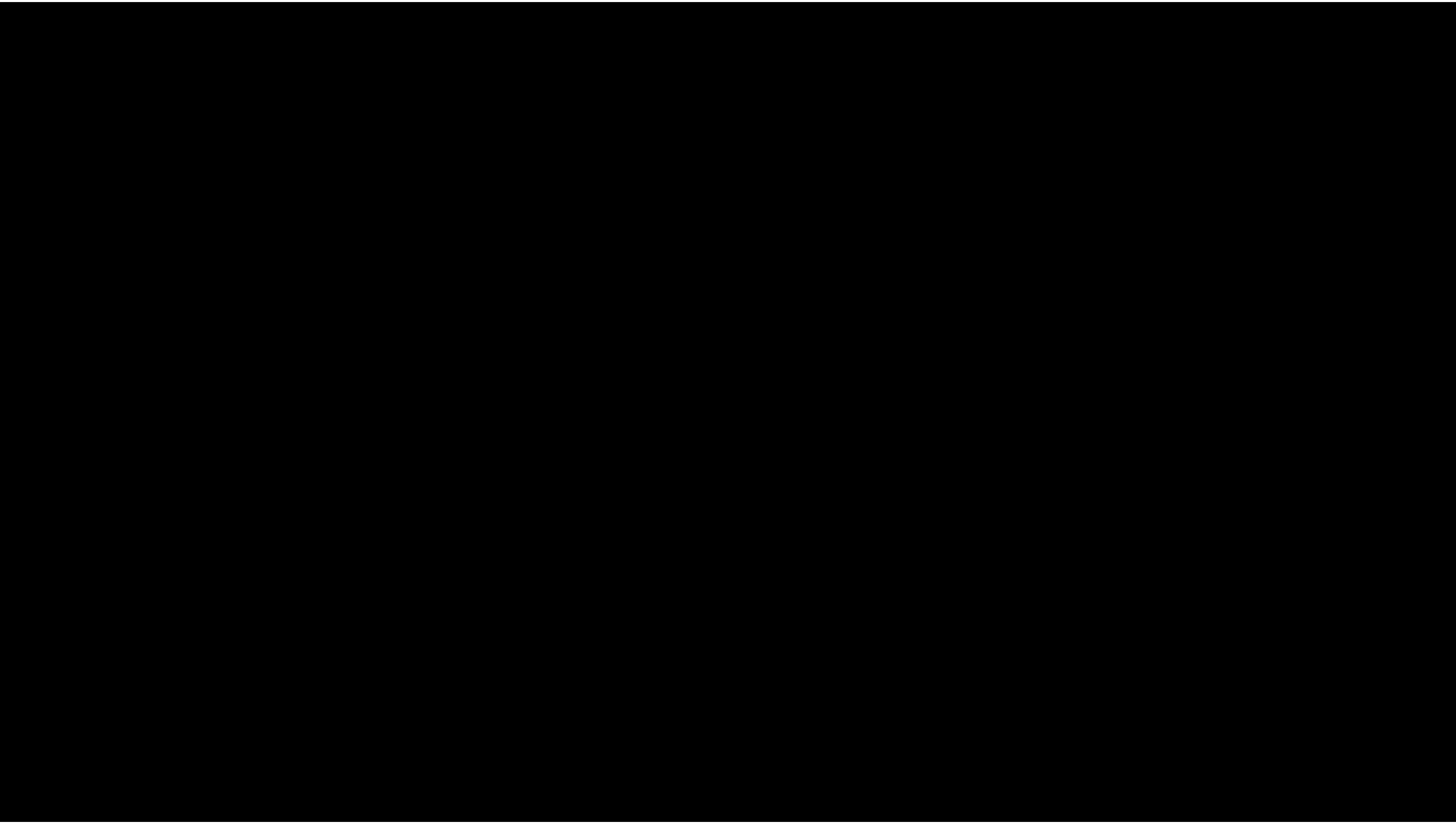

Magnetic field evolution in the core

Depending on the density and magnetic fields, you can have a mix of region with: (F) huge amount of tiny fluxtubes (with femtometer diameter) where magnetic fields are confined; (M) classical Meissner effect regions, inside which magnetic fields don't penetrate; (N) Normal matter

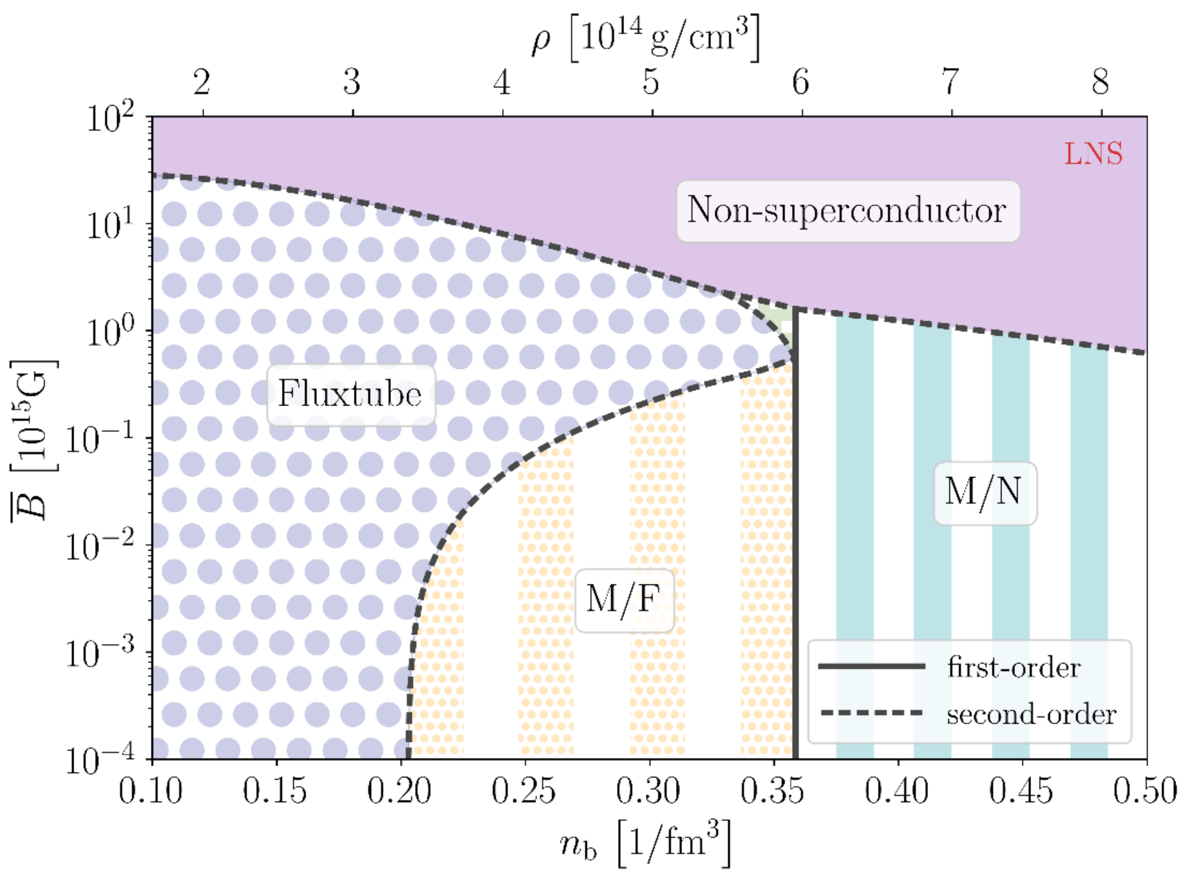

[Wood+ 2022]

Numerical simulations (crustal fields only)

The field in 3D tends to create small structures typically of the order of the crust size: Hall cascade, like in turbulence.

[Gourgouliatos & Hollerbach 2018]

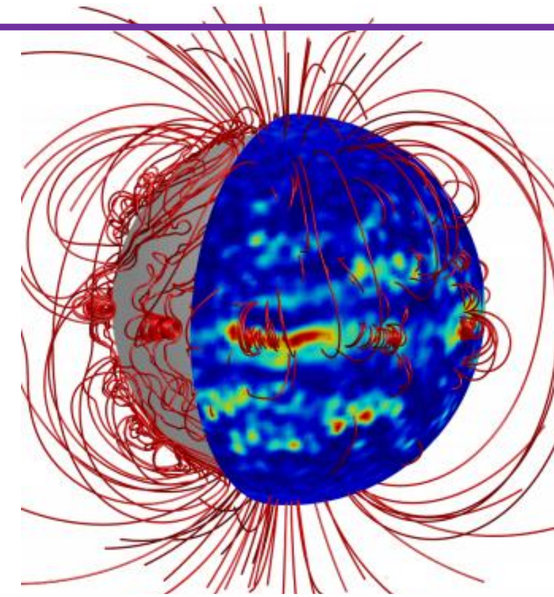

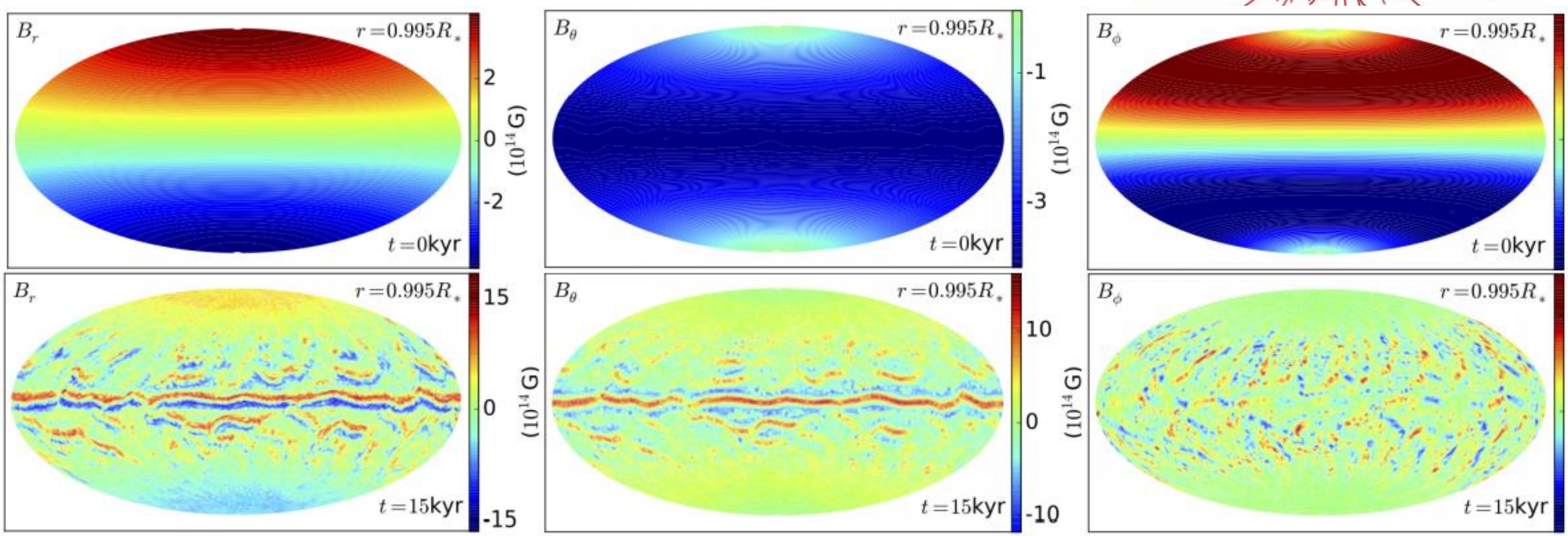

Fig. 2. Contour plot of the radial (left), latitudinal (middle) and azimuthal (right) component of the magnetic field at $r = 0.995R_*$ at $t = 0$ (top) and $t = 15$kyr (bottom)

Numerical simulations

Results depend on the amount of initial toroidal to poloidal field given.

For a toroidal dominance, the axis of the dipolar field can drift.

Growth of characteristic modes. The field in 3D is able to break the symmetry and create structures typically of the order of the crust size.

[Gourgouliatos & Hollerbach 2018]

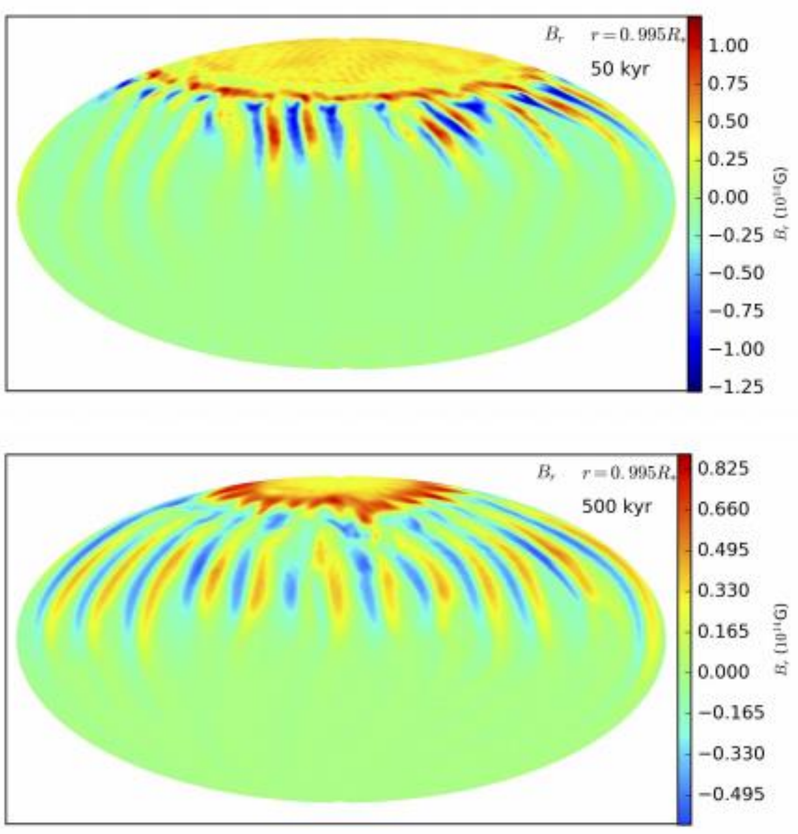

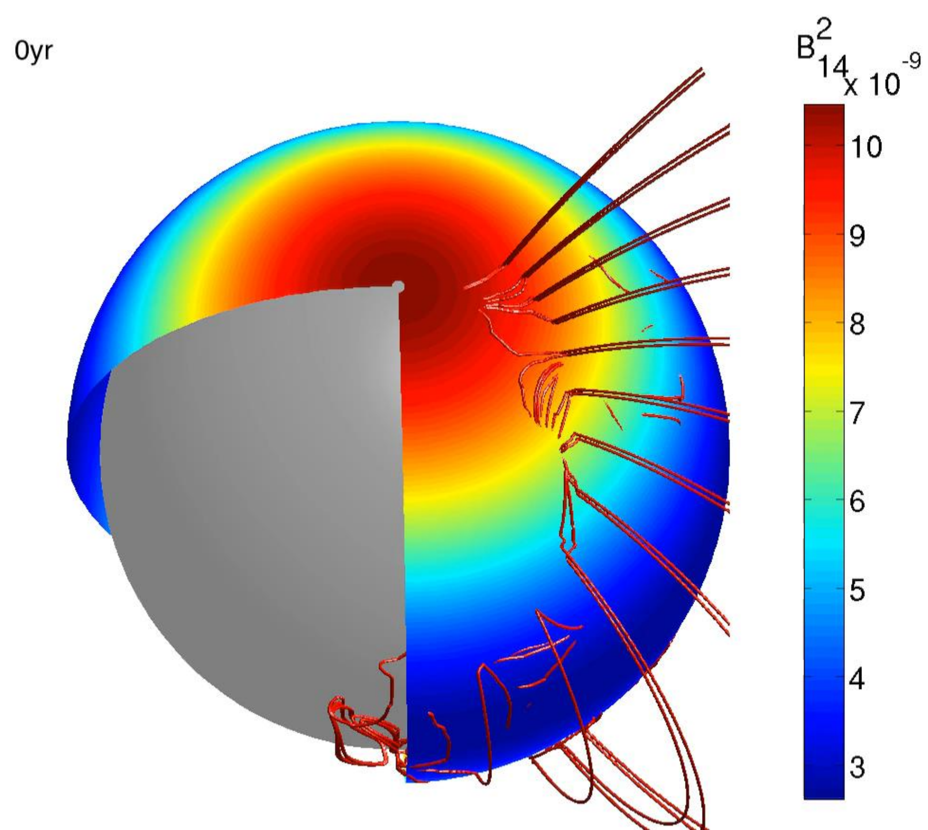

RESULTS FROM STATE-OF-THE-ART SIMULATIONS

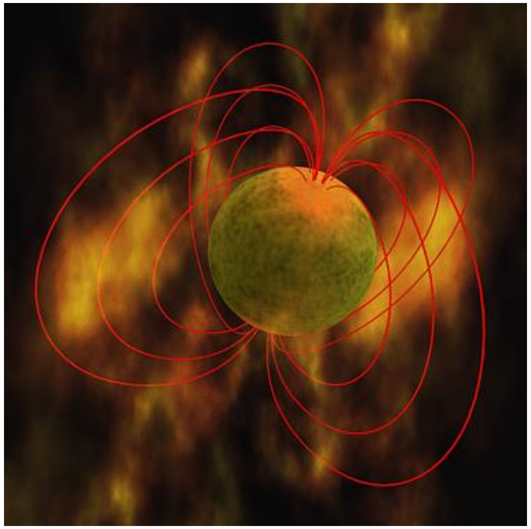

The role of the envelope model

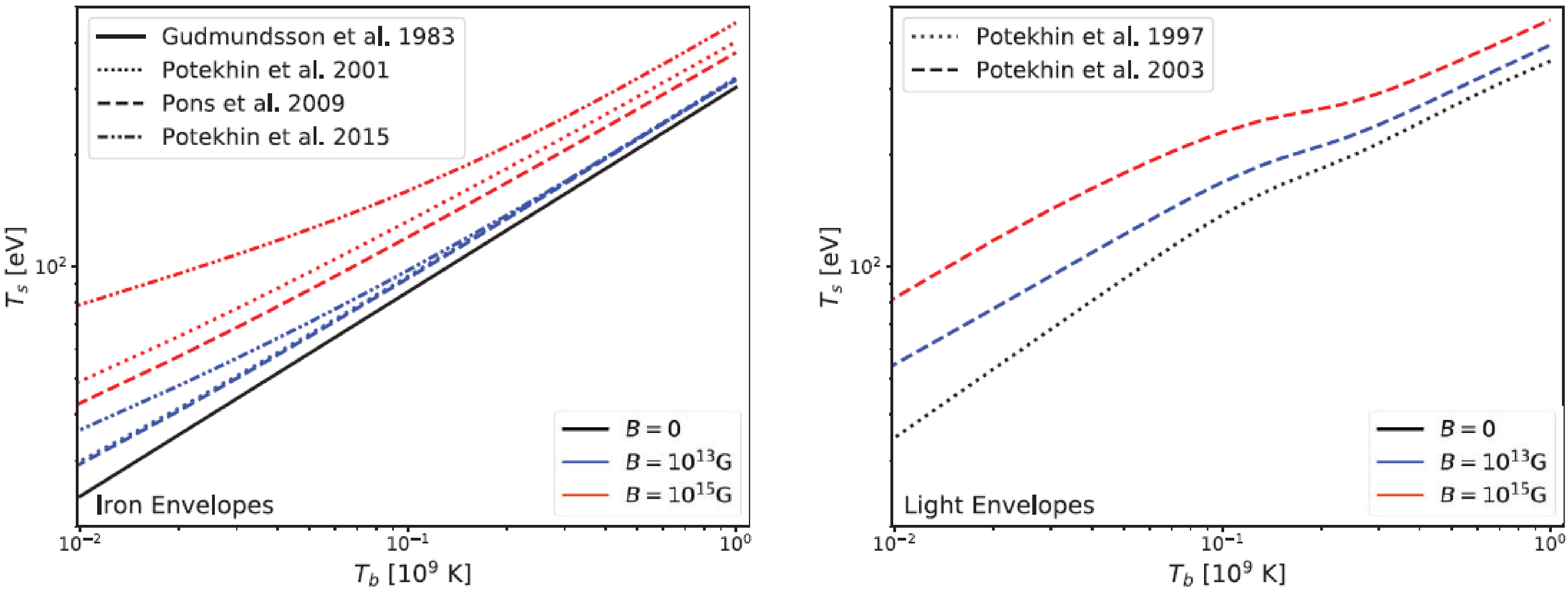

Figure 1. T_b–T_s relations of different envelope models. The non-accreted models are illustrated on the left and the fully accreted ones in the panel on the right. The studied envelopes are (i) non-magnetized (in black) (Gudmundsson et al. 1983; Potekhin et al. 1997) and (ii) magnetized (in colour) (Potekhin & Yakovlev 2001; Potekhin et al. 2003, 2015; Pons et al. 2009). For the latter, we consider two different values of a purely radial magnetic field strength (then, suitable for a polar T_s if the topology is a simple dipole): $B = 10^{13}$ (in blue) and 10^{15} G (in red).

[Dehman et al. 2023]

Magneto-thermal evolution

The role of the envelope model

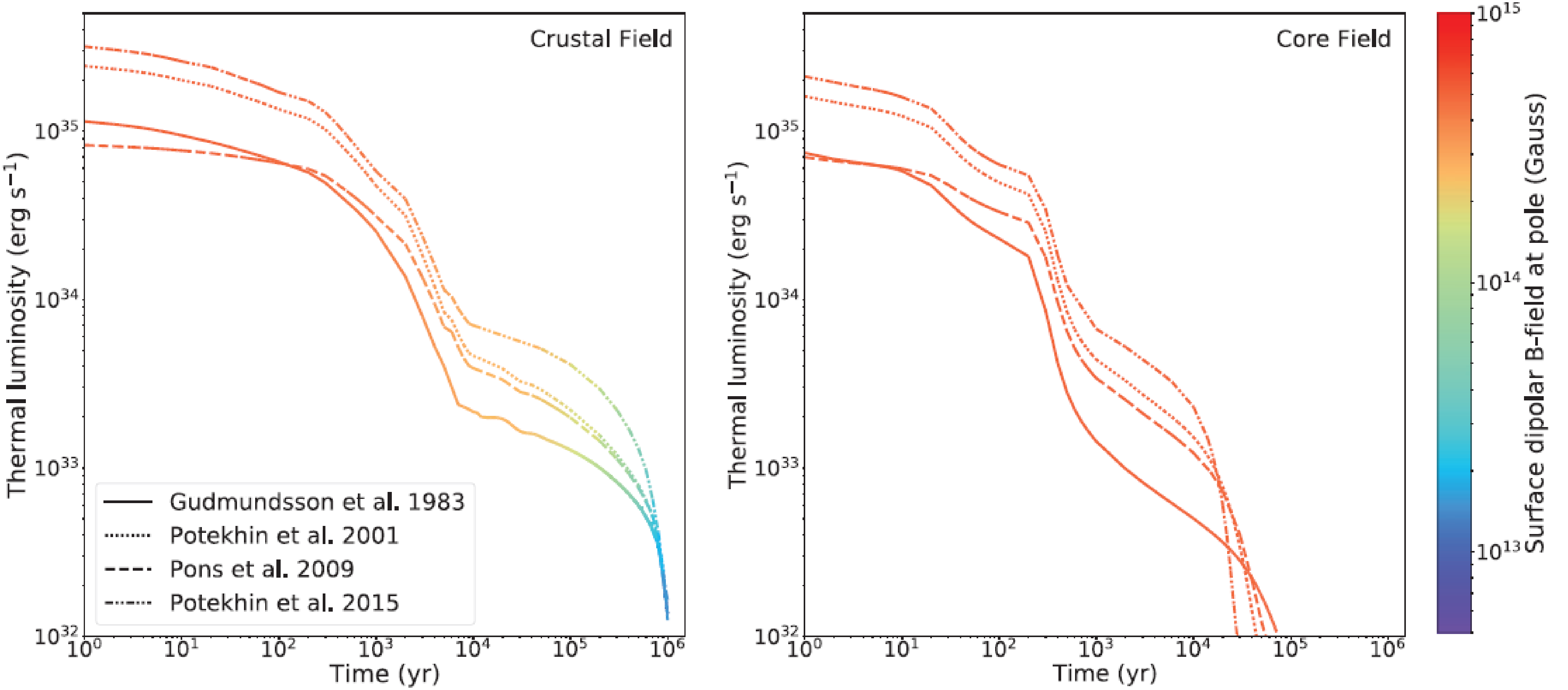

Figure 2. Luminosity curves of the four studied iron envelopes (Gudmundsson et al. 1983; Potekhin & Yakovlev 2001; Pons et al. 2009; Potekhin et al. 2015) with an initial magnetic field intensity at the polar surface of $B = 5 \times 10^{14}$ G (hereafter, the colourbar indicates its evolution). The left-hand panel corresponds to crust-confined topology, whereas the right-hand panel to core-dominant field topology.

[Dehman et al. 2023]

Numerical simulations

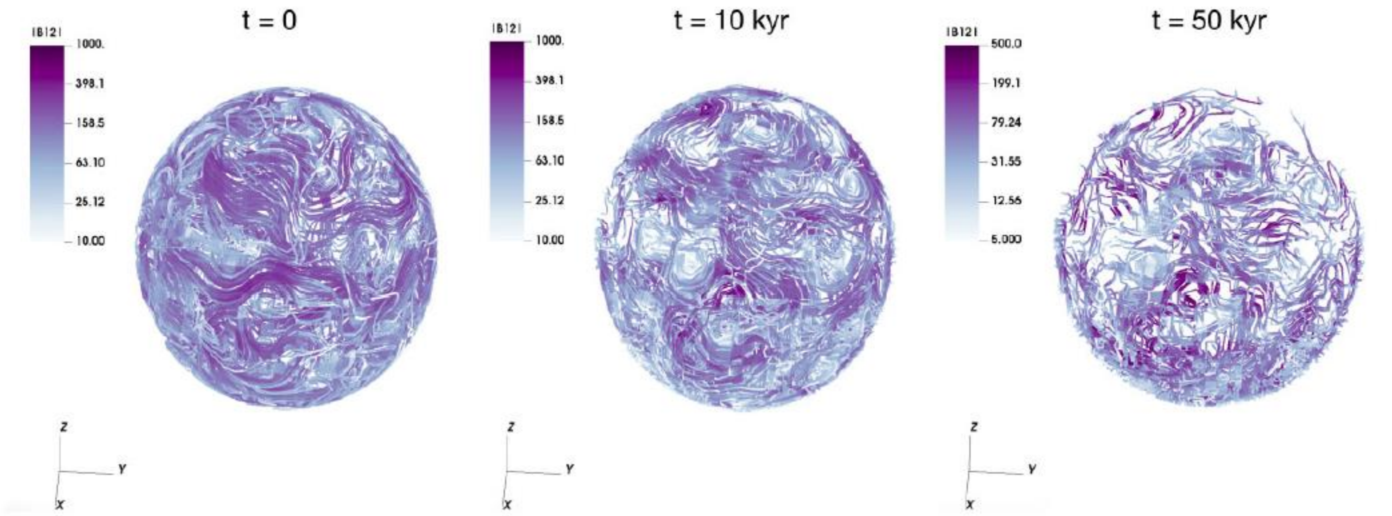

Figure 4. Field lines in the crust of an NS at $t = 0$ (on the left), $t = 10$ kyr (in the centre), and $t = 50$ kyr (on the right). The colour scales indicates the local field intensity in units of 10^{12} G.

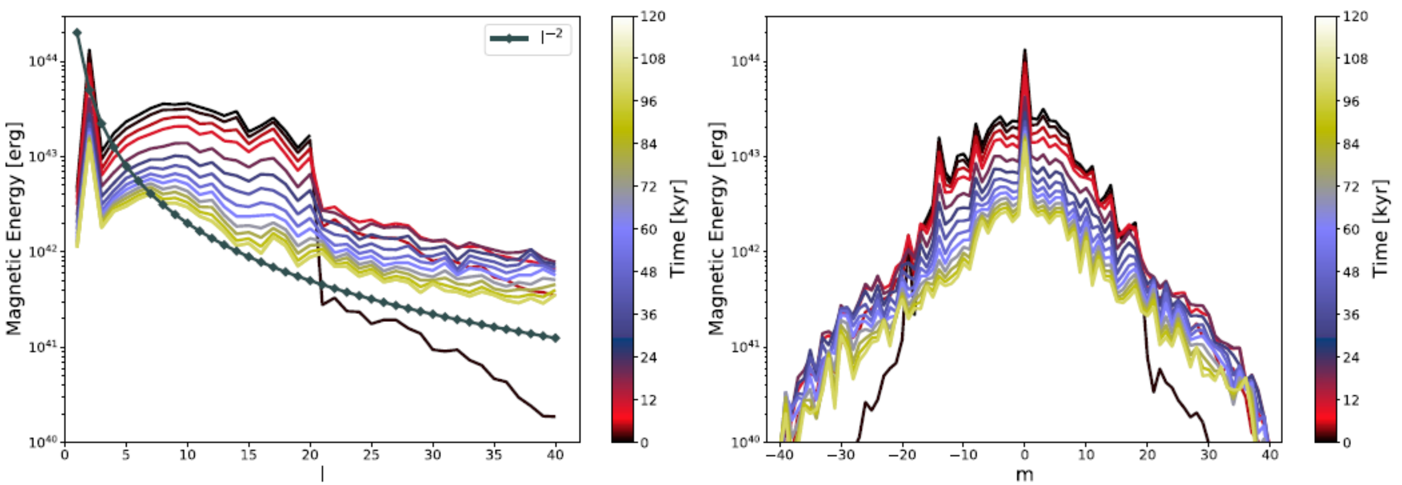

Figure 1. Spectrum of the total magnetic energy at different evolution time up to 100 kyr (Hall balance is reached in the system). Left panel: l – energy spectrum; right panel: m – energy spectrum.

[Dehman+ 2023]

Full simulations: results and observables

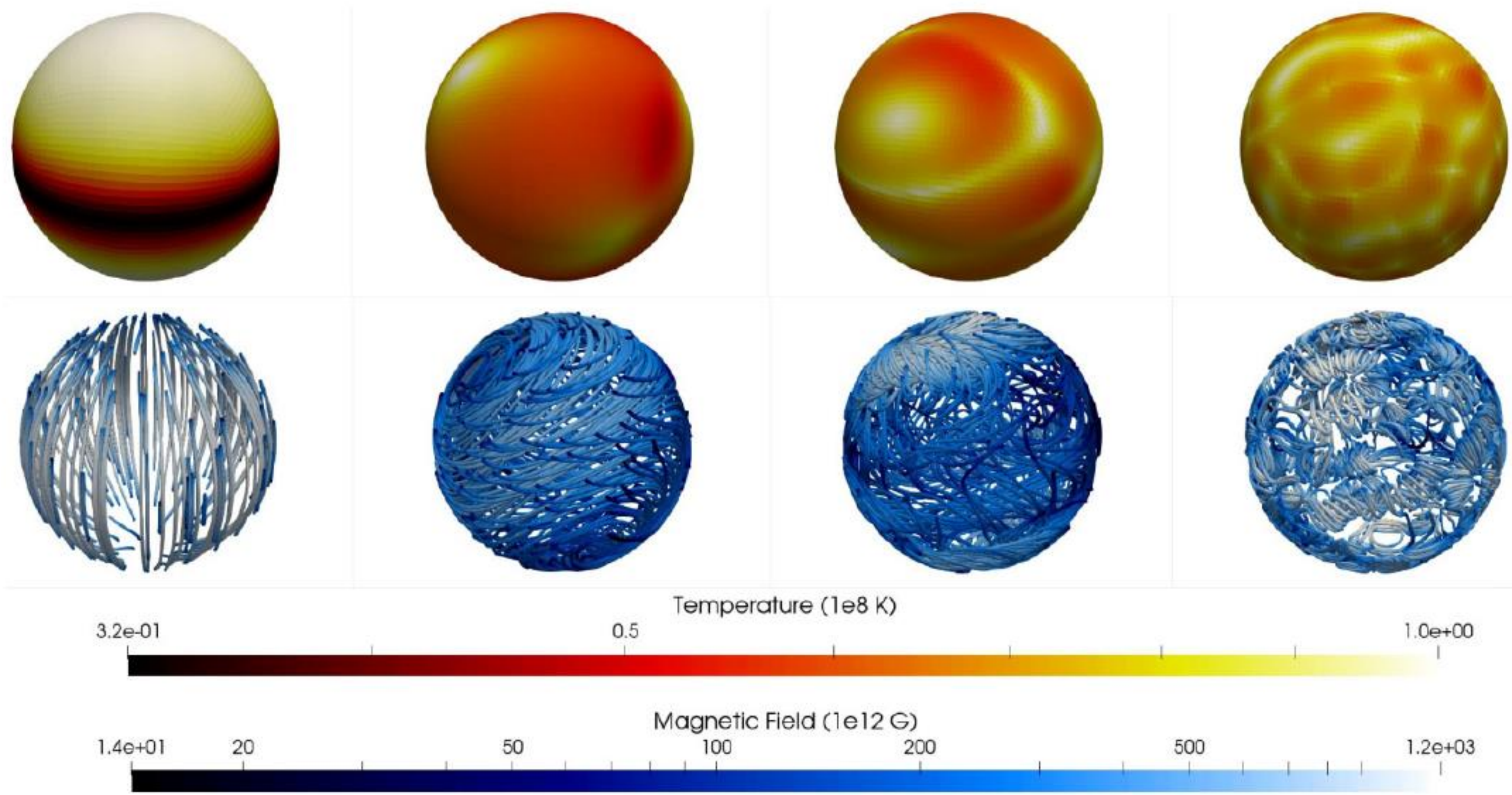

Figure 9. 3D rendering of the models *SLy4-M1.4-B14-L1*, *SLy4-M1.4-B14-L2*, *SLy4-M1.4-B14-L5*, and *SLy4-M1.4-B14-L10* (from left to right) at time $t = 2726$ yr. Top: temperature map at the base of the envelope T_b. Bottom: Magnetic field lines. The colour denotes the intensity of the field. All the simulations use the same mass of $M = 1.4\,\mathrm{M}_\odot$ and the EOS SLy4. The chosen resolution is $N_a = 31$, $N_r = 30$. In all these simulations, the magnetic field is not evolved.

[Ascenzi et al. 2024]

Full simulations: results and observables

Magnetic + thermal evolution + ray tracing:
light curves and spectra

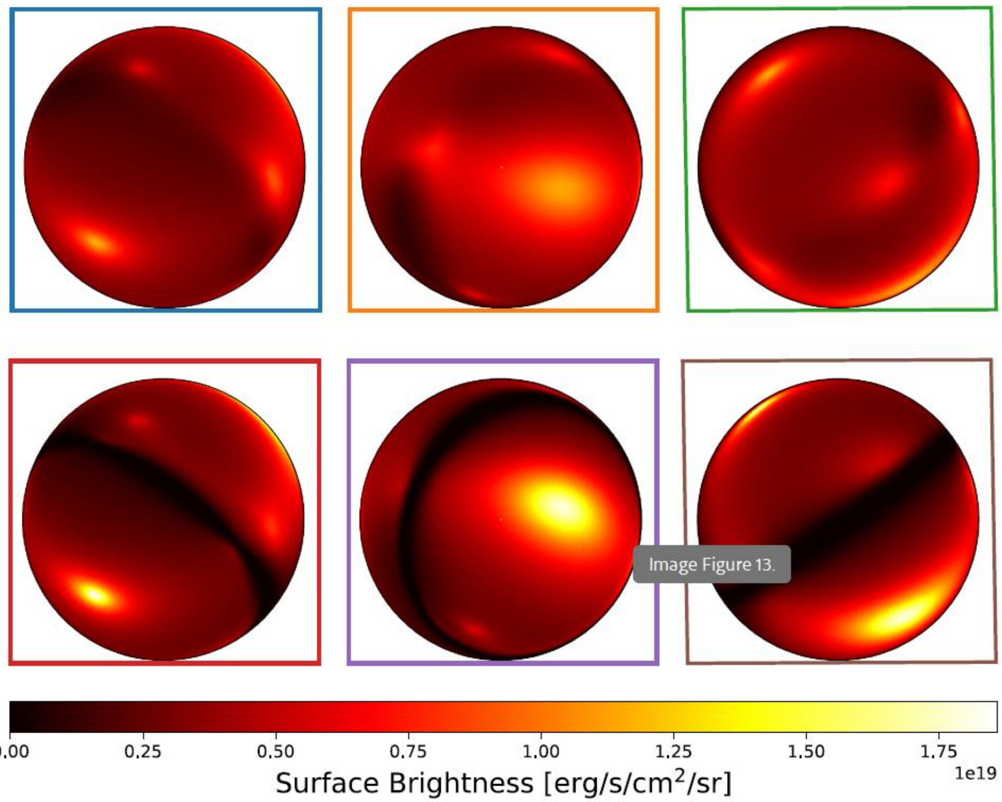

Figure 13. Surface brightness of the star projected on the observer plane at three different rotational phases. Top: Simulation with Gudmundsson envelope. Bottom: Simulation with the iron magnetized envelope. The rotational axis is horizontal in each image. The images refer to the three (per simulation) rotational phases highlighted in the right panel of Fig. 12. The colour of the frame around each image matches the colour of the dot in the previous figure to which the image refers. Note that the phases in the top row and in the bottom row are close but not exactly equal (refer to Fig. 12).

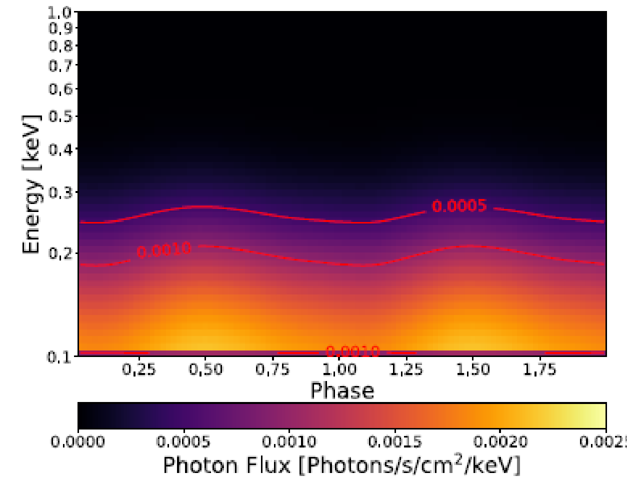

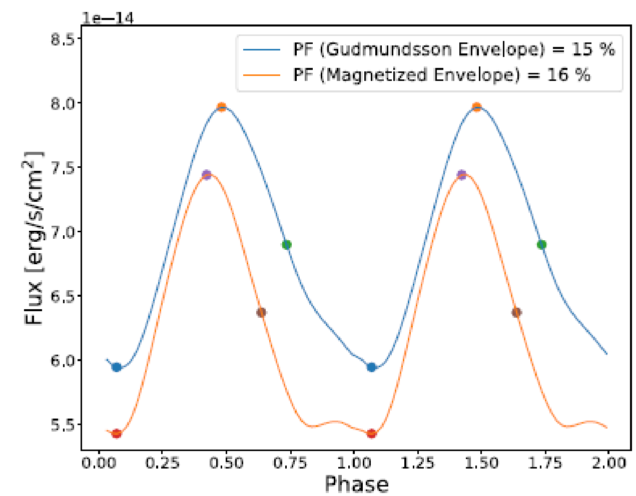

Figure 12. Same as Fig. 11 but for the simulation *Sly4-M1.4-B14-L2*. In the bottom panel coloured dots mark three different selected phases, coincident with the minimum (blue), the maximum (orange), and an intermediate (green) value of the flux. The orange curve represents the same run using an iron envelope model instead of the Gudmundsson envelope model. The coloured dots mark the minimum (red), maximum (purple), and an intermediate (brown) value of the flux.

[Ascenzi et al. 2024]

Simulations: application to magnetars

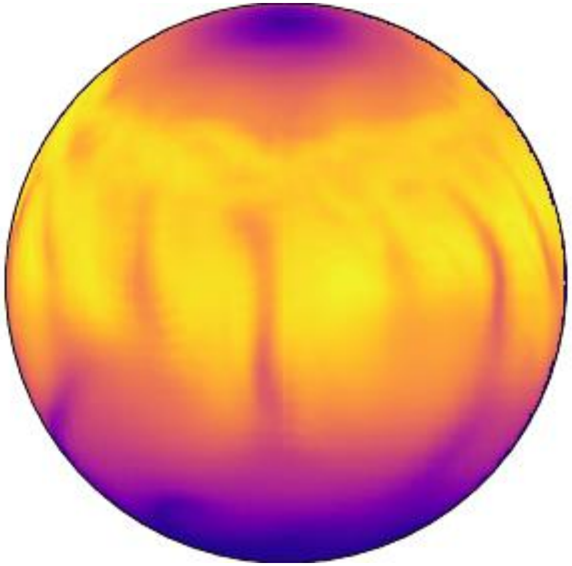

Strong, large-scale toroidal dipolar fields cause a dipolar-dominated distribution of temperature, which means high pulsed fraction (assuming a beamed emission).

Caveat: no cooling physics included (only anistropic conductivity)

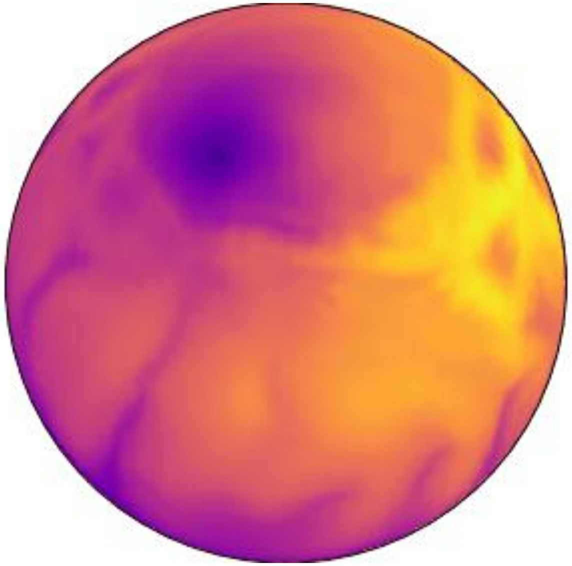

Igoshev et al. 2021 https://arxiv.org/pdf/2010.08553.pdf

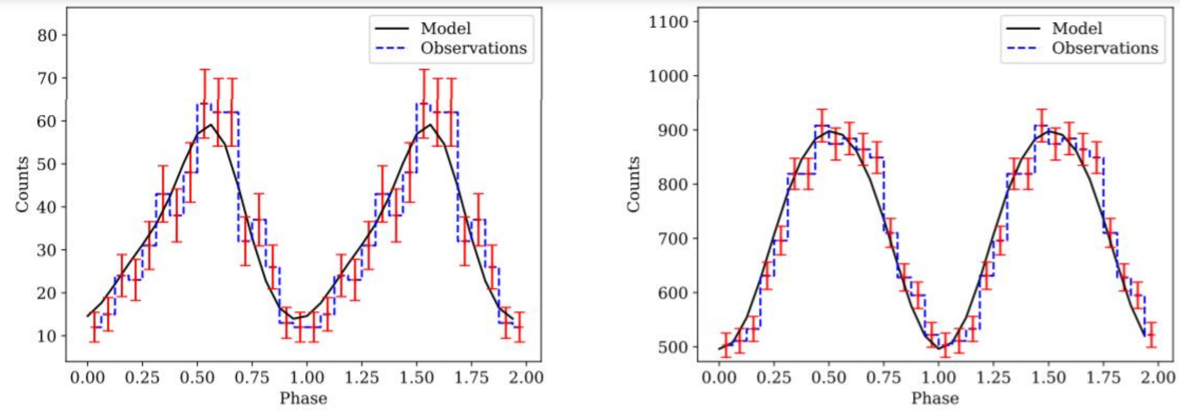

Fig. 2: Folded soft X-ray light-curve (300-2000 eV) for magnetars. Left panel: SGR 0418+5729, right panel: 1E 1547.0-5408. The dashed blue lines and red error bars

Simulations: tangled fields & CCOs

Tangled fields with low dipolar fields and “leopard spot” surface temperature imply low pulsed fractions.

Eventually these fields, possibly buried by postSN accretion, can re-emerge, increasing the dipolar fields and drawing peculiar tracks in the P-Pdot diagram (and low or even negative braking indexes, Viganò et al. 2012, Ho et al. 2012)

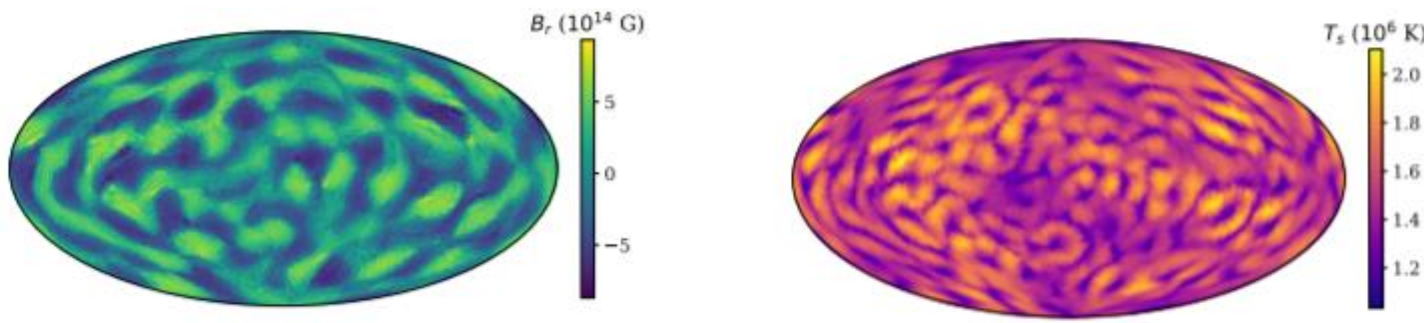

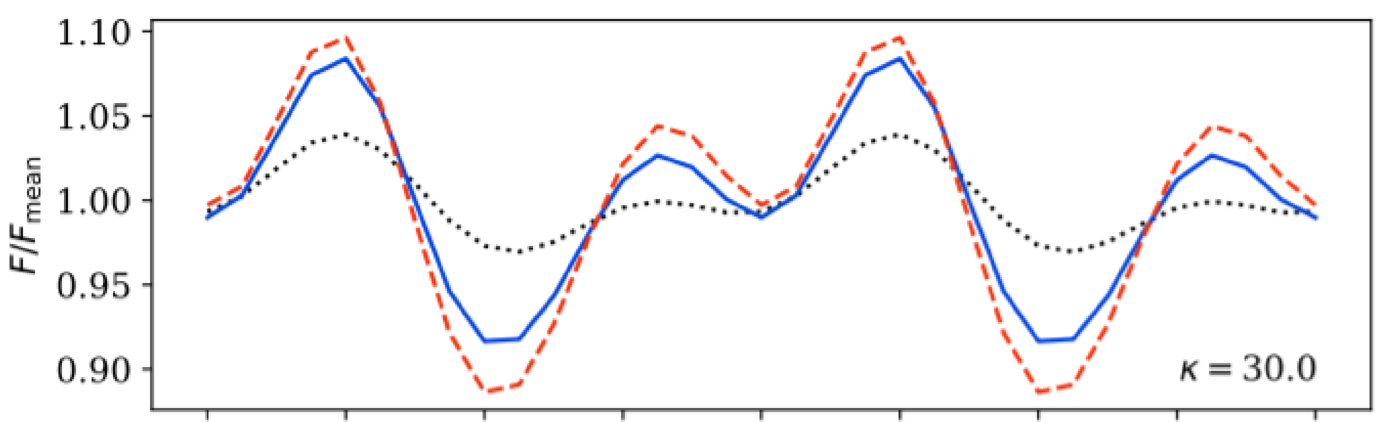

Gourgouliatos et al. 2020 [*https://arxiv.org/pdf/2005.02410.pdf*](https://arxiv.org/pdf/2005.02410.pdf)
Igoshev et al. 2021 [*https://arxiv.org/pdf/2101.08292.pdf*](https://arxiv.org/pdf/2101.08292.pdf)

Simulations: results and observables

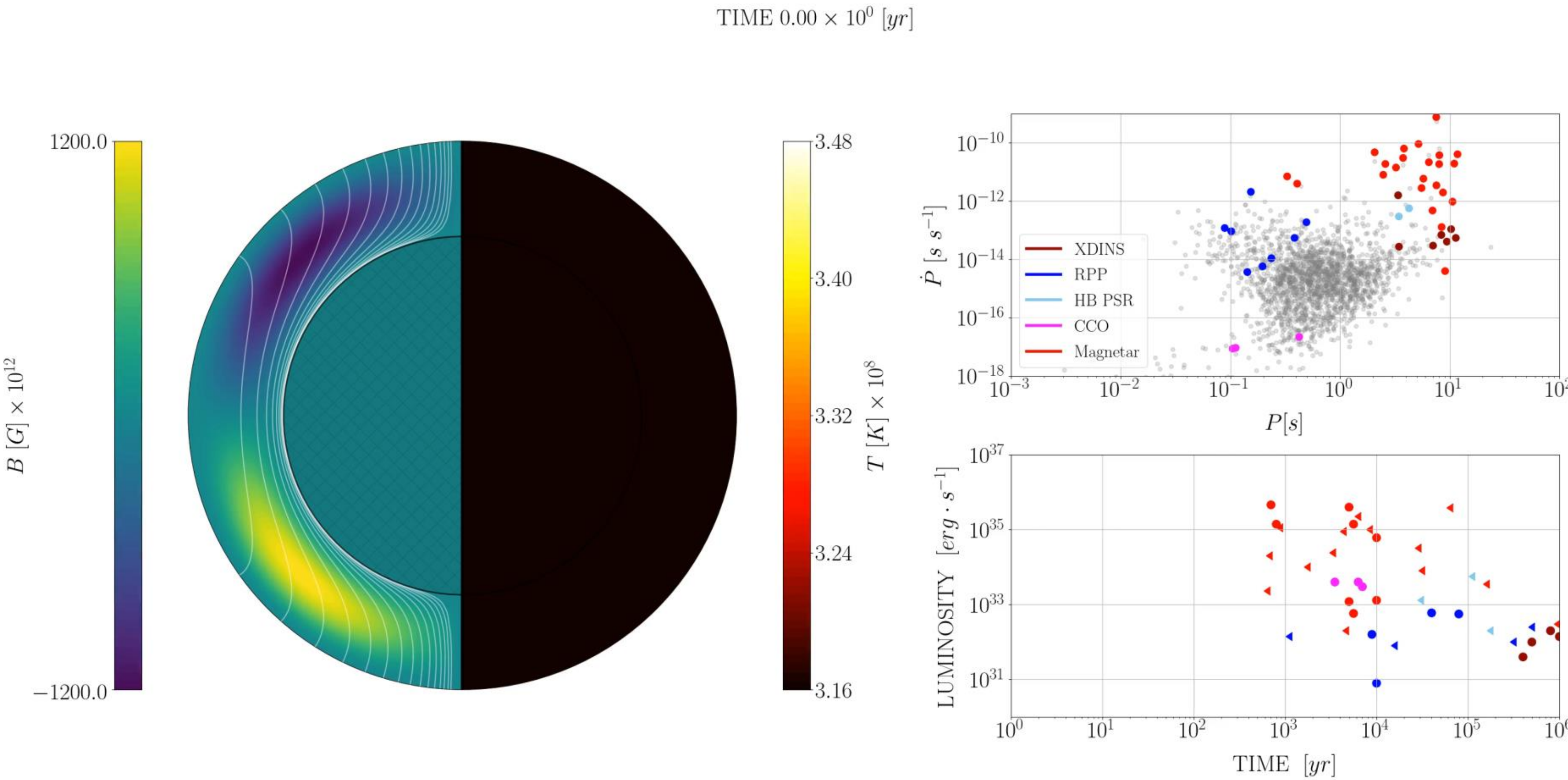

[C. Dehman credit]

Simulations applied to the observed population

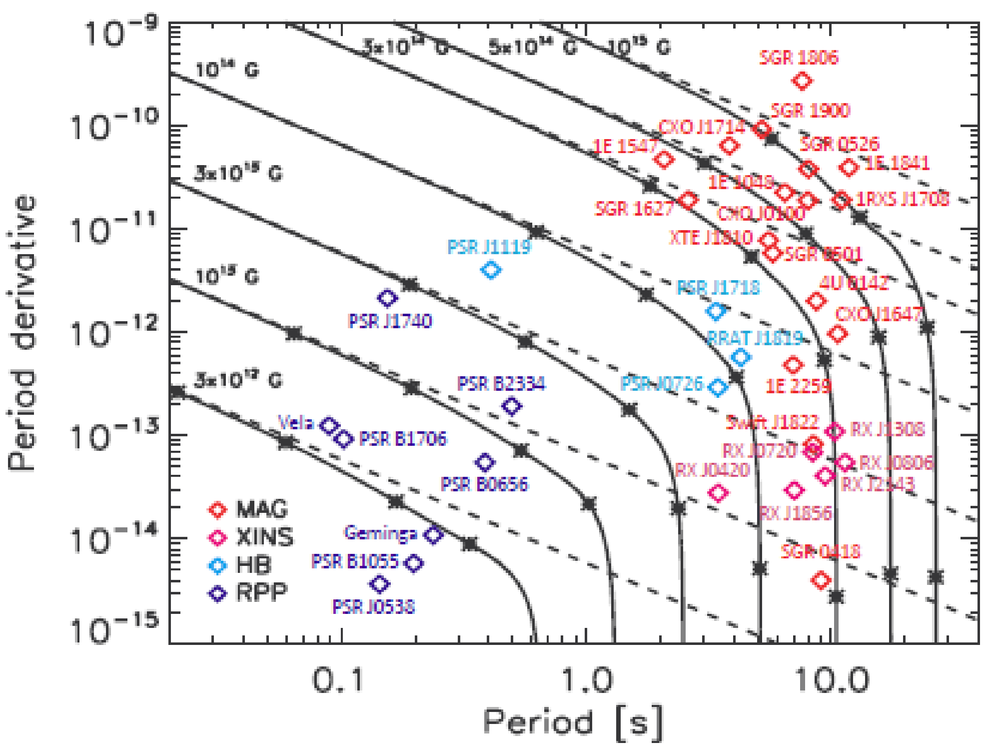

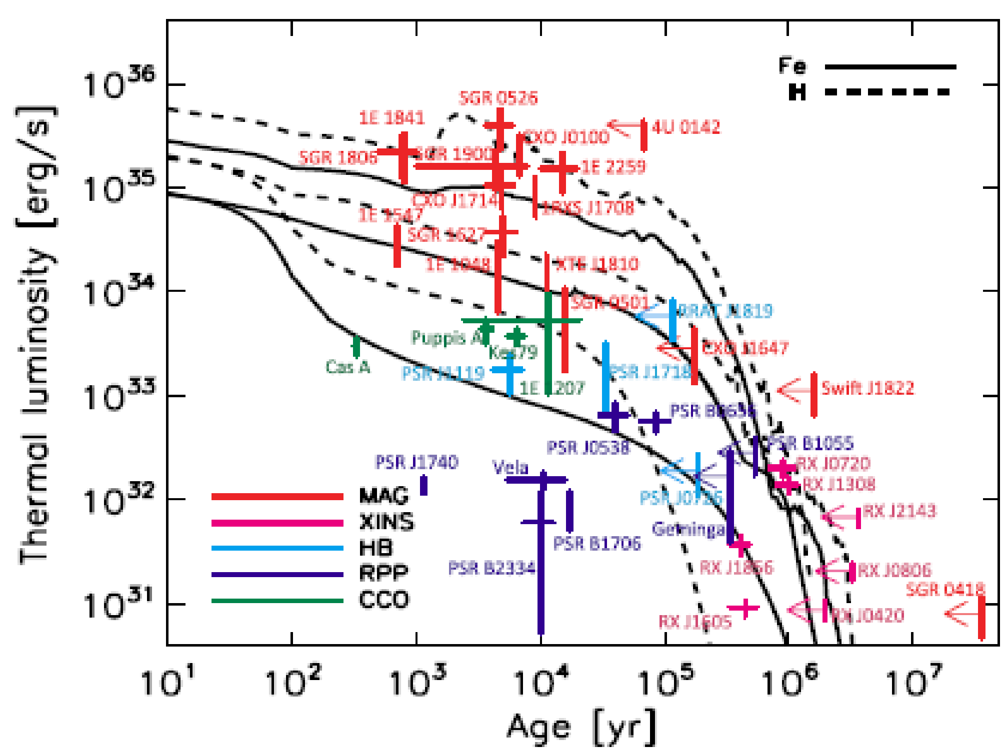

[Viganò+ 2013]

Reproducing the luminosity and timing property variety with magneto-thermal 2D models, varying only the initial B (confined to the crust).

(Caveats: 2D limitations, crust confinement, matching with potential solution outside, radii of inferred emission size are observed smaller than in simulations, no magnetospheric contributions considered…)

Magneto-thermal evolution

Simulations applied to the observed population

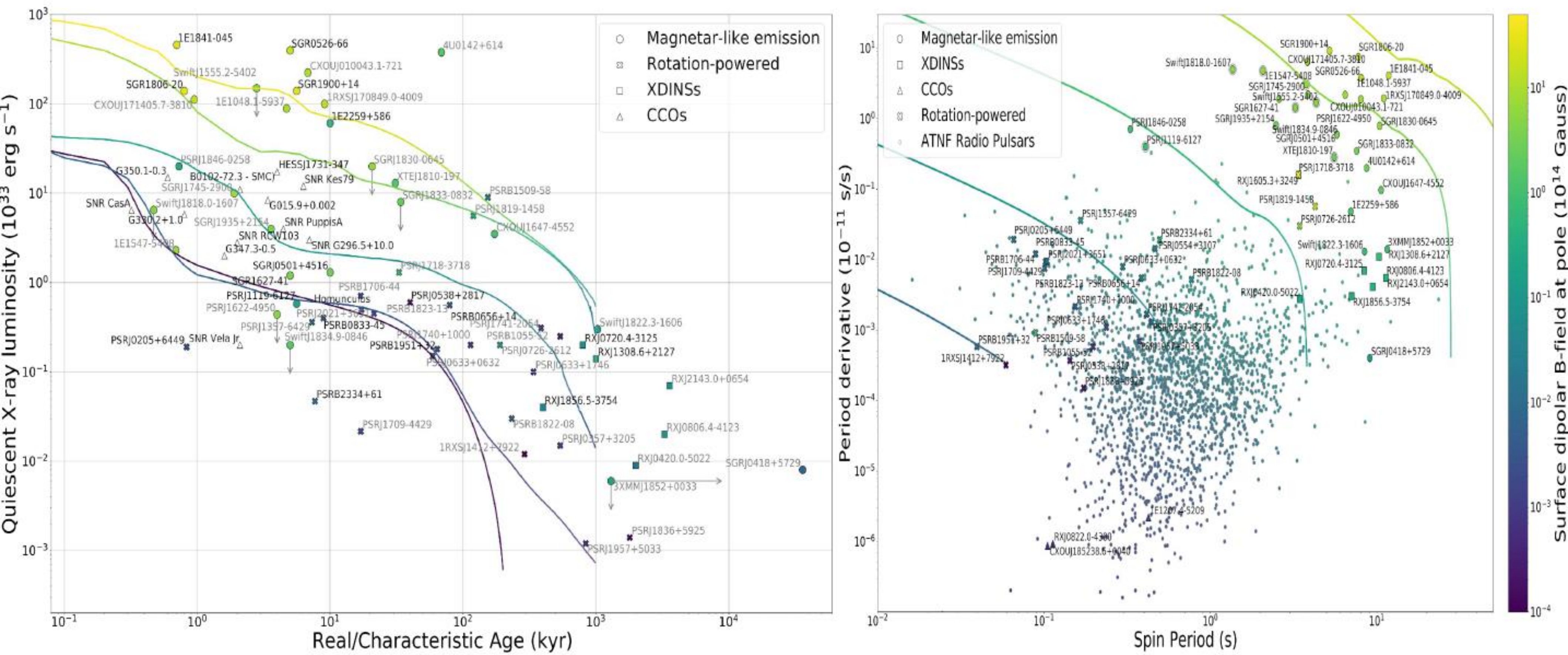

[Marino et al. in prep.]

Effects on the magnetosphere

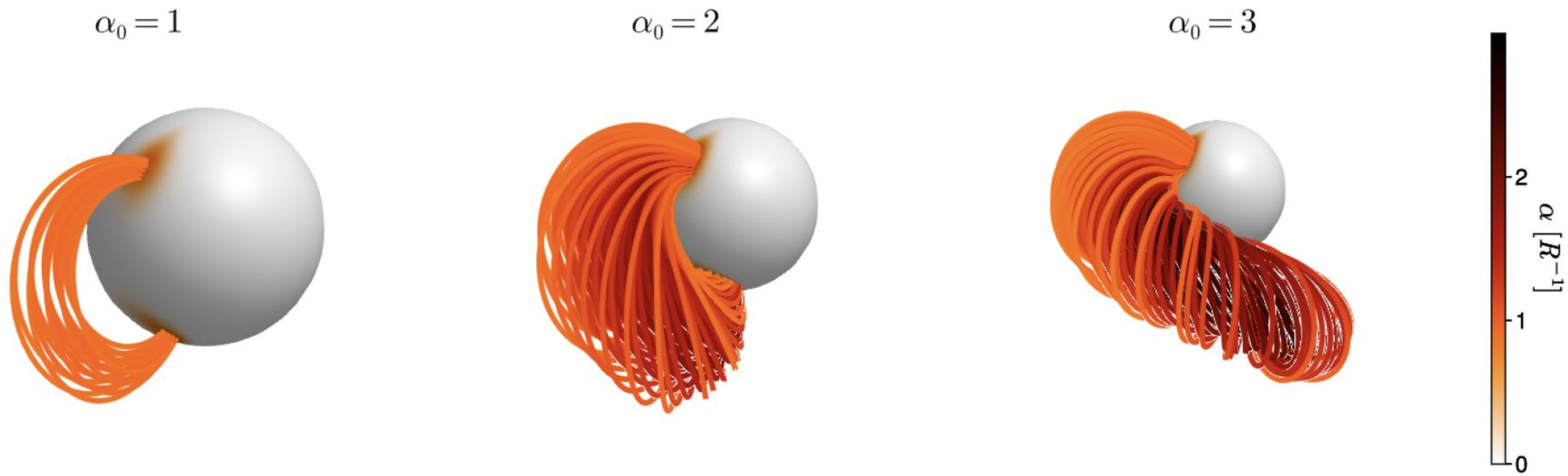

The internal dynamics of magnetic fields can twist the external field and lead to instabilities, related to the transient phenomena. *[Pons+ 2026, Carrasco+ 2020]*